REPORT NO. UMTA - FL - 06 - 0017 - 80 - 1

STATIC AND DYNAMIC TESTS OF FULL-SCALE DOUBLE-TEE GIRDERS FOR DADE COUNTY RAPID TRANSIT SYSTEM

METROPOLITAN DADE COUNTY
OFFICE OF
TRANSPORTATION ADMINISTRATION

OCTOBER 10, 1979

PREPARED FOR

U.S. DEPARTMENT OF TRANSPORTATION
Urban Mass Transportation Administration
Office of Technology Development and Deployment
Office of Rail and Construction Technology
Washington, D.C. 20590

STATIC AND DYNAMIC TESTS

OF FULL-SCALE DOUBLE-TEE GIRDERS

FOR DADE COUNTY RAPID TRANSIT SYSTEM

October 10, 1979

The preparation of this report has been financed through a grant from the U. S. Department of Transportation, Urban Mass Transportation Administration.

Technical Report Documentation Page

1. Report No.	2. Government Accession No.	3. Recipient's Catalog No.
UMTA-FL-06-0017-80-1		

4. Title and Subtitle	5. Report Date
Static and Dynamic Tests of Full Scale Double-Tee Girders for Dade County Rapid Transit System	October 10, 1979
	6. Performing Organization Code
	8. Performing Organization Report No.
7. Author(s) Thomas T. C. Hsu, Phd. P.E.	
9. Performing Organization Name and Address	10. Work Unit No. (TRAIS)
Metropolitan Dade County Office of Transportation Administration 44 W. Flagler St. Suite 9-14 Miami, Florida 33130	11. Contract or Grant No. FL-06-0017
	13. Type of Report and Period Covered
12. Sponsoring Agency Name and Address U. S. Department of Transportation Urban Mass Transportation Administration Office of Technology Development and Deployment Office of Rail and Construction Technology 400 7th Street, S.W., Washington, D.C. 20590	Final
	14. Sponsoring Agency Code

15. Supplementary Notes

16. Abstract

Demonstration tests were carried out on three full-size 80 feet long by 5 feet deep by 12 feet wide precast prestressed double-tee girders proposed for the aerial guideways of Dade County Rapid Transit System; use of this cross-section of girder was a first for any U.S. Transit System. Two of the three girders cast in Miami were shipped by rail to P.C.A. Laboratories, Skokie, Illinois for extensive static and dynamic testing, with the third girder being kept in Miami to monitor camber and loss of prestress. Static test results of uncracked and deliberately precracked girders, showed that service torsional rotations, which were in close agreement with a theoretical mixed torsion analysis, were small enough to ensure rider comfort. Fatigue resistance of the girders was fully established by two separate test spectra involving 5 and 6 million cycles of loading representing the cumulative damage of sixty years of operational life; no deterioration whatsoever was observed in terms of flexural and torsional stiffness, crack propagation or strand stresses. Post-cracking behavior of the girders showed adequate strength and ductility with an ultimate capacity of 1.6 times the required factored severe derailment loading including 100% impact. This test report concludes that the excellent behavior of the girders both from serviceability and strength considerations, substantiated all the design analyses and details used.

17. Key Words	18. Distribution Statement
Full Scale Tests, Double-Tee Girders Design Analysis, Double-Tee Girders Static and Dynamic Tests, Precast Girders	

19. Security Classif. (of this report)	20. Security Classif. (of this page)	21. No. of Pages	22. Price
		151	

Form DOT F 1700.7 (8-72) Reproduction of completed page authorized

CONTENT

TABLES

FIGURES

FIGURES

FIGURES

FIGURES

INTRODUCTION

Metropolitan Dade County, Florida, is now in the process of building a new rapid transit system of about 50 miles. The first-stage construction of this new system scheduled for completion in 1984, consists of 22.5 miles, and includes 21.5 miles of aerial guideways. The aerial structures to be used for the guideways are prestressed concrete double-tee girders - a first in the use of such a structure in a U. S. transit system.

The double tee design concept resulted from a study conducted by Kaiser Transit Group, the General Architectural and Engineering Consultant for Dade County Rapid Transit System. The study examined various cross-sectional configurations in different types of materials and alternative methods of construction, and narrowed the field down to the traditional box section and double tee section. The double tee girder was recommended for reasons of aesthethics as well as economy. It was estimated that the use of double tee may result in savings of up to $5 million.

It was decided at that stage to conduct more detailed technical studies, examining the various aspects of design and performance of the structure. It is recognized that torsional moments in a transit guideway are produced by wind load on the vehicles and structure, by the transverse horizontal nosing/lurching action of the vehicles on the rail, centrifugal force on curved track, etc.. Torsional rotation caused by these moments must be, therefore, controlled to provide riding comfort for passengers. This is accomplished through the analysis of the torsional stresses and the design of the structure accordingly. Such a study was conducted for this project by Dr. T. C. Hsu, and a report entitled "Torsion Analysis of Dade County Rapid Transit Aerial Guideways" was completed in April 1977. It showed that the torsional rotation can be controlled well within the prescribed tolerance limits.

The elastic torsional analysis, however, is applicable to the behavior of structures before cracking. The post-cracking torsional behavior of double-tee sections was not completely clear at this stage of investigation. However, it was known that large torsional moments occur in the case of severe derailment. For these reasons, testing of two approximately 5/8 scale models was conducted. These model girders were manufactured at Stresscon International, Inc., Miami, Florida and tested at the Construction Technology Laboratories of the Portland Cement Association, Skokie, Illinois in July, 1977. Another study by T. C. Hsu entitled "Torsion Tests of Double-Tee Girders for Dade County Rapid Transit Aerial Guideway" was completed in August, 1977. Tests conducted under this study showed that the girders behave satisfactorily, both from a safety as well as operational point of view.

In view of large capital investment involved, and the fact that a double tee had not been used on any rapid rail transit system, the U. S. Department of Transportation's Urban Mass Transportation Administration (UMTA) agreed to fund full-scale tests through a Research, Development and Demonstration (Section 6) grant. The full-scale tests were to serve three purposes: to prove the adequacy of all design methods, to check some of the construction and reinforcement details, and to verify the dynamic performance of the girders.

On March 10, 1978 a Structural Design Review Panel of seven eminent engineers was convened to examine the proposed design of the double-tee girders. This panel unanimously endorsed the double-tee design concept and urged the full-scale testing as proposed by the Kaiser Transit Group.

Preparatory work on the testing of full-scale girders began immediately after the recommendation of the Review Panel. Three girders were manufactured by Lone Star Florida, Inc./Stresscon from August to October of 1978. Two of these girders were shipped to the Construction Technology Laboratories of the Portland Cement Association and tested during the period from November 1978 to April 1979. This report describes the testing of these three girders and the analysis of the test results.

Finally, it is to be noted that on August 22, 1979, when the bids for the fabrication of the standard girders for the 21.5 mile phase 1 were opened, all the three bidders opted for the double tee alternative. Furthermore, the low bidder, R. T. Joint Venture, was $1.6 million below the engineers estimate. Since the box girders alternative was not bid on, direct comparison cannot be made. However, it is estimated that the selection of the double tee girders reduced the construction cost of the aerial guideway by about $6.2 million.

2. BACKGROUND

2.1 VEHICLE LOADINGS

The double tee girders were designed to carry a train of cars, each 75'-0" long, 10'-6" wide and 12'-1" high. Each car has two trucks with a center-to-center distance of 54'-0". Each truck consists of two axles 6'-6" apart.* Each axle has two wheels suitable for a track guage of 4 ft. 8-1/4 inc. The empty weight of the car is 78 KIPS, and the girders were designed to resist a normal full live load of 102.9 KIPS and a crush live load of 115.5 KIPS. The vertical impact factor is assumed to be 1.25 and the horizontal nosing/lurching force is taken as 10% of the vertical load; centrifugal forces are limited to a maximum of 6.3% of the design axle load (excluding impact) for curved track with a radius of 5200 feet.

2.2 DESIGN CRITERIA

2.2.1 Live Load

The design criteria used for live load in the tests are:

(1) Normal service load for tangent track (72^{k} vert. load + 31^{k-ft} torque/truck): 100% crush live load + 25% impact + 10% nosing/lurching + 27 mph wind.

(2) Abnormal service load for tangent track (72^{K} vert. load + 63^{k-ft} torque/truck): 100% crush live load + 25% impact + 10% nosing/lurching + 60 mph wind.

(3) Abnormal service load for curved track with radius of 5,200 ft. (72^{k} vert. load + 90^{k-ft} torque/truck): Abnormal service load (2) + eccentricity of chorded construction for 5200 ft. radius + centrifugal force of vehicle with 70 mph speed.

---

*The distance between axles of 6'-6" was later changed to 7'-6" which was used in the flange slab test of Chapter 9.

(4) Normal fatigue load on tangent track (64^{k} vert. load + 22.5^{k-ft} torque/truck): 89.1% crush live load + 25% impact + 10% nosing/lurching + 13.5 mph wind.

(5) Abnormal fatigue load on tangent track (72^{k} vert. load + 25^{k-ft} torque/truck): 100% crush live load + 25% impact + 10% nosing/lurching + 13.5 mph wind.

(6) Abnormal fatigue load for curved track with radius of 5,200 ft. (72^{k} vert. load + 48.5^{k-ft} torque/truck): Abnormal fatigue load (5) + Eccentricity of chorded construction for 5,200 ft. radius + centrifugal force of vehicle with 70 mph speed.

(7) Severe derailment load on tangent track (115.5^{k} vert. load + 346^{k-ft} torque/truck): Crush live load with 100% impact and maximum side shift of 3 ft.

(8) Factored derailment load on tangent track (162^{k} vert. load + 485^{k-ft} torque/truck): 1.4 times severe derailment load (7).

These criteria were checked in the following tests of Girders 2 and 3:

GIRDER	TESTS	CRITERIA USED
2	Initial Static Test	(1), (2), (3)
	Flexural Fatigue	(4), (5)
	Flexural Derailment	(7), (8)
3	Torsional Fatigue	(6)
	Torsional Derailment	(7), (8)
	Flange Bending & Punching (Derailment)	(7), (8)

2.2.2 Superimposed Dead Load

In addition to the live load caused by vehicles and wind, the weight of the track rails, rail plinth pads, power rail, guard rail, cableway, acoustic barrier, etc., will create superimposed dead loads (S.D.L.), which is assumed to be 0.81 kip/ft. of tangent track. In order to simplify the top surface of the test girder, it was necessary to add 0.04 kip/ft. of concrete. Hence, the S.D.L. for the test beam was taken as 0.77 kip/ft.

The superimposed dead load also creates a uniformly distributed torque due to the eccentric locations of the acoustic barriers, the third rail and the cableway. This torque is assumed to be 0.50 kips-ft/ft. of track.

In the case of derailment, it is assumed that the superimposed dead load is 1.1 (S.D.L.) + 0.1 (Girder weight of 2.31 kip/ft.). It is also assumed that the acoustic barrier (0.185 kip/ft. weight and 6.17 ft. from shear center) has been pushed off the girder during derailment. Consequently, the uniform vertical load becomes 0.88 kip/ft. and the uniformly distributed torque is 0.71 kip-ft/ft. This torque is in the direction opposite to the derailment torque.

In the testing of Girders 2 and 3, S.D.L. is simulated by two pairs of concentrated loads. In the flexural test of Girder 2, these concentrated loads are determined such that they create at the SR-4 gage locations (3.5 ft. from midspan) a moment identical to that caused by the uniformly distributed superimposed loads and torques. In the torsional test of Girder 3, the concentrated loads were determined to match the shear at 6 ft. from the support.

2.2.3 Fatigue Load for Test

The girders are designed for a service life of 60 years and a fatigue life of over 16 million cycles of loading during this period. The number of cycles are distributed as follows:

(1) Abnormal Fatigue Cycle (crush live load + impact, P = 144 kips): 250,000 cycles.

(2) Normal Fatigue Cycle (Normal full live load + impact, P = 128 kips): 6 million cycles.

(3) Reduced Normal Fatigue Cycle (87.1% normal full live load + impact, P = 112 kips): 10 million cycles.

For a 6-car train each of these three fatigue cycles consist of 40% high cycles (moment range from zero to 58P/4) and 60% of low cycles (moment range from 25P/4 to 58P/4).

Since the time required to apply 16.25 million cycles of loading with six types of moment range is prohibitive, it is necessary to devise some simple equivalent tests with reduced number of cycles and one or two types of high cycle moment range. Based on Minor's hypothesis of cummulative damages, Dr. John Fisher[12] has provided three equivalent tests of 7, 6 and 5 millions high cycles as follows:

Equivalent Test Spectrum	Abnormal Fatigue Cycle	Normal Fatigue Cycle	Total Cycles
A	250,000	6.82 million	7.07 million
B	3.20 million	2.80 million	6.00 million
C	5.05 million	0	5.05 million

Test Spectra B and C have been selected for Girders 2 and 3, respectively.

2.3 DESCRIPTION OF GIRDERS

The cross section and the details of the test girders is shown in Figs. 1a and 1b. The girder is 80 ft. long, 12 ft. wide, 5 ft. deep and weighs 94 tons. It has a 9 in. diaphragm at midspan and diaphragms at the ends. The dapped end is 2.5 ft. deep and 1'-5' long and the span between the centers of bearing is 78.5 ft. The two stems, each having an average width of 11.5 in., are 5 ft. c. to c.. The flange is 8 in. thick between the stems and tapered from 8 in. at the stem to 6-1/4 in. at the edge.

The girder is prestressed with 54 one-half in. diameter Lo-Lax strands. The strands are held down at two points 10.5 ft. from midspan. The eccentricities of the centroid of all strands are 35 in. and 15 in. at the midspan and at the ends, respectively.

The three girders were initially prestressed to different levels as follows:

Girder	1	2	3
Prestress per Strand (kips)	29.2	27.6	28,5

The prestresses in Girders 2 and 3 were reduced below the level of Girder 1 so that the prestress levels at the time of fatigue testing would be close to the effective prestress of Girder 1 after all losses have taken place. The final prestress loss for Girder 1 is calculated to be 23%.

The stems are reinforced with No. 4 stirrups at 10 in. spacing. This spacing is increased to 20 in. between the hold-down points and

is decreased to 4 in. near the ends. The longitudinal steel consists of 6 No. 4 bars per stem reduced to 2 No. 4 bars per stem in the central 12 ft. between the hold-downs. In the 3 ft. 5-1/4 in. length from the end, special reinforcement for the dapped end of the girder is provided according to the PCI Design Handbooks.(3)

The transverse reinforcement in the flange consists of No. 5 bars at 8 in. spacing at the top and No. 4 bars at the bottom. These bottom No. 4 bars are spaced at 8 in. between the stems and 16in. in the overhanging flanges. This arrangement is accomplished by staggering the bottom bars, each bar extending to the edge of the flange on one side and terminating just beyond the stem on the other side. The end of each bottom bar at the edge of the flange is bent up to form a closed loop with the top bar. The longitudinal bars in the flange consist of 8 No. 4 bars and 13 No. 3 bars distributed around the loop.

2.4 FLEXURAL DESIGN

Flexural design is based on the well=known principles of elastic behavior of prestressed concrete. The allowable stress at the bottom fiber is limited to $2.25\sqrt{f'_c}$ under 100% crush live load plus impact, and to zero under normal full load (89.1% crush live load) plus impact. The ultimate flexural strength of the test girder is 9,700 k-ft. which exceeds the required flexural strength of 7,620 k-ft. by 27%. In other words, flexural design of this double-tee girder is governed by allowable stresses.

A detailed analysis of a very similar girder is given in Ref. 4. This analysis is quite lengthy and includes a sophisticated method for calculation of prestress losses suggested by Dhondy. All these tedious design procedures have been simplified by the development of an electronic computer program. A detailed description of the computer program has been documented in a report by the writer.(5) The output of this program includes the transformed section properties, the maximum design moment, the flexural stresses, the prestress losses, the ultimate moment capacity, the release strength of concrete, the camber and the deflection due to dead and live loads.

2.5 TORSIONAL ANALYSIS

An elastic torsional analysis of the girder is given in Ref. 1. This analysis is based on Vlasov's mixed torsion theory for St.-Venant torsion and warping torsion.[6] This tedious torsional analysis has also been computerized.[1,5] The computer program can generate the following information:

(1) Sectional constants in mixed torsion analysis:
This includes the location of the shear center, the St.-Venant torsional constant, the sectorial moment of inertia and the dimensionless constant $k = l\sqrt{GC/EI_w}$

(2) The deformation and internal forces due to torsion:
This includes the rotation, the rotation per unit length, the bimoment, the St.-Venant torque and the warping torque. The end conditions may be fixed (100% warping restraint), hinged (zero warping restraint) or partially-hinged (actual dimensions of diaphragms).

(3) Stress diagrams due to unit force:
This consists of the shear stresses due to unit St.-Venant torque, the shear stresses due to unit warping torque and the longitudinal stresses due to unit bimoment.

This elastic torsional analysis is applied to design in two ways. First, to predict the torsional rotation of the girder under service loads, in order to ensure rider comfort. Second, to design the torsional steel under service loads.

Vlasov's elastic mixed torsion analysis was extended to the post-cracking stages for the study of derailment problems. This so-called "post-cracking mixed torsion analysis" has been developed by Hwang and the writer. This analysis has been used to design the torsional steel

under severe derailment loads.

The design of stirrups and longitudinal steel caused by shear and torque was based on the paper by Zia and McGee.[7] However, the minimum stirrup requirement was calculated according to a more recent paper by Zia and the writer.[8]

2.6 DESIGN OF DETAILS

One of the purpose of these tests is to check the suitability of the construction details. Design of these details can be found in Ref. 9. Three of these details are of prime concern:

(1) The re-entrant corner of the dapped ends:
Two bearing plates, each 3/4 in. by 6-3/4 in. by 16 in., are used at each end of the girder. Each bearing plate was anchored into the concrete by 4 No. 5 vertical bars and 8 horizontal bars (2 No. 9, 2 No. 7, 2 No. 6 and 2 No. 4). At the suggestion of Professor Ben Gerwick, this plate was extended into the end diaphragm by 3/4 in. to meet the closed galvanized stirrups of the end diaphragm. In this way the diagonal cracks usually developed at the reentrant corner may be arrested.

(2) The hold-down points:
Each hold-down device is designed to resist a hold-down force of 47 kips. This force introduces large stress concentration in the strands and in the concrete.

(3) The connections between the stem and the end diaphragm:
These regions require particular attention because (a) warping torsion creates tension in this region and (b) prestress is not fully effective in regions so close to the end.

To reinforce this region, two additional bars, (1 No. 8 and 1 No. 6, each 8 ft. long), are placed at the bottom of each stem near the end of the girder. Another fours No. 6 horizontal bars are placed at the bottom of each end diaphragm. Two of the four are bent and anchored into the stems. Similarly, two No. 6 U-shape horizontal bars connecting an end diaphragm to the stems are placed at approximately the mid-height of the girder.

2.7 PRODUCTION OF GIRDERS

The girders were manufactured at Lone Star Florida, Inc./Stresscon. A self-stressing reinforced concrete form with steel lining was designed by Givens as shown in Fig. 2a. The process of manufacturing the girders is shown in Fig. 2b. Details of the production process are given in Ref. 9.

2.8 TRANSPORTATION OF GIRDERS

The girders were transported by railroad from Miami, Florida, to Skokie, Illinois (Fig. 3). They were then trucked from the Skokie siding to the Construction Technology Laboratories of the Portland Cement Association. The process of threading a girder into the laboratory is shown in Fig. 4.

3. SCOPE OF TESTS

The scope of tests is summarized in the following Table:

GIRDER	LOAD CONDITION	OBJECTIVE OF TEST
1	None	a) Loss of Prestress b) Camber Growth
2	None	a) Natural Frequency
	Coupler at Midspan	b) Flexural and Torsional Stiffnesses c) Flexural Fatigue d) Flexural Derailment
3	Coupler at 0.21ℓ Coupler at 0.25ℓ	a) Torsional Fatigue b) Torsional Derailment
	Load at edge of flange	c) Flange Bending & Punching

A total of three girders were manufactured. Girder 1 was set-up in the yard of Lone Star, Florida, Inc./Stresscon to monitor the loss of prestress and the camber growth. Measurements were made periodically, about daily in the beginning and then gradually increased to monthly in the later stage.

Girders 2 and 3 were shipped to the Construction technology Laboratory of Portland Cement Association, Skokie, Illinois. A simple test was first made on Girder 2 to measure the natural frequency of the girder

in flexure and in torsion. Girder 2 was then subjected to loadings (symmetrical about midspan and eccentric with respect to centerline girder) to maximize the bending moment and the torsional rotation at midspan. The initial static testing was performed to study the flexural and torsional stiffnesses under design criteria (1), (2) and (3). It was first carried out on the uncracked girder, and then on the cracked girder after it was subjected to a vertical load exceeding twice the normal service load. Following the static test, the girder was subjected to 6-million cycles of fatigue load according to design criteria (4) and (5). Finally the girder was loaded under derailment condition to check design criteria (7) and (8). This loading was increased to ultimate capacity.

Girder 3 was subjected to loads on one-half span only. The load closest to the support was placed at a distance of 6.25 ft. therefrom. These load locations were chosen to satisfy two investigations simultaneously. First, to allow diagonal cracks, if any, to develop in the stem near the support under maximum shear and torsion. Second, to maximize as much as possible the shear at the re-entrant corners of the dapped ends. Girder 3 was first loaded statically in flexure to cracking before subjecting it to 5-million cycles of fatigue loads according to design criterion (6). It was then loaded to design criteria (7) and (8) under derailment conditions. This loading was increased to near ultimate capacity until the yielding of the stirrups.

An additional test was also made on Girder 3 to study the bending and punching capacities of the overhanging flange. This test is reported independently in Chapter 9.

4. MATERIALS

4.1 CONCRETE

The composition of the concrete mix was:

Cement: ASTM C150 Type III

Coarse Aggregate: ASTM C33 (Miami Oolite)

Sieve Opening	1"	3/4"	1/2"	3/8"	#4	#8
% passing by wgt.	100	99	64	32.6	3.1	1.8

Pea Rock: ASTM C33 (Miami Oolite)

Sieve Opening	1/2"	3/8"	#3	#4	#10	#16
% passing by wgt.	100	97	37	12	3.5	2.5

Fine Aggregate: ASTM C33 (Miami Oolite Screening)

Fineness modulus = 2.6.

Retardant: Daratard HC. ASTM C494. Type D
Air-Entrainment Agent: None.
Design mix per cubic yard*

	Girder 1	Girders 2 and 3
Cement	705 lbs.	680 lbs.
Coarse Aggregate	1600 lbs.	800 lbs.
Pea Rock	None	800 lbs.
Fine Aggregate	1280 lbs.	1280 lbs.
Water	36 gals.	33 gals.
Retardant	160-175 oz.	160-175 oz.
Slump	3-14 - 3-1/2	3" - 4"

*Concrete mix for Girder 1 was found to have workability less than desirable. The mix was then improved for Girders 2 and 3.

The cylinder compressive strength of concrete is summarized in the following Table:

Girder	Approx. 1 day	Approx. 28 days	At Test
1	4209 (16.5-19.5 hr.)	7572 (34 days)	----
2	4341 (19-20.8 hr.)	7597 (28 days)	7950 (53 days)
3	4097 (19.3-21 hr.)	7598 (28 days)	7953 (124 days)

Note that each value, in psi, in the Table is an average of 5 or 6 cylinders, each taken from a truck load. The values in brackets are the actual age of concrete tested.

The stress-strain curve of the concrete at test for Girder 2 is plotted in Fig. 5. This curve is an average for five cylinders. The secant modulus of elasticity, E_c, of this concrete is plotted in Fig. 6 as a function of the level of stress. It can be seen that the secant moduli are 3850 ksi and 3410 ksi at 0.1 f'_c and 0.5 f'_c, respectively. When compared to the modulus of elasticity recommended by the ACI Building Code 318-77, ($E_{code} = 57{,}000\sqrt{f'_c} = 5080$ ksi), the ratios E_c/E_{code} are 0.76 and 0.67 for stress levels of 0.1 f'_c and 0.5 f'_c, respectively. This low modulus of elasticity of local concrete is caused by the low modulus of elasticity of Florida Oolite aggregates.[10]

The direct tensile strengths of concrete were also measured. A 6 in. by 12 in. standard concrete cylinder was cut at both ends and was cleaned carefully. Two thick steel plates were epoxied onto the ends of the cylinder in a specially designed rig. Each steel plate was then attached to a spherical joint assembly and was tested in a universal testing

machine. The eleborate processes of preparing the concrete specimens and the use of the spherical joints were to ensure concentric tensile loading of the concrete cylinder and to avoid failure at the interfaces between the concrete and the steel plates. Even with such precuations, however, some cylinders still failed at the interfaces. Since the test results of such cylinders were conservative, these were included in the average if they have higher strength than those cylinders with failure in the concrete. These were neglected, however, if they have lower strength. The average direct tensile strengths of concrete of three or four cylinders were:

Girder 2: 396 psi at 68 days

Girder 3: 444 psi at 141 days

4.2 PRESTRESS STRANDS

1/2 in. Lo-Lax prestressed strands, Grade 270 and conforming to ASTM A416, were used in the girders. Six pieces of strands randomly selected were tested in a 200,000 lb. Wiedemann-Baldwin universal testing machine at the University of Miami. Steel discs were carefully glued onto one wire of a strand and the strains were measured by a mechanical Demec gauge over a length of 8 in. A typical stress-strain curve of strands is given in Fig. 7. The average modulus of elasticity was found to be 28,900 ksi and the average ultimate strength was 278 ksi. It is interesting to note that all the wires of the six strands broke at the jaw. The maximum strain was only 2% - 3%. It appears that Lo-Lax strands have somewhat less ductility than the stress-relieved strands, which usually do not break at the jaw.

Strains in the prestress strands were also measured by epoxying SR4 electrical strain gages onto one wire of each strand. It was found that the average modulus of elasticity was 33,700 ksi, considerably higher than those obtained by Demec gage. Since identical method was used to measure the strains in the strands of Girder 2, this higher modulus of elasticity was used to convert the measured strains into stresses for the strands in this girder.

4.3 MILD STEEL REINFORCEMENT

Mild steel reinforcement, Grade 60 and conforming to ASTM A615, was used for all non-prestressed reinforcement. 4 pieces of No. 4 bars randomly selected were also tested. A composite stress-strain curve of all four specimens is given in Fig. 8. This steel has a long yield plateau and an even longer strain hardening region. The average modulus of elasticity is 26,700 ksi and the yield stress is 61 ksi.

5. TEST SET-UPS

Both Girders 2 and 3 were simply supported in a similar manner as shown in Fig. 9. End diaphragms were restrained from twisting as shown schematically in Fig. 10. The loading systems, however, were different for the two girders. They are described as follows:

5.1 GIRDER 2

5.1.1 Initial Static Test

Three loading systems have been used to test Girder 2. The first was for initial static test to study the flexural and torsional stiffnesses. In this test two pairs of symmetrical loads, each identified as P_1 and P_2 in Fig. 11, were applied. For flexural moments without any torsion P_1 and P_2 should be applied equally. If P_1 was increased while P_2 was decreased, a torsional moment will also be generated. The loads were applied through a system of cross heads and tied rods[11] in Fig. 11. A general view of this test set-up has been given in Figure 9.

5.1.2 Flexural Fatigue Test

The second loading system was used for flexural fatigue test. Two MTS 110-kip capacity actuators were mounted on the girder as shown in Fig. 12. Actuators were provided with swivel heads at both ends. For maximum efficiency of the hydraulic system the piston of each actuator was clamped to the girder by two cross heads and two rods prestressed to 60 kips; this prestress will not affect the test results. Similar to the initial static test, the loads in the girders were identified as P_1 and P_2 in Fig. 11. The relative magnitude of loads P_1 and P_2 was obtained by controlling the eccentricity of the actuator relative to the center line of the girder. A general view of this test set-up is shown in Fig. 13.

5.1.3 Flexural Derailment Test

The third loading system was designed for derailment test. Four loads, designated as P_3 in Fig. 11, represent the center-lines of four axle loads of two derailed cars with the coupler located at mid-span; the other axles of the two cars would be located off the span. These loads are located 3 ft. from the center line of the girder. To accommodate the large deflection required to test the girder to failure, a system of cross heads, high strength Dywidag tie rods and high capacity rams were used. This system could take up the stroke of the rams after they are fully extended, so that the successive strokes of the rams could be added. In addition to the large derailment loads P_3, four small loads P_1 and P_2 were also applied to simulate the superimposed dead load on the girder. These loads were also applied through cross heads and rods and were maintained constant throughout the test. A general view of the test set-up is shown in Fig. 14.

5.2 GIRDER 3

5.2.1 Torsional Fatigue Test

Two loading systems have been used to test Girder 3. The first was torsional fatigue test as shown in Fig. 15b. Two pairs of loads, each designated by P_1 and P_2, were placed 7 ft. and 28 ft. from the end. These loads were induced by two 110-kip actuators attached to the girder in the same way as Girder 2, (Fig. 12).

The girder was cracked before the dynamic loads were applied. Since the two actuators did not have sufficient capacity to crack the girder, two auxiliary loads identified as P_5 were added. P_5 was accomplished by cross-heads, tied rods and a ram. This auxiliary equipment was removed before the commencement of the fatigue test.

The precracking process produced flexural cracks in the vicinity of the load P_5 in a region 12 ft. wide from 7 ft. west to 5 ft. east of P_5. A small crack about 5 in. long and inclined at about 25^o to horizontal was also observed at the south side of the west re-entrant corner.

5.2.2. Torsional Derailment Test

The second loading system of Girder 3 was for derailment test as shown in Fig. 15c. This load system was identical to that for Girder 2 except that the locations of the loads were moved closer to the support.

6. INSTRUMENTATIONS

6.1 LOADS

Universal load cells mounted on the MTS rams were calibrated before testing and were used to measure loads during the fatigue load tests. Forces applied at each loading point during the initial static test and the derailment test were measured by precalibrated compression load cells.

6.2 TRANSLATIONS

Vertical translations relative to the laboratory floor were measured at 19 points in Girder 2, and at 13 points in Girder 3. The cross sections where the measurements were made are indicated by alphabet letters in Fig. 11a (for Girder 2) and in Fig. 15a (for Girder 3). Locations of measurement at each cross section are given by numbers 1 to 5 in Fig. 16a. Using this code the locations of measurement for vertical translations have been summarized in Table 1. Longitudinal translations were also measured at the ends of the girders as shown in Fig. 16b.

Both vertical and longitudinal translations were measured by potentiometers with a sensitivity of 0.001 in. Each potentiometer was connected through hinges to a thin steel plate glued onto the girder. These hinges eliminated the interference of small movement of the girder in the plane perpendicular to the direction measured.

Deformation of the cross section during static and derailment tests were measured at two sections in Girder 2, and at one section in Girder 3. At each section a rigid frame was attached to the girder right on top of the two stems. Eight LVDT or DCDT gages were attached to the frame as shown in Fig. 17. In Girder 2, one frame was located at quarter point

of the girder and the other frame was 10 ft. from midspan in the same half of the girder. In Girder 3, only one frame was used at the quarter point in the half span that was loaded.

6.3 TORSIONAL ROTATIONS

Six rotation gages designed by the writer were used to measure the torsional rotations along the girder. Rotations for Girders 2 and 3 were measured at the locations shown in Fig. 18.

Each rotation gage consists of a heavy 9-lb steel cylinder hung by a thin strip of spring steel to an aluminum angle, which is attached to the bottom face of the girder. Four SR-4 electrical strain gages are epoxied onto both sides of the spring steel strip to form an electrical Wheatstone bridge. When the girder rotates, the heavy steel cylinder tends to remain vertical, resulting in bending of the spring steel strip. The bending strains of the spring steel strip are monitored by the SR-4 gages and the output voltage of the Wheatstone bridge is fed into a recorder. Precalibration between the output voltage and the torsional rotation shows that the sensitivity of the rotation gage is 0.01 degree per division.

6.4 STRAIN GAGES

SR4 electrical strain gages were epoxied to the strands and reinforcing bars before casting. 24 gages were attached to the strands in both stems of Girder 2 at two symmetrical sections 3.5 ft. from midspan. At each of the four locations, two gages each were glued to the first and second strands of the innermost row counted from the bottom. One gage was glued to the 9th strand at the top and the last gage was placed on either the fourth or sixth strand. To force the cracks to occur at the four gage locations a crack former was placed at each location between the bottom fibre of

the stem and the bottom strand. All gages were monitored during the derailment test, but only six gages were selected for recording during the dynamic test.

31 SR4 gages were epoxied onto the stirrups in the stems and in an end diaphragm of Girder 3. The locations of these gages are shown in Fig. 19. Two gages, located nearest to the end of the heavily-loaded stem on the outside leg of stirrups, were selected for periodical reading during the dynamic test. All gages were monitored during the derailment test.

In the test some gages were found to be dead and the accuracy of some live gages was also questionable. All unreliable gages have been discarded in this report.

6.5 CRACKS

Cracks were marked with black felt pens and photographs were taken. At some load stages maximum crack widths were selected and were measured by illuminated hand microscopes.

For the dynamic test of Girder 2, one of the largest cracks were selected for monitoring. An LVDT was attached to two brackets glued onto the concrete surface on each side of the crack. In this way this crack width was monitored continuously.

6.6 RECORDINGS

Data from load cells, rotation gages, potentiometers and SR4 gages were recorded by a digital data acquisition system. All the data were later reduced to engineering units and tabulated by a mini-computer.

6.7 LOSS OF PRESTRESS

Losses of prestress were measured in all three girders. Losses due to friction, anchorage seating and relaxation of strands was first measured before casting of concrete. The elastic

shortening was then obtained from measurements before and after the cutting of strands. Loss of prestress due to creep, shrinkage and relaxation was measured periodically thereafter. The measurements were taken daily in the early age and the interval was gradually increased to about once a month at the later age.

Five to ten hours after the concrete was cast in the form, 3/8 in. diameter steel discs were countersunk and epoxied onto the inside faces of the two stems at two symmetrical sections 3 ft. - 6 in. from midspan. To accommodate the installation of those steel discs, four special windows were provided in the skin of the steel form. These windows are accessible from the outside by two tunnels under the bed.

Loss of prestress was measured by a Demec mechanical gage and a Whittemore mechanical gage. At each of the four locations of measurement, two steel discs were placed 8 in. apart to accommodate the Demec gage length and another two steel discs were placed 10 in. apart for the Whittemore gage. These steel discs were located approximately 5 in. above the bottom face of the stem at the centroidal line of the prestress strands. The loss of prestress before and shortly after the cutting of strands was calculated from the measurements at these four locations.

After a girder was lifted out of the form, steel discs were attached to four more locations on the outside faces of the two stems, opposite to those installed previously on the inside faces. The loss of prestress thereafter were calculated from the measurements at all eight locations.

In view of the fact that temperature fluctuated greatly during the life of a concrete girder, particularly in the early age as shown in Fig. 20, the strain caused by temperature must be subtracted from the strain measured directly by the Demec or Whittemore mechanical gages.

This temperature strain was measured by the same mechanical gages from an auxiliary steel bar with two fixed discs. This steel bar was attached to the face of the concrete at the location of measurement until the temperature of the bar was identical to that of the concrete. To convert the temperature strain of the auxiliary steel bar to the temperature strain of concrete we multiply the former by the ratio of the coefficient of expansion of concrete to that of steel.

6.8 CAMBER GROWTH

Camber was measured immediately after the girder was removed from the form and periodically thereafter. Measurements were taken daily in the early age and the interval has been gradually lengthened to approximately once a month.

Measurement of camber was made simply by a long piano wire and a scale. The piano wire was stretched tightly from both ends of the girder by hooks and weights. Measurements were made at four locations, namely under the two stems and under the tips of the two overhanging flanges.

7. TEST PROGRAMS AND PROCEDURES

7.1 GIRDER 2

7.1.1 Initial Static Test

The initial static test program for Girder 2 to study the flexural and torsional stiffnesses of the girder was summarized in Table 2. The test procedures could be divided into three parts:

(1) Static test of Uncracked Girder (load stages 1 to 26)

(2) Cracking of the girder (Looad stages 27 to 51)

(3) Static Test of Cracked Girder (Load stages 52 to 76)

In the uncracked static test, the 26 load stages can be divided into six groups:

(a) Apply superimposed dead load (load stages 1 to 5)

(b) Apply bending moments with increment of 6 kips for P_1 and P_2 (load stages 6 to 11)

(c) Apply torsional moments with increment of 15 k-ft. i.e., 3 kips force times 5 ft. level arm. (load stages 12 to 17).

(d) Unload torsional moments with decrement of 30 k-ft. (load stages 18 to 20).

(e) Unload bending moments with decrement of 12 kips for P_1 and P_2 (load stages 21 to 23).

(f) Unload superimposed dead load (load stages 24 to 26).

After the uncracked static test, Girder 2 was cracked. This process was made with small load increments because crack length was very sensitive to loads shortly after cracking. Initial cracks were found at the crack formers (where the SR4 strain gages were located) at load stage 29. The actual P_1 and P_2 were 47.5 kips each and the

crack width were less than 0.001 in.. Normal cracking in the constant moment region between the hold-down points occurred at load stage 35, with $P_1 = P_2 = 55.7$ kips. These loads correspond to a modulus of rupture of about 350 psi. The maximum crack width was 0.002 in.. The process to crack the girder was terminated at load stage 50 when the crack length reached 1.5 ft., $P_1 = 67.5$ kips, $P_2 = 66.0$ kips and the maximum crack width was 0.006 in.. A composite photo of the crack pattern at this load stage is shown in Figs. 21a and 21b. This crack pattern was chosen to satisfy three conditions: (a) The crack should extend above all the strands in the constant moment region in order to stabilize the strain measurements of the strands in the fatigue test. (b) The cracks should not be too long, because the high sensitivity of cracks at this load stage was desirable to study the crack propagation in the fatigue test. (c) Cracks should have started outside the constant moment region. This critical region just outside the load points P_1 and P_2 (see Fig. 11) are subjected to large shear and moment and therefore should be carefully observed.

The third part of the initial static tests from load stages 52 to 76 was identical to the first part from load stages 1 to 26. These later load stages produced flexural and torsional stiffness for cracked section.

7.1.2 Flexural Fatigue Test

Girder 2 was subjected to 6.02 million cycles of dynamic load according to Fisher's equivalent Test Spectrum B at a frequence of approximately 2.5 cycles/sec. The target fatigue test program was given in Table 3. However, the actual fatigue program was somewhat different as recorded in Table 4. The differences were due to the change in midtest from a 7-million cycle program to the 6-million cycle. It was also caused

by the equipment instability of the MTS controller. A comparison of the target and actual test program was given in Fig. 22. The two programs should be equivalent according to Minor's Hypothesis of cumulative damages.

The 6-million cycle test program as suggested by Fisher et al[12] consisted of 3.2-million cycles of 100% crush live load plus impact according to design criteria (5) and 2.8-million of normal full load (89.1% of crush live load) plus impact according to design criteria (4). The torsional moments due to 10% nosing and 13.5 mph wind were also imposed on the girder. It was assumed that half of all torsional moments were positive and half were negative. The combination of two levels of vertical loads and the two directions of torsional moments resulted in four loading conditions I, II, III and IV, listed in Tables 3 and 4.

Table 3 showed that both load conditions I and II were split into two equal parts, one at the beginning and one at the end of the test. In other words, the heavily-loaded stem will receive the maximum P_1 load of 53.9 kips both at the beginning and at the end of the fatigue test. Such test history should be conservative if the load history has an effect on the fatigue strength as some investigators have suggested.

The load history was designed to minimize the number of changes of the load eccentricity, while maintaining some dispersion of the four load conditions. This test program required only three changes of the load eccentricity. (See Fig. 12)

It should also be noted that the superimposed dead loads should be simulated by P_1 = 12.9 kips and P_2 = 7.6 kips. However, these were

changed to P_1 = 12.0 kips and P_2 = 8.5 kips in load condition I to maintain a constant load eccentricity of 5 in.. This increases slightly the stress range in the heavily-loaded stem and, therefore, should be conservative. Similar justifications should apply to the other three load conditions.

In the fatigue test, dynamic correction must be made to account for the inertia of the girder. Dynamic loads were controlled such that the deflection produced due to cyclic loading corresponded with the measured minimum and maximum static deflections. The dynamic deflections were measured by LVDT's (Linear Variable Differential Transformer) at midspan. Repetitive load varied sinusoidally from minimum to maximum. Loads and deflections were monitored periodically throughout the test; also, the static tests were repeated to establish the effect of creep deflection.

7.1.3 Flexural Derailment Test

The derailment test program for Girder 2 is summarized in Table 5. Loads P_1 and P_2 were calculated such that these loads, combined with the self weight of the girder, simulated the required factored self and superimposed dead loads. Loads P_1 and P_2 were first applied and maintained constant throughout the test. The factored derailment load (see Fig. 11) was then applied by varying P_3 in the following sequences:

(a) P_3 was loaded in four increments up to 57.8 kips, (load stage 9, 10) corresponding to the unfactored, derailment load (=2 times the crush live load) and the design criterion (7). It was then unloaded to find the residual cracking deflections and rotations as a measure of the serviceability of the girder after a severe derailment.

(b) Repeat (a) for second cycle.

(c) P_3 was loaded in increments up to 80.9 kips (load stage 26), corresponding to factored derailment load (2.8 times the crush

(c) continued

live load and the design criterion (8),) and then unloaded to find the residual deformations.

(d) P_3 was loaded in increments to 131 kips (load stage 43-45), corresponding to 28 in. deflection of the heavily-loaded stem. The load was taken as the ultimate load which was 60% higher than the required ultimate (factored) derailment load (= 4.5 times the crush live load.)

In the derailment test, the loads, deflections, rotations and strand strains were recorded after each increment. Crack pattern was traced on the heavily-loaded stem on one end diaphragm at selected load stages. Photographs were also taken for the final crack pattern. The maximum crack widths at selected load stages were also recorded.

7.2 GIRDER 3

7.2.1 Torsional Fatigue Test

Before the torsional fatigue test, Girder 3 was first cracked by a load system shown in Fig. 15b. The loads $P_1 = P_2$ were applied by two MTS actuators, while the two loads P_5 was achieved by an auxiliary system of cross heads and tie rods. The sequence of loading to crack the girder is given in Table 6. The midspan deflections were also measured by potentiometers and were recorded in the Table. The pattem of cracking was photographed and produced in Fig. 22A. The maximum crack length was about two feet.

Girder 3 was subjected to 5.05 million cycles of loadings according to Fisher's equivalent test Spectrum C, at a frequency of 4.0 cycles per second. The test program was shown in Table 7. It can be seen that all load cycles were 100% crush live load plus impact according to design criteris (5). These were divided equally into load conditions I & II

7.2 continued

assuming that half of all the torques were positive and half were negative. The fatigue test began and ended with load condition I, which is the more severe case for the heavily-loaded stem.

The stimulated superimposed dead loads for Girder 3 should be P_1 = 11.6 kips and P_2 - 4.8 kips. These were adjusted slightly so that a constant eccentricity could be maintained within each load condition.

7.2.2 Torsional Derailment Test

The derailment test program for Girder 3 is summarized in Table 8. As for girder No. 2, loads P_1 and P_2 stimulating the factored dead loads were first applied and then maintained constant throughout the test. The derailment load P_3 was then added in two steps:

(a) P_3 was first loaded in small increments up to 58.2 kips (load stages 16, 17; Table 8) corresponding to the unfactored derailment load (=2 times the crush live load.) It was then unloaded to find the residual deflections and rotations as a measure of the serviceability of the girder after a severe derailment.

(b) P_3 was applied in increments to 146.1 kips (load stage 47, Table 8) corresponding to 5.0 times the crush live load which represented 78.5% excess over the required (ultimate) factored derailment load.

In the derailment test, the loads, deflections, rotations and stirrup strains were recorded after each increment. Crack patterns were traced on the outside face of the heavily-loaded stem, on the heavily-loaded end diaphragm and on midspan diaphragm. Photographs were taken for the final crack pattern and the maximum crack widths were recorded at some selected load stages

8. TEST RESULTS AND ANALYSIS

8.1 GIRDER 1

8.1.1 Loss of Prestress

Loss of prestress in Girder 1 was given for the first 180 days in Fig. 23. It could be seen that the measurements made by Demec and Whittemore gages were very close. Loss of prestress increased very rapidly up to 13% in the first three or four days and then slowed down to approach the theoretical 23% loss asymptotically.

A comparsion of the experimental prestress loss with the theoretical prediction was shown in Fig. 24. This figure indicated that the experimental value was slightly higher than the theoretical value in the early age and that this trend was reversed in the later age. In general, however, the correlation between theory and test was good.

8.1.2 Camber Growth

The growth of camber for Girder 1 was plotted in Fig. 25. It includes both the measured cambers and the theoretically predicted cambers. It could be seen that the measured cambers were approximately 7% less than the predicted cambers after about one month of age.

8.2 GIRDER 2

8.2.1 Natural Frequencies

The natural frequencies of the uncracked Girder 2 were measured in flexure and in torsion before the initial static test. The girder has been set-up on the supports as shown in Fig. 9 (without the loading systems and without tightening the hold-down rods at support). Two LVDT's were installed at midspan near the north and south edges

of the flanges to monitor continuously the vertical deflection during vibration. The vibration was started by a sudden impulse and was recorded by a Hewlett-Packard strip chart recorder operating at a speed of 2 inches per second. A sinusoidal curve was obtained, from which the natural frequencies were determined.

The natural frequency in flexure was obtained by applying a vertical impulse at midspan, so that the girder vibrated in a vertical direction. The natural frequency was measured to be 4.6 cycles per second. This is very close to the calculated theoretical value of 4.45 using the following equation

$$f = \frac{\pi}{2\ell^2}\sqrt{\frac{EI}{m}}$$

where E = modulus of elasticity of concrete (3,850 ksi)

I = transformed moment of inertia (813,731 in^4)

m = mass per unit length = w/g, where w is the weight per unit length (2.3 kips/ft.) and g is 32.2 ft/sec^2.

ℓ = span of beam (78.5 ft.)

The natural frequency in torsion was obtained by applying a horizontal impulse at the bottom of the stem at midspan. This created a torsional vibration about the shear center, which was picked up by the vertical LVDT's. The horizontal vibration, however, was ignored by the vertical LVDT's. In this way, the natural frequency in torsion was found to be 9.2 cycles per second.

The theoretical natural frequency in torsion can be calculated by the following equation, if the warping torsional resistance is ignored:

$$f = \frac{1}{2\ell}\sqrt{\frac{GC}{i}}$$

where G = modulus of rigidity of concrete (1,610 ksi)

C = St. Venant torsional constant (76,235 in.^{4})

i = moment of inertia of mass per unit length

= $(\gamma/g)\, I_p$, where γ is the unit weight (139 lb/cu.ft) and I_p is the polar moment of inertia about shear center (254.4 ft.^{4})

ℓ = clear span between end diaphragms (75'-2").

This equation gives a theoretical natural frequency of 5.9 cycles per second. Comparing this value with the measured frequency (9.2 cycles per second) shows that the warping torsional stiffness has greatly increased the torsional natural frequency of the girder.

8.2.2 Initial Static Load

8.2.2.1 Vertical Deflections - Midspan deflections at the center line were plotted as a function of truck loads from load stages 5 to 11 in Fig. 26. (See Table 2 for load stages). At these load stages of the uncracked girder, the behavior was elastic.

A theoretical straight line was also included in Fig. 26. This line was derived from the well-known flexural theory using (a) the transformed section at midspan for the moment of inertia, I and (b) the actual modulus of elasticity of concrete, E_c, measured from standard concrete cylinders (see Fig. 5). E_c was taken as the secant modulus at the stress level of 0.1 f'_c. (see Fig. 6). At this stress level, $E_c = 0.76\ (57{,}000\sqrt{f'_c})$, where a

reduction factor 0.76 was incorporated into the ACI Code expression.

Comparison of the theoretical straight line with the test data showed excellent correlation. The elastic stiffness was found to be 101 kips/in. At a truck load of 72 kips, corresponding to crush live load plus impact, the midspan deflection was 0.71 in.

A curve for loads vs. midspan deflections was also given for cracked girder in Fig. 27. This curve, which was obtained from load stages 55 to 61, remained straight (i.e. elastic). Fig. 27 showed that the flexural stiffness of cracked girder was 97 kips/in. This was 4% lower than that for the uncracked section. At a truck load of 72 kips the midspan deflection was 0.74 in.

Deflections along the girder axis were shown in Fig. 28 for both the uncracked and the cracked sections. In view of symmetry, the former was plotted on the left half-span while the latter on the right. The experimental curves of all six load stages were included. Two load stages, namely 47.6 kips and 71.8 kips for the uncracked section, were chosen to compare with the theoretical curves. It could be seen that the correlation was excellent throughout the girder.

8.2.2.2 Torsional Rotations - Midspan torsional rotation was plotted as a function of truck torque from load stages 11 to 17 in Fig. 29. At load stage 17, the girder was uncracked (see Table 2).

Three theoretical curves were also included in Fig. 29 for (a) rigid end diaphragms (100% warping restraint), (b) no end diaphragms (zero warping restraint), and (c) 22 in. thick end diaphragms. 22 in. was the average thickness of a dapped end diaphragm shown in the insert in Fig. 29. This simplification was necessary because the computer program was written to treat only

uniform end diaphragms.[1,5] In the analysis the span of girder was taken as 75 ft. 2 in., the net span of the girder between the inner faces of end diaphragms. The St.-Venant torsional constant, C, and the warping moment of inertia, I_w,were assumed to be uncracked and non-transformed. The modulus of rigidity was taken as $G_c = E_c/2(1+\mu)$, where $\mu = 0.2$ and $E_c = 0.76\ (57{,}000\sqrt{f'_c})$.

The two theoretical curves for rigid end diaphragms and for no end diaphragms provided the upper and lower limits for the test curves. The test curve, however, had a slope (torsional stiffness) 6% greater than the theoretical curve with 22 in. thick end diaphragms. This small difference may be caused by the following three reasons: (1) the average thickness of 22 in. may have underestimated the stiffness of the dapped end diaphragm, because the torsional stiffness of the diaphragm is proportional to the third power of the thickness. (2) the effect of reinforcement was neglected in assuming a non-transformed section for St.-Venant torsional constant C, and warping moment of inertia, I_w. (3) The Poisson's ratio $\mu = 0.2$ may have been assumed too high.

The midspan rotations obtained from tests in Fig. 27 and the corresponding differential deflections at midspan are given below for the three design criteria (1), (2) and (3).

DESIGN CRITERIA (see page 3)	(1) Normal Service Load Tangent Track	(2) Abnormal Service Load, Tangent Track	(3) Abnormal Service Load, Curved Track
TORQUE/TRUCK (kip-ft.)	31	63	90
MIDSPAN ROTATION (deg.)	0.033	0.067	0.095
DIFF. DEFLECTION (in.)	0.035	0.070	0.099

The above table shows that when a girder of tangent track is subjected to normal and abnormal service loads, the differential deflection at midspan would be 0.035 in. and 0.070 in. respectively. These deflections were less than 5% and 10%, respectively, of the deflections under vertical service loads. Such negligible rotations due to lateral loads should ensure the rider's comfort.

Loads vs. midspan rotation curve was also given for cracked girder in Fig. 30. This curve was derived from load stages 61 to 67. It showed that the torsional stiffness after cracking was identical to that before cracking. Apparently the prestress had closed up the flexural cracks and the girder behaved as though it had never been cracked.

Torsional rotations along the girder were given in Fig. 31, for both the uncracked and the cracked sections. The curves for the uncracked section was plotted on the left half-span while those for cracked section on the right half-span. Two load stages, namely 58.8 kip-ft. and 91.9 kip-ft. for the uncracked section, were chosen to compare with the theoretical curves (22 in. diaphragms). The correlation was quite satisfactory, but appeared to be better at 1/6 and 1/3 span than at midspan.

8.2.3 Flexural Fatigue Tests

8.2.3.1 Stiffness - During the fatigue test, the test was stopped from time to time so that the static deflections could be measured. It was found that the static deflection at the end of the test was very close to that at the beginning. In other words, no apparent deterioration of the stiffness was observed.

8.2.3.2 Cracks -The crack width of the largest crack was monitored throughout the test. In the beginning of the fatigue test the crack

width was measured to be 0.001 in. under load condition I. This crack width remained essentially the the same at the end of the fatigue tests under the same load condition I.

8.2.3.3 Strains in Strands - The stress ranges in the prestressed strands were measured during the last half of the fatigue tests for load conditions I and IV and were recorded in the following Table. Both these load conditions have $(P_1 + P_2)$ min = 20.5 kips and $(P_1 + P_2)$ max = 92.5 kips. The only difference was the load eccentricity indicated in the Table.

LOAD CONDITION	ECC.	STEM	STRESS RANGE (ksi) *	AVE
IV	1.5 in. NORTH	SOUTH	6.4-7.3	6.7
		NORTH	5.8-8.7	7.1
I	5.0 in. SOUTH	SOUTH	5.8-6.9	6.3
		NORTH	4.7-8.0	6.1

*4 strand measurements were used in the south stem while 11 were used in the north stem.

A theoretical flexural analysis has also been carried out on Girder 2 to find the relationships among moment, curvature, steel strands from zero load to failure. The tedious analysis utilized a trial and error method to satisfy simultaneously the three conditions, namely equilibrium, compatibility and stress-strain curves. The actual stress-strain curves of prestressed strands and concrete were used. The stress-strain curve of concrete was very closely approximated by a second-order parabola. This analysis showed that under a load range from $(P_1 + P_2)_{min}$ = 20.5 kips to $(P_1 + P_2)_{max}$ = 92.5 kips, the stress range of the strands should be

7.0 ksi.

The theoretical stress range of 7.0 ksi should be compared with the measured stress range shown in the above table. It can be seen that the measured stress ranges compared very well under load condition IV. The measured stress ranges were somewhat smaller than the theoretical prediction, however, in load condition I. This discrepency was probably due to the difficulties of installing strain gages on prestressed stands and the instability of the MTS actuators during this period of testing.

8.2.4 Flexural Derailment Test

8.2.4.1 Vertical Deflections - The midspan deflections at the center line of girder 2 were plotted as a function of axle loads in Figs. 32a and 32b. Fig. 32a magnifies the strains and showed clearly the three unloading cycles and their resulting residual deflections. The measured curve should also be compared to the elastic theory for uncracked section. Hence, the ratios of the measured deflection to the uncracked theoretical deflection and the residual deflections were given below for the three design load stages.

Load	$\frac{\text{Meas. Defl.}}{\text{Uncr. Theo. Defl.}}$	Residual Deflection (in.)
Crush Live Load	1.06	
Unfactored Derailment (2 x Crush Live Load)	1.46	0.09, 0.11
Factored Derailment (2.8 x Crush Live Load)	2.17	0.22

The above table shows that at a load of 2 times the crush live load, corresponding to design criterion (7), the midspan deflection at

center line was only 46% greater than that predicted by the elastic theory for uncracked section and the average residual deflection was about 0.10 in.

Fig. 33 showed the deflections along the center-line axis. Due to symmetry, only half of the span was measured for each load stage. Four load stages were plotted namely, 1 times, 2 times, 2.8 times and 3.8 times the crush live load. The measured deflections under crush live load were compared with the theoretical curve for uncracked section. The correlation was satisfactory throughout the girder.

In a similar way, the midspan deflections of the heavily-loaded stem were plotted as a function of axle loads in Figs. 34 and 35. Fig. 34 showed that the residual deflections under 2 times the crush live load and 2.8 times the crush live load were 0.14 in. and 0.36 in. respectively, Fig. 35 also showed that the test terminated when the midspan deflection of the heavily - load stem reached 28 in. The deflections along the heavily-loaded stem were recorded in Fig. 36 for the four load stages designated.

8.2.4.2 Torsional Rotations - The midspan rotations of Girder 2 were plotted as a function of axle torques in Figs. 37 and 38. A theoretical straight line based on uncracked section was also included in these figures. The ratios of the measured rotations to the theoretical rotations were given below for the three design load stages. The residual rotations of the three unloading cycles were also included.

Load	Meas. Rotation / Uncr. Theo. Rotation	Residual Rotation (deg.)
Crush Live Load	1.0	-
Unfactored Derailment Load (2 x Crush Live Load)	1.49	0.045, 0.047
Factored Derailment Load (2.8 x Crush Live Load)	2.43	0.17

The above table showed that at a load of 2 times the crush live load, corresponding to design criterion (7), the midspan torsional rotation was only 49% greater than that predicted by theory for uncracked section. The residual rotation at this load was only about 0.046 degree, corresponding to a differential stem deflection of 0.049 in.. Fig. 38 also showed that the test was terminated when the midspan rotation reached 6.8 degrees.

Torsional rotations along the girder were recorded in Fig. 39. Only half of the span was measured because of symmetry. Four load stages were plotted. The measured rotations under crush live load were compared with the theoretical curve for uncracked section. The correlation was found to be excellent.

In view of the small residual deflections and rotations under severe derailment load, it can be concluded that the girders should remain serviceable even after the derailment of vehicle, as defined in the Load Criteria.

8.2.4.3 Ultimate Load - The ultimate load was determined from Figs. 32b and 35 to be 131 kips. When this load was reached and maintained constant, deflection and rotation continued to increase . The test was discontinued when the maximum deflection under the heavily-

loaded stem was 28 in. and the maximum rotation was 6.8 degrees. The termination was necessary, because (1) the gaps at the ends of the girders between the bottom corner and the support blocks were exhausted due to elongation of the bottom fibers, and (2) the vertical tied rods for P_1 was touching the inner face of the heavily load stem and the tie rods for P_3 was dangerously bent above the slab on top of the cross heads. The large deformation of the girder at ultimate load was shown in Fig. 14.

The ultimate load of P_3 = 131 kips corresponds to 4.5 times the crush live load. This load is 2.25 times the severe derailment load (design criterion (7)) and 1.61 times the factored derailment load (design criterion (8)).

8.2.4.4 Strains in Strands - The strains measured in the prestress strands were plotted as a function of axle load P_3 in Fig. 40. Those measurements in the south stem (or heavily loaded stem) were indicated by squares while those in the north stem by circles. These experimental measurements were compared to the theoretical curve based on a sophiscated flexural analysis described in 8.2.3.3. It can be seen that the trend of the experimental points is very well described by the theoretical curve. Fig. 40 also showed that the strains in the south stem were greater than the theoretical prediction, while those in the north stem were less. This clearly showed the effect of torsional moments in the derailment tests.

8.2.4.5 Crack Development - A general view of Girder 2 under derailment load has been given in Fig. 14. The cracking pattern of the heavily-loaded stem were photographed along the girder in sections and a composite picture was shown in Fig. 41. The process of crack development in the derailment test was as follows: The vertical

flexural cracks was observed to have reopened at stage 6 when P_3 = 45.8 kips (see Table 5). The maximum crack width began to develop and reached 0.008 in. at P_3 = 58.9 kips (2 times crush live load). It continued to increase to 0.019 in. when P_3 = 80.9 kips (2.8 times crush live load). At load stage 25 (P_3 = 67.4 kips) flexural shear cracks began to develop outside the load points in the vicinity of the quarter points. This was followed by the web shear cracks near the supports when the load reached P_3 = 82.6 kips.

It can be seen from Fig. 41 that all the cracks are well distributed, resulting in small crack width. In terms of cracking the girder behaved admirably in general. There was one crack at midspan, however, that required examination. This crack began to open very rapidly when P_3 reached 106 kips and eventually caused the failure of the girder. This phenomenon was apparently caused by stress concentration of the midspan diaphragm and will be discussed in the next section 8.2.4.6.

8.2.4.6 Midspan Diaphragm - Figs. 42a and b show an interesting observation; i.e. the development of horizontal cracks in the stem at midspan below the bottom face of the diaphragm. These horizontal cracks started to develop rapidly at P_3 = 106 kips and destroyed the bond between the strands and the surrounding concrete. As a result, the girder behaved like an unbonded girder in this region, and one vertical flexural crack could widen very rapidly.

The cause of the horizontal cracks is explained in Fig. 43. When one stem of a double-tee girder is subjected to a concentrated load, part of this load must be transferred to the other stem by

the midspan diaphragm. In other words, the diaphragm exerts an upward shear on the stem being loaded. This shear stress created vertical tension just below the bottom face of the diaphragm and produced the observed horizontal cracks.

No cracks were found in the midspan diaphragm itself throughout the test. However, a fine crack was observed between the diaphragm and the heavily loaded stem at high loads near ultimate.

8.2.4.7 End Diaphragms - The diagonal torsional cracking of one end diaphragm is shown in Fig. 44. The cracking of the stem at the junction with the inner face of an end diaphragm is shown in Fig. 45. This typical cracking is produced by the differential bending of the two stems (or warping torsion). Since these cracks occurred at loads beyond the design derailment load (i.e. 2 times the crush live load), they satisfy completely the serviceability requirements.

8.2.4.8 Sectional Deformation - No appreciable changes of the cross sectional contour were observed until the load P_3 exceeded 100 kips. This statement was true for both the cross sections measured, namely, at quarter span and at 10 ft from midspan. At load approaching failure, the change of the sectional contour appeared to be irratic and therefore was not reported herein.

8.2.4.9 Construction Details - Cracks at the reentrant corners started at load stage 25 (P_3 = 67.4 kips). Since this is the same load stage when flexural shear cracking occurred near the support, it appeared that the reentrant corner did not cause any premature cracking. The crack widths at the reentrant corners also remained small throughout the derailment test. No distresses whatsoever were observed at the hold-down points.

8.3 GIRDER 3

8.3.1 Torsional Fatigue Tests

8.3.1.1 Stiffness - Static deflections were taken from time to time during the period of the fatigue test. No change of stiffness was found throughout the test.

8.3.1.2 Cracks - Cracking of the girder prior to fatigue test produced flexural cracks in the stems (Fig. 22A) and one 5 in. long inclined crack (about 25 deg. to horizontal) at the reentrant corner of the dapped end. All these cracks did not propagate during the fatigue test.

8.3.1.3 Strains in Stirrups - The strains of two stirrups were monitored periodically throughout the fatigue test. The gages were placed at No. 1 and No. 2 location on the outer leg of stirrup in the heavily-loaded stem. (see Fig. 19) Since these stirrups are located nearest to the support and the gages are on the face where torsional stress and shear stress are additive, the measured strains should be critical. The very small strains observed in these stirrup legs during the test indicated that the concrete had not been cracked.

8.3.2 Torsional Derailment Test

8.3.2.1 Vertical Deflections - The midspan deflections at the center line of Girder 3 was plotted as a function of axle loads in Figs. 46 and 47. Fig. 46 shows the unloading cycles after loading to 2 x the crush live load (design criterion (7)) and the resulting residual deflections. The residual deflections were 0.070 in. immediately after unloading and 0.049 in. after 1.3 hours. A theoretical curve based on elastic analysis of uncracked section was also included in Figs. 46 and 47. This theoretical curve coincided with the measured curve

well beyond the crush live load. At 2 x the crush live load (unfactored derailment load) the measured midspan deflection was only 5% greater than the theoretical value for uncracked girder.

Fig. 48 showed the deflections along the longitudinal centerline axis of Girder 3. Curves were plotted for three load levels at 1.0 times, 2.0 times and 2.8 times the crush live load. Comparison of the test curves and the theoretical curves showed that the agreement was good throughout the girder at the first two load levels. It should be pointed out that the curves were not symmetrical about midspan.

In a similar way, the midspan deflections of the heavily-loaded stem were plotted as a function of axle loads in Figs. 49 and 50. Fig. 49 showed that the residual deflections under 2 times the crush live load were 0.087 in. immediately after unloading and 0.057 in. after 1.3 hours. The deflections along the heavily-loaded stem were also recorded in Fig. 51.

8.3.2.2 Torsional Rotations - The midspan rotations of Girder 3 were plotted as a function of axle torques in Figs. 52 and 53. Fig. 52 gave the residual rotation of 0.024 in. after unloading from a load of 2 times the crush live load. This residual rotation did not decrease with the passage of 1.3 hours.

Figs. 52 and 53 also included a theoretical curve based on uncracked section and 22 in. thick end diaphragms. It can be seen that the measured torsional stiffness (slope of the curve) is 13% greater than the theoretical torsional stiffness. Comparing this error with the corresponding error of 6% in the initial static test of Girder 2 (Figs. 29 and 30), it appeared that the underestimation of the end

diaphragm stiffness discussed in 8.2.2.2 had a greater effect on Girder 3 than on Girder 2. Apparently, the stiffness of the end diaphragm had a greater strengthening affect on the torsional stiffness of the girder when the loads were applied close to the support (Girder 3) than when the loads were symmetrical about midspan (Girder 2).

The measured and theoretical torsional rotations along Girder 3 were plotted in Fig. 54, at three load levels. The unsymmetrical shape of the curves was evident, especially at high loads.

8.3.2.3 Ultimate Load - The test was terminated when the load P_3 reached 146 kips, corresponding to 5.0 times the crush live load. This load is 2.5 times the severe derailment load (design criterion (7)) and 1.78 times the factored derailment load (design criteria (8)). At this load level the midspan deflection of the heavily loaded stem was 7.5 in. (Fig. 50) and the midspan rotation was 2.8 degrees (Fig. 53). The stirrups in the most highly stressed region have also yielded. Figs. 59 to 61 showed the cracking condition at this load level. It should be noted that the ultimate capacity of Girder 3 has not yet been reached.

8.3.2.4 Strains in Stirrups - The stresses in the stirrups were summarized in Figs. 55 to 58. The location of the gages were given in Fig. 19. Fig. 55 gave the stresses in the outer legs of stirrups in the heavily-loaded south stem. It can be seen that three of the gages close to the support have yielded before termination of the test. The other five gages, further away from the support, have substantial stresses but did not yield.

Fig. 56 gave the stresses in the inside legs of stirrups in the heavily loaded south stem. The stresses in these stirrups were substantially less than the yield stress since the stresses due to shear and the stresses due to torsion are subtractive.

Fig. 57 showed the stresses in the outer legs of stirrups in the north stem. The stresses in these gages were very small. In other words, the shear and torsional capacity of this stem had barely been utilized.

Fig. 58 gave the stirrup stresses in the end diaphragm. The average stress was about 20 ksi, which was about one-third of the yield stress.

8.3.2.5 Crack Development - The previously induced vertical flexural cracks in the heavily-loaded south stem was observed to reopen at a load of P_3 = 51.3 kips. These cracks developed very slowly. The maximum crack widths was only 0.003 in. at P_3 = 58.2 kips (2 times crush live load), and became 0.010 in. at P_3 = 108.7 kips. Fig. 59 showed the flexural cracking pattern at 5.0 times the crush live load (2.5 times the severe derailment load). The cracks were well distributed and finely spaced.

The flexural shear crack started to spread at the high factored derailment load of P_3 = 80.9 kips (2.8 times crush live load). These cracks first occurred between the innermost load point and the midspan, and then spread toward the east support. Most of these shear cracks lied within the hold-down points where the stirrup spacing was 20 in. The crack widths of these shear cracks developed very rapidly, reaching 0.050 in. at P_3 = 108.7 kips and 0.090 in. at P_3 = 139.6 kips. The cracking pattern of these shear

cracks in the vicinity of midspan was given in Fig. 60.

8.3.2.6 Re-entrant Corner of Dapped End - The pre-existing small crack (see Section 5.2.1) at the re-entrant corner of the dapped end first re-opened at a low load of P_3 = 14.4 kips with a maximum crack width of 0.002 in.. This maximum crack width, however, increases very slowly and reached only 0.005 in. at the derailment load of P_3 = 58.2 kips. It was 0.011 in. at P_3 = 108.7 kips and 0.017 in. at P_3 = 140 kips. The cracking patterns are shown in Fig. 61a at P_3 = 58.2 kips (2 times crush live load) and in Fig. 61b at P_3 = 146.1 kips (5 times cruch live load).

8.3.2.7 Joint Between Stem and End Diaphragm - The joint crack between the stem and the end diaphragm was first observed at P_3 = 51.3 kips. This crack developed rapidly, and the crack width was recorded to be 0.010 in. at the derailment load of P_3 = 58.2 kips. At higher loading this crack continued to widen, reaching 1/8 in. at P_3 = 110 kips. This was accompanied by spalling of concrete and longitudinal splitting at the bottom of the stem. Figs. 62a and 62b showed the condition of this joint at 5 times crush live load or 2.5 times severe derailment load (P_3 = 146 kips).

8.3.2.8 End Diaphragm - The pattern of diagonal torsional cracking at the west end diaphragm is shown in Fig. 63 following the termination of test (P_3 = 146.1 kips). These cracks developed very slowly. The maximum crack width was 0.008 in. at the severe derailment load of P_3 = 58.2 kips. They became 0.015 in. at P_3 = 108.7 kips and 0.040 in. at P_3 = 139.6 kips.

8.3.2.9 Midspan Diaphragm - Midspan diaphragm was observed to develop torsional cracks only at the very high load of P_3 = 146.1 kips. This

was 5.0 times the crush live load. The cracking pattern on both sides of the diaphragm is shown in Fig . 64.

It should be noted that the local horizontal cracks in the stem at midspan, which was very prominent in Girder 2, (Figs. 42a and 42b) also existed in Girder 3. These local horizontal cracks are shown in Fig. 65. Their widths, however, were small.

8.3.2.10 Sectional Deformation - No appreciable deformation of the cross-sectional contour was observed until P_3 reached 80.9 kips. At the termination of the test at P_3 = 146.1 kips, the contour deformation was still very small.

9. BENDING AND PUNCHING TEST OF FLANGE SLAB

9.1 OBJECTIVES

An additional test was made on Girder 3 to study the bending and punching behavior of the overhanging flange slab under derailment condition. Two wheel loads, 7 ft.-6in. apart, were assumed to be located at a distance 8-1/4 in. from the edge of the flange, just inside the 7 in. wide curb. The bearing area of each wheel was assumed to be 2 in. by 8 in..

The purpose of this test was three-fold:

(1) To check the bending or punching capacity of the flange slab and the behavior of the flange under derailment design criteria (7) and (8).

(2) To check the validity of two equations proposed by Tudor Engineering Co. for the effective width E, over which a wheel load could be dispersed at the face of support of the overhanging flange. These two equations are:

$$E = 0.85\,x + 5.5' \leqslant 7.5' \qquad (9.1)$$

$$E = 1.4\,x + 2.2' \leqslant 7.5' \qquad (9.2)$$

where x is the distance in feet from the load to the face of supports and $1.75' < x < 3.0'$. The top bars (No. 5 at 8 in. spacing) in the overhanging flange of the test girders were calculated on the basis of Eq. (9.1). Using Eq. (9.2), however, the top bars would have to be increased to No. 6 at 8 in. spacing.

(3) To check the adequacy of the longitudinal distribution reinforcement provided in the overhanging flange.

9.2 TEST SET-UP AND INSTRUMENTATION

Two loading points, P_4, were established at sections G and H as shown in Fig. 66a. These load points, each representing one wheel load, were 7 ft. - 6 in. apart and were located 8-1/4 in. from the edge of the flange (Figs. 66b and 66c). The load at each point was transmitted to the slab through a 2 in. x 3 in. x 8 in. steel block with a bearing surface of 2 in. by 8 in.. The relative position of the steel block with respect to the curb and the reinforcement was given in Fig. 66d.

Each load was applied through a system of crossheads and tie rods (Fig. 67a) and was activated by a ram. The oil pressure for the two rams was supplied from the same pump to provide simultaneous loading of equal pressure. Each of the two loads was measured by a 50-ton precalibrated load cell. It was found that the two loads may differ as much as 11% due to friction in the rams and the hoses.

Deflections of the flange were measured by potentiometers each mounted on a steel tube connected rigidly to both stems of the girder as shown in Fig. 67b. A potentiometer was provided for each load point at approximately 5 in. from the center of the load point on the straight line connecting the two load points.

The loads and the deflections were recorded continuously by two x-y plotters.

9.3 TEST PROGRAM

Each wheel load P_4 was increased in increment with the target values of 5, 10, 15, 20, 25 and 28.9 kips. The last value was two times the crush live load according to the severe derailment criterion (7). The flange was then unloaded to find the residual deflection. Following

an hour of rest, the flange was reloaded in three steps to a target value of 28.9 kips.(Severe Derailment Load, Criterion 7). The load was further increased with small increments of 3 kips to 40.5 kips, or 2.8 times crush live load according to factored derailment criterion (8). Finally, the load was increased to failure.

9.4 TEST RESULTS

The test results were summarized in Table 9. The load-deflection relationship was plotted in Fig. 68 using the average value of the two loads and the average value of the two deflections. At a load P_4 = 20.9 kips, the very fine pre-existing cracks caused by torsional derailment test on top of the flange reopened. At a load P_4 = 26.0 kips new cracks on top of the flange began to develop in roughly concentric circles around the two loads. These cracks multiplied and widened to a maximum crack width of 0.005 in. and an average crack width of 0.004 in. at P_4 = 29.9 kips. This load corresponded approximately to 2.0 times the crush live load. After unloading, the residual deflection was about 20% and the maximum crack width was less than 0.001 in.

Reloading of the flange showed that the load-deflection relationship was quite linear up to P_4 = 29.7 kips (see Fig. 68). At this load crack widths were also the same as those before unloading. When the load was increased to P_4 = 41.7 kips, corresponding approximately to 2.8 times the crush live load, the average crack width became 0.010 in.

At P_4 = 44.6 kips cracks began to open on the bottom face of the flange. This crack developed inward about half way to the stem. Failure occurred abruptly and loudly by punching shear around load point H, at an average P_4 value of 47.1 kips. This failure load was 3.26 times the crush live load or 1.63 times the derailment load. After failure

at load point H, load point G was loaded individually until failure at P_4 = 51.3 kips. Failure was again due to punching shear. It was interesting to note that some ductility was observed before this abrupt failure. This apparent ductility might be caused by the deformation around the bearing area or might be due to the yielding of reinforcement in the slab. Fig. 69 showed the cracking pattern, and Figs. 70 and 71 showed the mode of failure at load points H and G. respectively.

9.5 SUMMARY STATEMENTS

(1) The flange was able to resist 1.6 times the severe derailment load (3.2 times crush live load). This capacity exceeded the design requirement of 1.4 times the severe derailment load. At the derailment load the cracking condition and the residual deflection were tolerable.

(2) Although the flange slab did not fail in bending, it is possible to state that Eq. (9.1) for the effective width is conservative. Consequently, the top bars of No. 5 at 8 in. spacing is adequate to satisfy the design criterion.

(3) The longitudinal distribution reinforcement appears to be satisfactory for the girder. Additional reinforcement is not expected to improve the behavior of the overhanging flange.

(4) The pre-existing cracks introduced during the derailment test of Girder 3 had very little effect on the results of the test.

10. CONCLUSIONS

1. The girders behave elastically both in flexure and in torsion well beyond the abnormal service load of 72 kips vertical load plus 63 kip-ft. torque per truck. At this load, the maximum midspan deflection was 0.71 in. and the maximum midspan rotation was 0.067 deg., corresponding to a differential stem deflection of 0.070 in. These small deformation should ensure rider comfort.
2. Introduction of flexural cracks due to accidental overload or environmental factors (secondary stresses) does not change the elastic behavior of the girders, both torsionally and flexurally, well beyond the abnormal service load level.
3. The flexural behavior of the girders can be accurately predicted by the well-known flexural theory, both before and after cracking. In this calculation the modulus of elasticity is taken as:

$$E_c = 0.76\ (57{,}000\ \sqrt{f'_c}\ )$$

The reduction factor 0.76 reflects the actual property of the Florida oolite concrete.

4. Torsional behavior of the girders in the elastic range can be reasonably predicted by Vlasov's elastic mixed torsion analysis, taking into account both the St.-Venant torsional resistance and the warping torsional resistance.
5. The natural frequencies of the girders are 4.6 cycles per second in flexure and 9.2 cycles per second in torsion. These natural frequencies are much higher than those of the vehicles.
6. Girder 2 and Girder 3 have been subjected to different test spectra of 6 million cycles and 5 million cycles, respectively, of dynamic loading, equivalent to 60 years of service life. No deteriorations whatsoever

have been observed in the girder in terms of flexural and torsional stiffnesses, crack propagation and stresses in the strands.

7. Under severe derailment load (crush live load with 100% impact and a maximum sideshift of 3 ft.), the maximum midspan deflection and rotation were 1.72 in. and 0.61 degree, respectively. These deformations were only 46% and 49%, respectively, greater than those predicted by the elastic theory. The residual deformations were also very small (0.11 in. for deflection and 0.047 degree for rotation). In other words, the girders remained serviceable after severe derailment.
8. The ultimate load of Girder 2 was 2.25 times the severe derailment load, or 1.61 times the factored derailment load (load factor of 1.4)
9. The stirrups were designed by the elastic mixed torsion analysis under abnormal service load and by the "post-cracking mix torsion analysis" under factored derailment load. This resulted in No. 4 bars at 10 in. spacing between the hold-down points and the points 3' - 3½" from support. This design was found by tests to be very conservative.
10. Prestress losses and cambers can be predicted to a reasonable accuracy. The small camber growth after installation of the rails is expected to improve rider comfort.
11. Cracks were very few in number and crack width very small at the re-entrant corners of the dapped ends, and at the end diaphragms under abnormal service load. No distresses whatsoever had been observed at the hold-down points.
12. The midspan diaphragm appears to have introduced local stress con-

centration in the stem resulting in local horizontal cracks and the opening of one large crack near ultimate. Since this process occurred at very high load near failure (1.9 times the severe derailment load), it did not detract from the generally excellent behavior of the girder.

13. It is recommended that the center diaphragm of the girder be retained for the Stage I construction of the Dade County Rapid Transit aerial guideway, since it may have contributed to the ultimate strength of the girder. However, future research is desirable to find out whether the midspan diaphragm can be eliminated for the Stage II construction.

14. The overhanging flange is able to resist 1.6 times the severe derailment load (3.2 times crush live load). The reinforcement provided in the flange of the test girder appears to be adequate.

15. In view of the observed separation between stem and end diaphragm at the joint, when the girder is subjected to derailment loading, it is recommended that all main reinforcement from the end diaphragm be extended into the stems with full anchorage.

11. RECOMMENDATIONS

The excellent behavior of the tested girders both in serviceability and in strength substantiated all the analysis and design methods used. The tests demonstrated conclusively that double-tee girders are viable standard girders for the aerial guideways of mass rapid transit systems. It is recommended, therefore, that this prestressed double-tee girder be an approved alternative for the aerial guideway for the Stage I construction of the Dade County Rapid Transit System.

12. REFERENCES

1. Hsu, T.T.C., "Torsion Analysis of Dade County Rapid Transit Aerial Guideways", Report to Kaiser Transit Group, April 12, 1977.

2. Hsu, T. T. C., "Torsion Tests of Double-Tee Girders for Dade County Rapid Transit Aerial Guideways", Report to Kaiser Transit Group, August 23, 1977.

3. PCI Design Handbook, Prestressed Concrete Institute, First Edition, 1971. Second Edition, 1978.

4. Dhondy, S. and Jaurequi, I., "Detailed Calculations of 79 ft. Effective Span Double-Tee Girders for Tangent Double Track". Internal Report of Kaiser Transit Group, Aug. 1977.

5. Hsu, T. T. C., "Computerization of Flexure and Torsion Design for Dade County Rapid Transit Aerial Guideways". Report to Kaiser Transit Group, May 29, 1978.

6. Vlasov, V. Z., "Thin Walled Elastic Beams", 2nd Edition, Moscow, 1958. Translated into English in 1961, available from the National Technical Information Service, U. S. Department of Commerce, Springfield, Virginia.

7. Zia, P. and McGee, D., "Torsion Design of Prestressed Concrete", Journal of the Prestressed Concrete Institute, Vol. 19, No. 2, March-April, 1974.

8. Zia, P. and Hsu, T. T. C., "Design for Torsion and Shear in Prestressed Concrete". Preprint 3424 ASCE Fall Meeting, Chicago, Oct. 16-20, 1978.

9. Givens, W., "Review of the Design and Producibility of Double-Tee Test Girders for Stage I - Rapid Transit System Metropolitan Dade County Transportation Improvement Program . Final Report to Kaiser Transit Group, Feb. 1979.

10. Collins, J. and Hsu, T. T. C., "Properties of Florida-Oolite Concrete". Journal of Testing and Evaluation. ASTM, Vol. 5, No. 3, March 1977.

11. Hanson, N. W., Hsu, T.T.C., Kurvits, O. A. and Mattock, A. H., Facilities and Test Methods of PCA Structural Laboraoty - Improvements 1960-65", PCA Development Department Bulletin, D 91, 28 pp. 1965.

12. Fisher, J. W., Hwang, T. and Slutter, R. G., "Selection of A Fatigue Load Test Spectrum for a Pretensioned Concrete Double-Tee Girder". Report to Kaiser Transit Group, March, 1978.

13. METRIC CONVERSION TABLE

MEASUREMENT	ENGLISH UNIT	METRIC UNIT
LENGTH	1 inch (in. or ")	2.540 centimeter (cm)
	1 foot (ft. or ')	0.3048 meter (m)
	1 yard (yd.)	0.9144 meter (m)
	1 mile (mi.)	1.609 kilometer (km)
AREA	1 sq. inch ($in.^2$)	6.452 sq. centimeter (cm^2)
	1 sq. foot ($ft.^2$)	0.09290 sq. meter (m^2)
	1 sq. yard ($yd.^2$)	0.8361 sq. meter (m^2)
	1 sq. mile (mi^2)	2.589 sq. kilometer (km^2)
VOLUME OR STATIC MOMENT	1 cu. inch ($in.^3$)	16.39 milliliter (ml) or cm^3
	1 cu. foot ($ft.^3$)	28.32 liter (l)
	1 cu. yard ($yd.^3$)	0.7646 cu. meter (m^3)
	1 ounce (oz.), U.S. Fluid	29.57 milliliter (ml) or cm^3
	1 gallon (gal.)	3.785 liter (l)
MOMENT OF INERTIA	1 $in.^4$	41.62 cm^4
	1 $ft.^4$	0.008631 m^4
SECTORIAL MOMENT OF INERTIA	1 $in.^6$	268.5 cm^6
	1 $ft.^6$	0.0008018 m^6
FORCE	1 pound (lb.)	4.448 newton (N)
		0.4536 kilogram force (kg-f)
	1 kilopound (kip or k)	4.448 kilonewton (kN)
	1 ton (200 lb.)	0.9072 metric ton (1000 kg)
DISTRIBUTED FORCE	1 lb./ft. (plf)	14.59 N/m
	1 kip/ft. (klf)	14.59 kN/m
	1 lb./in. (pli)	175.1 N/m
STRESS	1 $lb./in.^2$ (psi)	6.895 kN/m^2
	1 $kip/in.^2$ (ksi)	6.895 MN/m^2
	1 $lb./ft.^2$ (psf)	47.88 N/m^2
	1 $kip/ft.^2$ (ksf)	47.88 kN/m^2
DENSITY	1 $lb./ft.^3$	0.1571 kN/m^3
MOMENT	1 lb.-in.	0.1130 N-m or 1.152 kg-cm
	1 lb.-ft.	1.356 N-m or 13.83 kg-cm
	1 kip-in (k-in.)	0.1130 kN-m or 11.52 kg-m
	1 kip-ft. (k-ft.)	1.356 kN-m or 138.3 kg-m
TEMPERATURE	1°Fahrenheit (°F)	(°F-32)/1.8 Celsins (°C)

Table 1. LOCATIONS OF VERTICAL TRANSLATION MEASUREMENTS

GIRDER	TEST	SECTION	POINT
2	INITIAL STATIC AND DERAILMENT	WEST DIAPH	2 4
		A-A	1, 2, 3, 4, 5
		B-B	1, 2, 3, 4, 5
		C-C	1, 2, 3, 4, 5
		EAST DIAPH	2 4
	FATIGUE	WEST DIAPH	3
		C-C	1 3 5
		EAST DIAPH	3
3	DERAILMENT	WEST DIAPH	2 4
		A-A	2 4
		B-B	2 4
		C-C	2, 3, 4
		F-F	2 4
		EAST DIAPH	2 4
	FATIGUE	WEST DIAPH	2
		C-C	2 4
		EAST DIAPH	2

TABLE 2 INITIAL STATIC TEST PROGRAM - GIRDER 2

LOAD STAGE	UNCRACKED STATIC TEST			REMARK	LOAD STAGE	CRACK GIRDER		LOAD STAGE	CRACKED STATIC TEST			REMARK
	P_1 (k)	P_2 (k)	T (k-ft)			P_1 (k)	P_2 (k)		P_1 (k)	P_2 (k)	T (k-ft)	
1,2	0	0		APPLY S.D.L.	27	0	0	52	0	0		APPLY S.D.L.
3	4.3	2.5			28	46	46	53	4.3	2.5		
4	8.6	5.1			29*	48	48	54	8.6	5.1		
5	12.9	7.6			30	50	50	55	12.9	7.6		
6	18.9	13.6		FLEXURAL TEST (6 KIPS INCREMENT)	31	52	52	56	18.9	13.6		FLEXURAL TEST (6 KIPS INCREMENT)
7	24.9	19.6			32	53	53	57	24.9	19.6		
8	30.9	25.6			33	54	54	58	30.9	25.6		
9	36.9	31.6			34	55	55	59	36.9	31.6		
10	42.9	37.6			35**	56	56	60	42.9	37.6		
11	48.9	43.6	0		36	57	57	61	48.9	43.6	0	
12	51.9	40.6	15	TORSION TEST (15k-FT INCREMENT)	37	58	58	62	51.9	40.6	15	TORSION TEST (15k-FT INCREMENT)
13	54.9	37.6	30		38	59	59	63	54.9	37.6	30	
14	57.9	34.6	45		39	60	60	64	57.9	34.6	45	
15	60.9	31.6	60		40	61	61	65	60.9	31.6	60	
16	63.9	28.6	75		41	62	62	66	63.9	28.6	75	
17	66.9	25.6	90		42	63	63	67	66.9	25.6	90	
18	60.9	31.6	60	UNLOAD TORQUE	43	64	64	68	60.9	31.6	60	UNLOAD TORQUE
19	54.9	37.6	30		44	65	65	69	54.9	37.6	30	
20	48.9	43.6	0		45	66	66	70	48.9	43.6	0	
21	36.9	31.6		UNLOAD VERT.LOAD	46	67	67	71	36.9	31.6		UNLOAD VERT.LOAD
22	24.9	19.6			47	0	0	72	24.9	19.6		
23	12.9	7.6			48	0	0	73	12.9	7.6		
24	8.6	5.1		UNLOAD S.D.L.	49,50***	67	67	74	8.6	5.1		UNLOAD S.D.L.
25	4.3	2.5			51	0	0	75	4.3	2.5		
26	0	0						76	0	0		

*Cracking at stress raiser; $P_1=P_2=47.5^k$; Max. crack width $< 0.001"$

**Cracking in flexural region; $P_1=P_2=55.7^k$; Max. crack width $\simeq 0.002"$

***Crack length reach 1.5 ft; $P_1=67.5^k$, $P_2=66.0^k$; Max. crack width $\simeq 0.006"$

TABLE 3 TARGET FATIGUE TEST PROGRAM - GIRDER 2

(6-MILLION CYCLE)

LOAD CONDITION	LOAD CYCLE (MILLIONS)	P_1 (KIP)	P_2 (KIP)	REMARK		
				CLL+I	TORQUE	LOAD ECC. (IN.)
I	0.800	12.0[1] 53.9	8.5[1] 38.6	100%[2]	+(N+W)[3]	5.0 S
II	0.700	12.0 49.4	8.5 35.1	89.1%	+(N+W)[4]	5.0 S
III	1.400	9.8[1] 40.4	10.7[1] 44.1	89.1%	-(N+W)	1.3 N
IV	1.600	9.7[1] 43.9	10.8[1] 48.6	100%	-(N+W)	1.5 N
II	0.700	12.0 49.4	8.5 35.1	89.1%	+(N+W)	5.0 S
I	0.800	12.0 53.9	8.5 38.6	100%	+(N+W)	5.0 S
	6.000					

[1]Superimposed Dead Loads should be simulated by $P_1 = 12.9^k$, $P_2 = 7.6^k$, but were changed to maintain a constant load eccentricity indicated.

[2]CLL + 25% impact gives $P_1 = P_2 = 36^k$

[3]10% nosing + 13.5 MPH wind = 25^{k-ft}

[4]10% nosing + 13.5 MPH wind = 22.5^{k-ft}

TABLE 4. ACTUAL FATIQUE TEST PROGRAM - GIRDER 2

LOAD CONDITION	LOAD CYCLES (MILLIONS)	P_1 (KIP)	P_2 (KIP)	REMARK		
				CLL+I	TORQUE	LOAD ECC.(IN.)
I	0.610	12.0 53.9	8.5 38.6	100%	+(N+W)	5.0 S
II	1.081	12.0 49.4	8.5 35.1	89.1%	+(N+W)	5.0 S
III	1.196	9.8 40.4	10.7 44.1	89.1%	-(N+W)	1.3 N
IV	1.632	9.7 43.9	10.8 48.6	100%	-(N+W)	1.5 N
III*	0.200	9.7 40.4	10.8 44.7	89.1%	-(N+W)	1.5 N
II	0.311	12.0 49.4	8.5 35.1	89.1%	+(N+W)	5.0 S
I	0.990	12.0 53.4	8.5 38.6	100%	+(N+W)	5.0 S
	6,020					

* An eccentricity of -1.5 in. was used instead of the -1.3 in.. This was done to avoid the changing of actuator position and should be conservative.

TABLE 5. DERAILMENT TEST PROGRAM - GIRDER 2

LOAD STAGE	P_3 (kips) TARGET	P_3 (kips) ACTUAL (AV.)	REMARK	LOAD STAGE	P_3 (kips) TARGET	P_3 (kips) ACTUAL (AV.)	REMARK
1-3*	0	0	Apply P_1,P_2	22	0		
4	14.4	12.3		23	57.8	56.7	
5	28.9	27.9[1]	Crush L. L.	24	63.5	62.3	
6-8	43.3	45.8		25	69.3	67.4	F.S. Crack
9,10	57.8	58.9[2]	2.0xCrush L. L.	26	80.9	80.9[3]	2.8xCrush L. L.
11	28.9	31.7		27	0		
12-15	0	0		28	80.9	79.3	
16	14.4	11.9		29-30		82.6	W. S. Crack
17	28.9	27.8		31		93.8	
18	43.3	44.2		32-34		106[4]	3.7xCrush L. L.
19,20	57.8	57.7		35		110	3.8xCrush L. L.
21	0	0		36-39		120	
				40-42		127	
				43-45		131	4.5xCrush L. L.

Simulated Superimposed Dead Load P_1 = 7.9k P_2 = 15.4k

[1]Max. crack width = 0.001 in. (cracks did not reopen)

[2]Max crack width = 0.008 in

[3]Max. crack width = 0.019 in.

[4]Max. crack width = 0.187 in. (one crack open at midspan)

TABLE 6. LOADING TO CRACK GIRDER 3

LOAD STAGE	(P_1+P_2),* kips at 6'-3" **	(P_1+P_2), kips at 27'-3"	$2P_5$,* kips at 30'-3"	MIDSPAN DEFLECTION (IN.)
1,2	0	0	0	0
3	9.8	10.0	0	0.057
4	20.0	20.6	0	0.115
5	30.1	30.6	0	0.170
6	40.2	40.7	0	0.227
7	50.4	50.9	0	0.287
8	60.5	60.5	0	0.343
9	70.6	70.4	0	0.401
10	80.6	81.8	0	0.465
11	90.4	91.4	0	0.525
12	95.5	97.3	0	0.559
13	95.4	102.1	0	0.590
14	95.6	101.0	7.2	0.625
15	95.3	101.3	15.4	0.666
16	95.7	100.9	26.3	0.720
17	95.7	101.1	39.4	0.790
18	95.7	100.4	53.2	0.858
19	95.7	101.4	66.3	0.936
20	95.6	100.9	80.4	1.015
21	95.8	100.4	86.9	1.059
22	95.8	101.5	89.4	1.090
23	95.8	100.3	91.8	1.100
24	95.6	100.7	95.8	1.132
25	95.6	101.9	95.9	1.157

* See Fig. 15b, $P_1 = P_2$.

** Distance measured from center of support.

TABLE 7. FATIGUE TEST PROGRAM - GIRDER 3

LOAD CONDITION	LOAD CYCLES (MILLION) TARGET	LOAD CYCLES (MILLION) ACTUAL	P_1 (kip)	P_2 (kip)	REMARK CLL+I	REMARK TORQUE	REMARK LOAD ECC.(IN.)
I	1.2625	1.352	10.6[1] 57.3	5.8[1] 31.1	100%[2]	(N+W+E+C.F.)[3]	8.9 S
II	2.525	2.450	8.8[1] 47.3	7.6[1] 41.1	100%	(-N-W+E+C.F.)[4]	2.1 S
I	1.2625	1.247	10.6 57.3	5.8 31.1	100%	(N+W+E+C.F.)	8.9 S
	5.050	5.049					

[1]Superimposed dead loads should be simulated by P_1 = 11.6 kips, P_2 = 4.8 kips but were changed to maintain a constant load eccentricity indicated.

[2]CLL + 25% impact gives $P_1 = P_2$ = 36 kips

[3]10% nosing + 13.5 mph wind + Ecc. for 5200 ft. radius + C.F. for 70 mph = 48.5$^{k-ft.}$

[4]10% nosing - 13.5 mph wind + Ecc. for 5200 ft. radius + C.F. for 70 mph = 1.5$^{k-ft.}$

TABLE 8 DERAILMENT TEST PROGRAM - GIRDER 3

LOAD STAGE	P_3 (Kips)	REMARK	LOAD STAGE	P_3 (Kips)	REMARK
1-3	0	Apply P_1, P_2 [1]	25	21.9	
4.5	5.8		26	29.3	CLL
6	7.9		27	33.6	
7	10.1		28	44.7	
8	12.3		29	58.1	2.0xCLL[3]
9	14.4	Reentry corner crack reopen .002"	30	63.9	
10	17.8		31	69.7	
11	25.0		32	76.1	
12	29.0	CLL (28.9)	33,34	80.9	2.8xCLL (80.9)
13	33.6		35	89.8	
14	43.9		36	98.9	
15	51.3	Joint crack[2] open Flex. cracks reopen	37	100.6	
16,17	58.2	2.0xCLL (57.8)[3] End Diaph. cracks	38,39	108.7	3.8xCLL (109.8)[3]
18	30.8		40	117.8	
19,20	0		41	129.2	
21	3.2		42	131.2	
22	5.9		43	137.6	
23	11.7		44,46	139.6	4.8 CLL[3]
24	18.1		47	146.1	5.0 CLL (144.5) Midspan diaph. cracks.

[1] Simulated superimposed dead loads P_1 = 6.6 kips, P_2 = 12.8 kips.

[2] Joint crack is crack between the stem and the end diaphragm.

[3] Max. crack widths are (in inches):

P_3	FLEXURE	FLEXURAL SHEAR	REENTRY CORNER	END DIAPH.	JOINT[2]
58.1	.002	-	.005	.008	.010
108.7	.010	.050	.011	.015	.120
139.6	.015	.090	.017	.040	.500

TABLE 9. RESULTS OF FLANGE SLAB TEST.

STAGE LOAD	LOAD P_4 (KIPS)			DEFLECTIONS (in.)			REMARK
	G*	H*	AV.	G	H	AV.	
0	0	0	0	0	0	0	
1	5.5	5.0	5.3	.007	.005	.006	
2	11.0	9.8	10.4	.016	.013	.015	
3,4	16.1	15.0	15.6	.027	.025	.026	
5	21.5	20.2	20.9	.045	.043	.044	Existing Cracks Open
6	26.8	25.2	26.0	.068	.067	.068	New Cracks Open
7	30.8	29.0	29.9	.086	.086	.086	2.0 x CLL (P_4=28.9^k), W_{max} = .005"
8	0	0	0	.018	.017	.018	20% Res. Defl., W_{max} = .001"
9	0	0	0	0	0	0	
10	11.0	10.0	10.5	.022	.022	.022	
11	22.0	20.0	21.0	.048	.046	.047	
12	31.1	28.3	29.7	.072	.070	.071	2.0 x CLL (P_4=28.9^k) W_{max} = .005"
13	34.1	31.2	32.7	.083	.080	.082	
14	37.7	34.3	36.0	.103	.100	.102	
15	41.0	37.2	39.1	.116	.113	.115	
16	43.6	39.8	41.7	.133	.134	.134	2.8 x CLL (P_4=40.4^k) W_{max} = .010"
17	46.6	42.6	44.6	.143	.145	.144	Cracks Open On Underside of Flange
18	49.1	45.0	47.1	-	FAILED	-	3.26 x CLL, (P_4=47.1^k)
19	0	0	0	.019	-	-	
20	51.3	0	-	FAILED	-	-	3.55 x CLL, (P_4=51.3^k)

*Location of Wheel Load (see Figs. 66a and 66b)

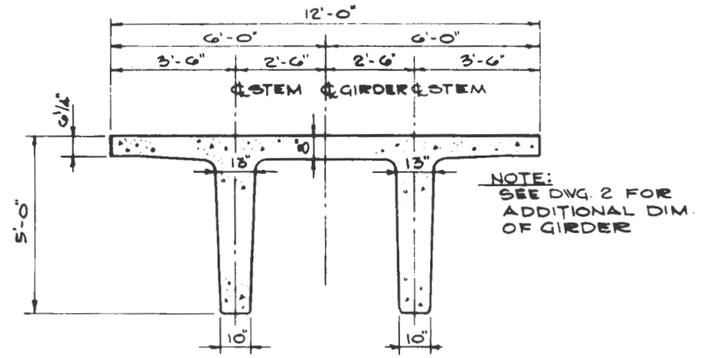

NOTE:
SEE DWG. 2 FOR ADDITIONAL DIM. OF GIRDER

CROSS SECTION

SCALE: ½"=1'-0"

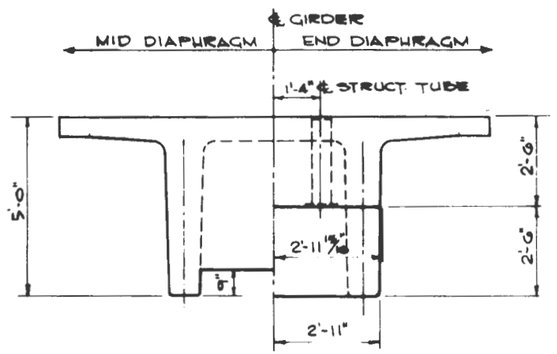

MID ℄ END DIAPHRAGM

SCALE: ½"=1'-0"

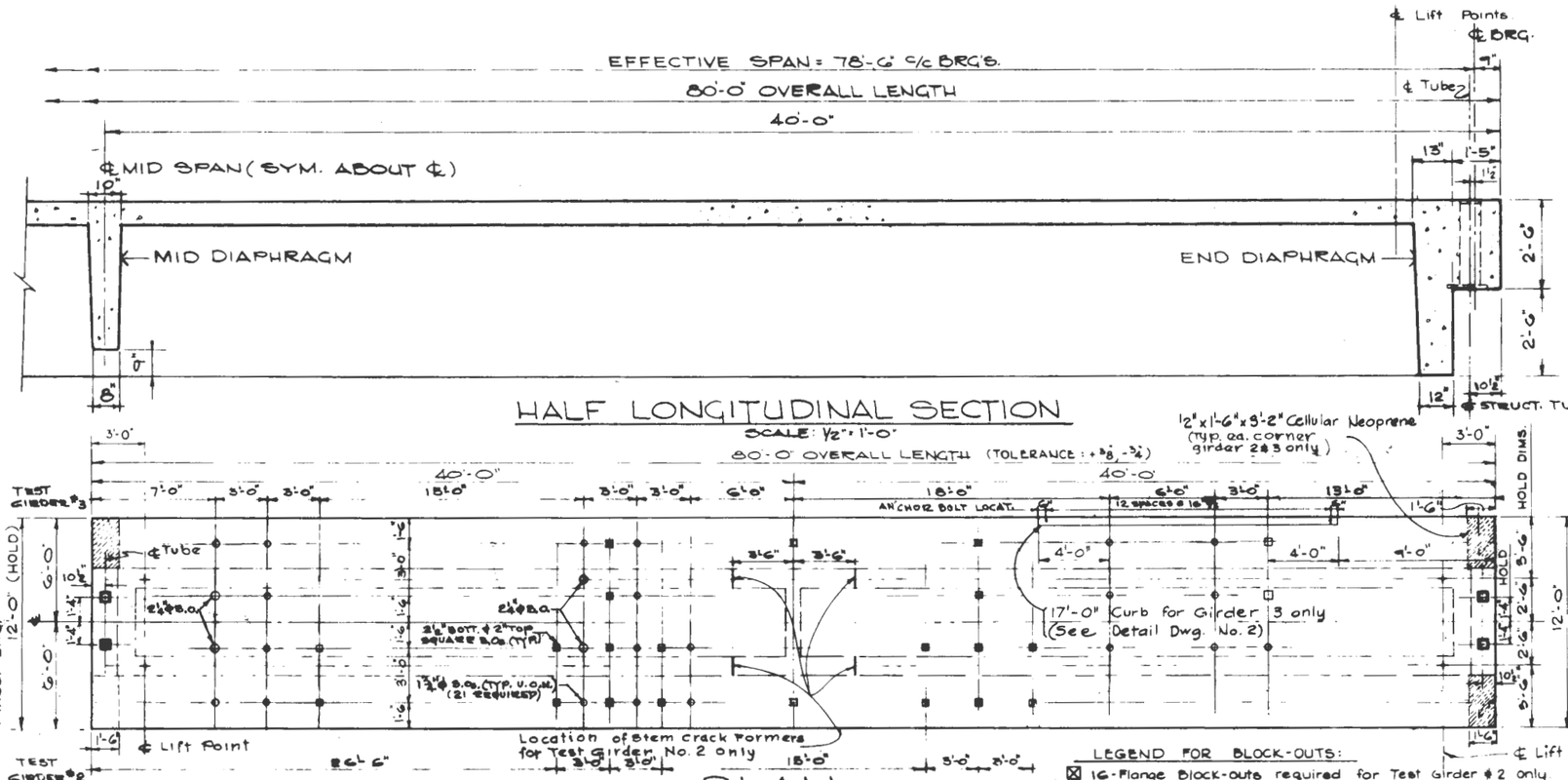

HALF LONGITUDINAL SECTION

SCALE: ½"=1'-0"

PLAN

Scale 1"=4'-0"

12"x1'-6"x9'-2" Cellular Neoprene (typ. ea. corner girder 2&3 only)

LEGEND FOR BLOCK-OUTS:

- 16-Flange Block-outs required for Test Girder #2 only.
- 31-Flange Block-outs required for Test Girder #3 only.
- 6"ø Tubes required for all 3 Test Girders. See Dwg No 8 for details.

TOLERANCE FOR ℄ BLOCK-OUT LOCATIONS

All locations to be measured from ℄ girder Field tolerance: ± ⅜" in any direction.

Plan above shows: ① Locations round and square flange block-outs for Test Girders Nos. 2 & 3 only and ② Locations of 4 Stem Crack Formers for Test Girder No. 2 only. (shown thus). See Dwg No 3 & 4 for details of (a) Crack Formers and (b) Additional Flange Reinforcement around block-outs.

GENERAL NOTES

A. MATERIAL DATA:

1. Concrete:
Strength: f'c = 6400 psi at 28 days
f'ci = 4000 psi at release
Cement: ASTM C150, Type III (Min. 7 sacks/cyd; Max 7½ sacks/cyd)
Coarse Aggregate: Miami Oolite - ASTM C33 Max size ¾"
Fine Aggregate: Miami Oolite Screenings
Water: Potable
Slump: 2½" to 3" (Maximum)
Admixture: Daratard HC-F as manufactured by W R Grace Company (ASTM C444 - Type D) or approved equivalent

2. Reinforcing Steel:
ASTM A615 Grade 60 unless otherwise noted.
Galvanize only (1½ mil ± thickness) stirrups MK5E01 MK5E01A and MK 5E02

3. Prestressing Strand: ▲
Low Relaxation (Stabilized) ½"ø - 270K LO-LAX (Florida Wire & Cable Co) or approved equivalent.

4. Structural Steel:
Plates and Structural Shapes: ASTM A-36
Tubing: ASTM A501; fy = 36 ksi
Hot-dip Galvanized only Bearing ℄ No 1 and Tubing Assembly ℄ No 2

B. TEST CYLINDERS

Six Standard Test Cylinders per truck-load of concrete. Precaster shall retain 2 cylinders per truck-load to determine release and 28-day strength and ship remaining 4 cylinders per truck-load to test lab at Skokie to determine Compressive and tensile strengths and modulus of elasticity. Test cylinders to be shipped to lab shall be packed carefully in wood crate.

C. PRODUCTION DATA

Refer notes on Dwg No 8

D. DUNNAGE POINTS

* Cantilever Dimension X during hauling can vary from 2'-0" (min.) to 8'-0" (max.) It is desirable to reduce dimension X as much as possible.

▲ Precaster shall provide and deliver to University of Miami bundle of 4 cm lengths of strand, each 5'-0" long, selected at random from each pack used.

NO.	DATE	BY / CHK.	APP.	REVISIONS
4	11-6-78 VP			Neoprene, orientation ℄ B.O.s, TYPE & QTY.
3	9-19-78 VP	SD	MK	GIRDER NO 3 FLANGE CURB
				/
1	8-7-78 VP	SD	MK	ADD. 3 B.O.s FOR TEST GIRDER #3

DESIGNED I. Jauregui/S.D. 3/30/78
DRAWN C. Quintana 8/20/78
CHECKED M Nunez 4/11/78
APPROVED M Nunez 4/11/78

Dade County Transportation Improvement Program

APPROVED ____ DATE ____

THE KAISER TRANSIT GROUP a joint venture
KAISER ENGINEERS, DIVISION OF HENRY J. KAISER COMPANY
HARRY WEESS & ASSOCIATES LTD.
POST, BUCKLEY, SCHUH & JERNIGAN, INC.
CARR SMITH AND ASSOCIATES, INC.
SCHIMPELER-CORRADINO ASSOCIATES

APPROVED D Weesner DATE 5/18/78

FULL-SIZE DOUBLE TEE TEST GIRDERS

PLAN, SECTIONS & GENERAL NOTES

SCALE AS NOTED | DRAWING 1 | Fig. 1a

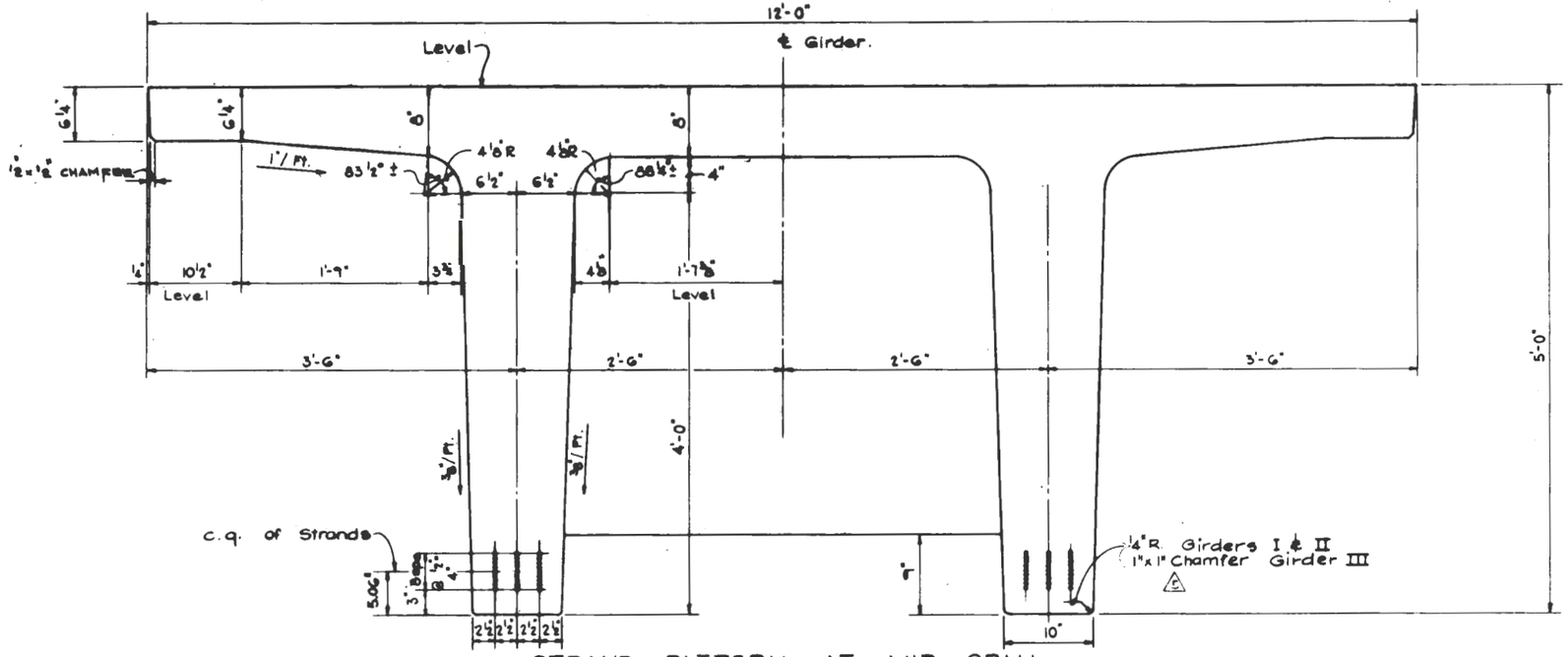

STRAND PATTERN AT MID SPAN (Strand Pattern same up to 10'-6" ea side (hold-down locations) of ℄ Girder (Midspan)

54 - ½"ϕ (270 K) Low-Relaxation (stabilized) strands at Pi kips ea. (Design Initial Force - See Table Dwg. No. 2 and Note No. 2 Dwg. No. 8)

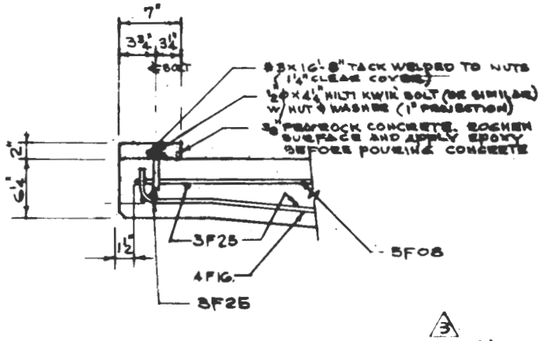

CURB DETAIL (GIRDER #3 ONLY)
See Plan Dwg. No. 1

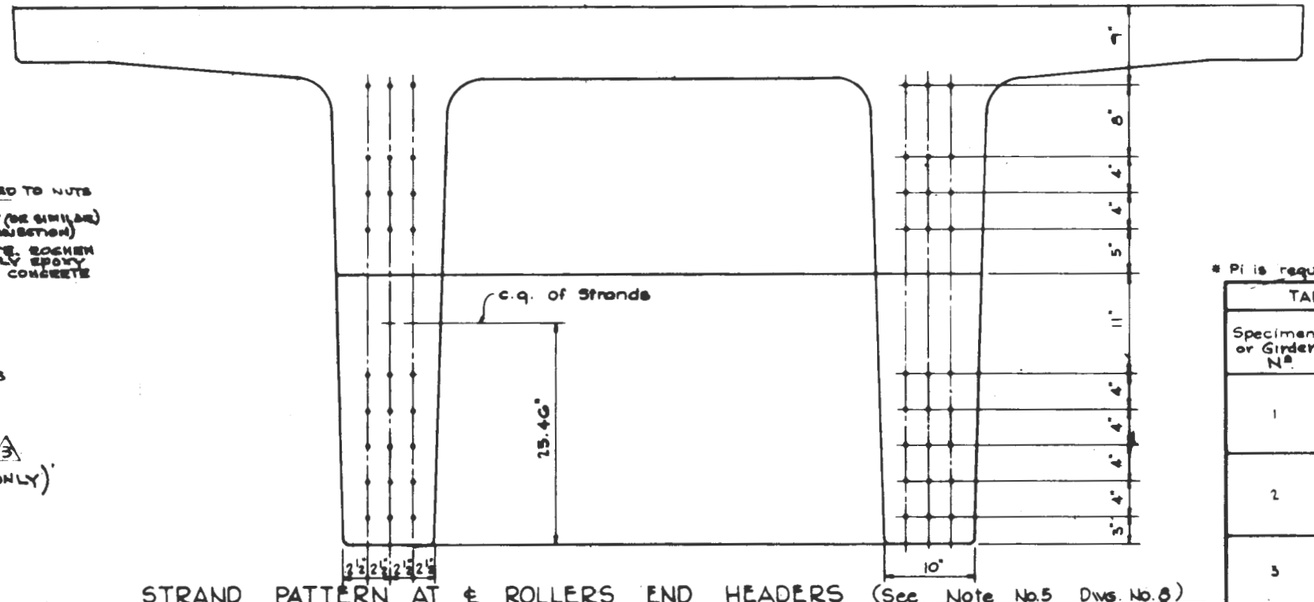

STRAND PATTERN AT ℄ ROLLERS END HEADERS (See Note No. 5 Dwgs. No. 8)

* Pi is required design initial force per strand at midspan girder.

TABLE FOR DESIGN INITIAL PRESTRESSING		
Specimen or Girder No.	Initial Design Force Pi in Kips/Strand*	REMARKS:
1	29.2k	Retain in Precaster's Yard to Monitor Camber Growth and Total Loss of Prestress
2	27.90k	Send to Test Lab.- Age of Specimen Estimated to be 30 to 40 days (t) when test commences.
3	28.10k	Send to Test Lab.- Age of Specimen Estimated to be 60 to 70 days when test commences.

I. Imaseta/S.D. 3/29/78					
DESIGNED DATE					
I.E. Varona 3/30/78					
DRAWN DATE					
CHECKED 4/11/78					
APPROVED DATE	1	7-6-78	WH		STEM CHAMFERS, CURB DETAIL & TABLE
	2	7-19-78	WH		FORCES IN TABLE, STRAND QTY, CURB DETAIL
	3	7-25-78	WH		FORCES IN TABLE FOR 28 DAY EST. PRESTRESSING
	4	8-7-78	WH		FORCES IN TABLE FOR DESIGN INIT. PRESTRESSING
	5	8-17-78	WH		FORCES IN TABLE FOR DESIGN INIT. PRESTRESSING
APPROVED DATE	NO.	DATE	BY	APP.	REVISIONS

Dade County Transportation Improvement Program

THE KAISER TRANSIT GROUP a joint venture

KAISER ENGINEERS, DIVISION OF HENRY J. KAISER COMPANY; HARRY WEESE & ASSOCIATES LTD.; POST, BUCKLEY, SCHUH & JERNIGAN, INC.; CARR SMITH AND ASSOCIATES, INC.; SCHNEIDER-CORRADINO ASSOCIATES

APPROVED DATE 5/10/78

FULL-SIZE DOUBLE TEE TEST GIRDERS

CROSS-SECTION & STRAND PATTERN

SCALE 1½"=1'-0" | DRAWING 2 | Fig. 1b

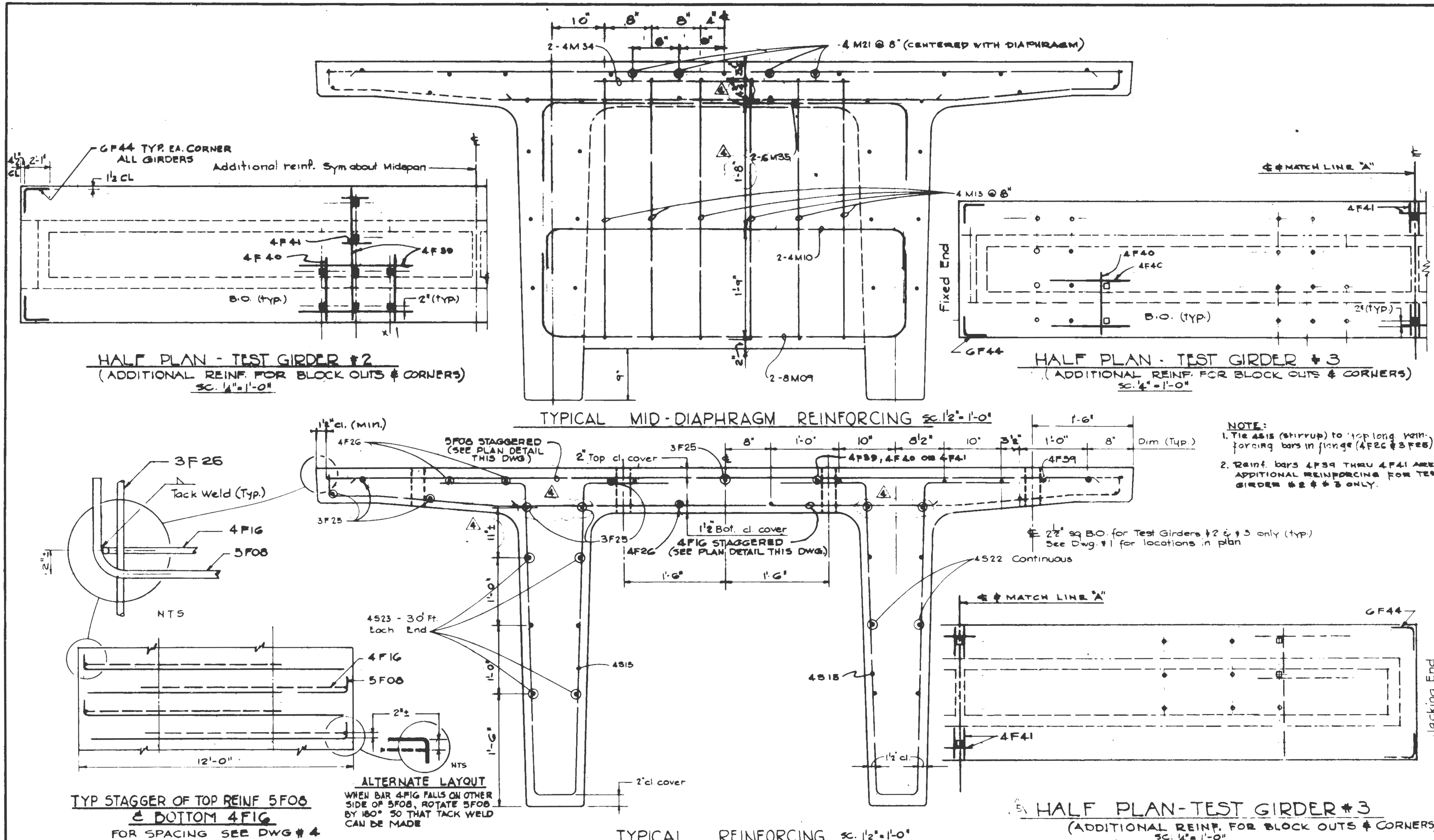

NO.	DATE	BY/CHK.	APP.	REVISIONS
5	10-6-78			ROUND B.O. W/O ADD REINF FOR #3 GIRDER
4	9-19-78			LOCATION OF BARS 6M35 & 3F25
3	8-25-78			NEW PLAN DETAIL & 4M21 BAR DIMENSION
2	8-7-78			SIZE/QTY/LENGTH/LOCATION BARS; 4F39, 4F40, 3F25, 4F26, 4S23, 4F16, 8M09, 4M21, 4M34, 6M35
1	6-5-78			TOP AND BOTT. FLANGE CLEAR COVER

DESIGNED: I. Taurasu / S.D. DATE: 3/30/78
DRAWN: I.E. Vorona DATE: 3/30/78
CHECKED: DATE: 4/11/78
APPROVED: DATE: 4-11-78

Dade County Transportation Improvement Program

THE KAISER TRANSIT GROUP a joint venture
KAISER ENGINEERS, DIVISION OF HENRY J. KAISER COMPANY
HARRY WEESE & ASSOCIATES LTD.
POST, BUCKLEY, SCHUH & JERNIGAN, INC.
CARR SMITH AND ASSOCIATES, INC.
SCHIMPELER-CORRADINO ASSOCIATES

APPROVED — DATE 5/10/78

FULL-SIZE DOUBLE TEE TEST GIRDERS

MIDSPAN DIAPHRAGM DETAILS & TYPICAL REINFORCEMENT

SCALE: AS SHOWN | DRAWING: 3 | Fig. 1C

Note: Move stirrup and/or transverse flange reinforcement nominally in the event of conflict with flange block-outs located on Dwg No. 1) so as to provide clear cover of 3/4" between rebar and edge of block-out

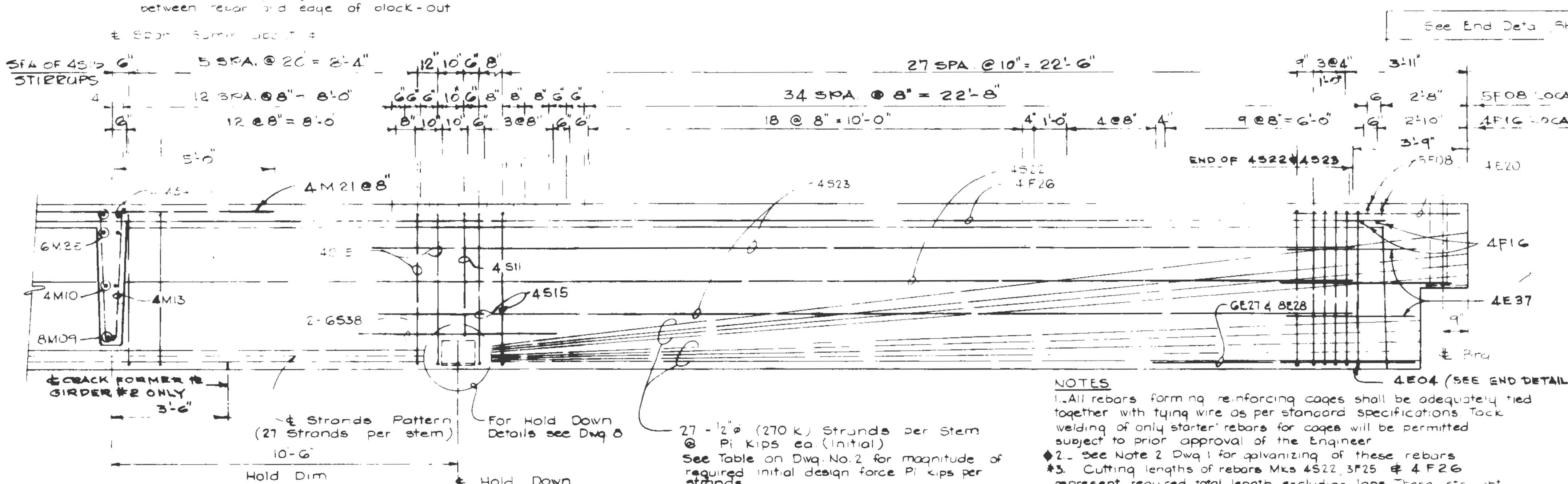

HALF LONGITUDINAL SECTION

Scale 1/2" = 1'-0"

NOTES
1. All rebars forming reinforcing cages shall be adequately tied together with tying wire as per standard specifications. Tack welding of only starter rebars for cages will be permitted subject to prior approval of the Engineer.
◆2. See Note 2 Dwg 1 for galvanizing of these rebars.
✱3. Cutting lengths of rebars Mks 4S22, 3F25 & 4F26 represent required total length excluding laps. These straight longitudinal rebars shall be made from multiple shorter lengths determined by length of reinforcing cages. Avoid laps thru midspan diaphragm. Required lap length = 1'-6" for #3 rods and 2'-0" for #4 rebars.
†4. Bars 4F39, 40 & 41 for girders Nos. 2 & 3 only see Dwg 5

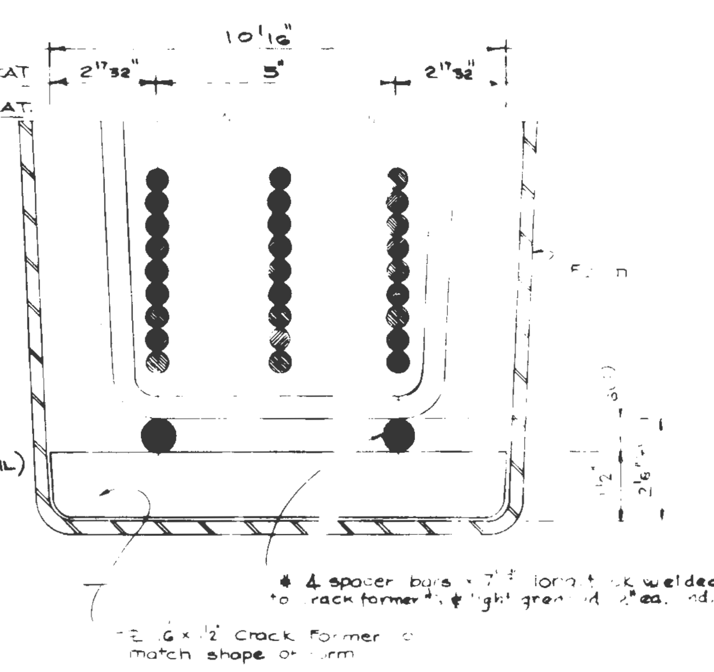

CRACK FORMER DETAIL TEST GIRDER #2

For Location of Crack Formers see Plan Dwg #1

LEGEND

BAR NUMBER
LOC. OF BAR IN GIRDER
SIZE OF BAR
MK No. = 4 E 14

E = END DIAPHRAGM
F = FLANGE
M = MID DIAPHRAGM
S = STEM

▲ Before fabrication of rebars and reinforcement cages, precaster should verify all the bending diagrams and cutting lengths to ensure fit, minimum cover and details as shown on the drawings.

REINFORCING SCHEDULE (QUANTITY PER GIRDER)							
STRAIGHT BARS				BENT BARS			
MARK	SIZE	No. REQ'D.	LENGTH▲	MARK	SIZE	No. REQ'D	LENGTH▲
				3E17	3	16	4'-3"
				4E03	4	36	5'-7"
4E20	4	10	5'-8"	4E17	4	20	4'-6"
4E36	4	2	3'-0"	4E04 A	4	16	9'-3"
6E27	6	4	8'-0"	4E04	4	32	4'-11 1/2"
6E33	6	4	4'-2"	4E05	4	40	9'-5"
8E24	8	6	11'-6"				
8E28	8	4	8'-0"				
4S22	4	4	✱72'-6	5E14	5	24	4'-3"
4S23	4	16	30'-0"				
6S38	6	8	6'-0"				
4E37	4	16	4'-6"	5E02 ◆	5	24	9'-4"
3F25A	3	1	16'-8"				
3F25	3	13	✱75'-0"	5E12	5	16	8'-4"
3F30	3	16	4'-6"	5E18	5	14	3'-4"
4F26	4	6	✱75'-0"	5E01 ◆	5	8	9'-6"
4F29	4	24	4'-6"	5E01A ◆	5	8	9'-5"
†4F39	4	For Girder 3 [illegible]	11'-6"	6E19	6	4	4'-0"
†4F40	4	[illegible]	6'-0"	6E06	6	2	7'-0"
†4F41	4	[illegible]	3'-0"	6E07	6	6	7'-6"
4M34	4	2	3'-8"	6E42	6	4	10'-0"
				4S15	4	164	12'-0"±
4M21	4	4	10'-0"	4S11	4	8	6'-4"±
4E31	4	12	4'-2"				
4F43	4	10	5'-0"	4M10	4	2	6'-3"
				4M13	4	6	9'-3"
				8M09	8	2	7'-6"
			◆ See Note 2	6F44	6	4	4'-0"
			✱ See Note 3	4F16	4	114	9'-0"
			† (See Note 4)	5F08	5	116	12'-0"
				6M35	6	2	7'-5

BENDING DIAGRAM▲

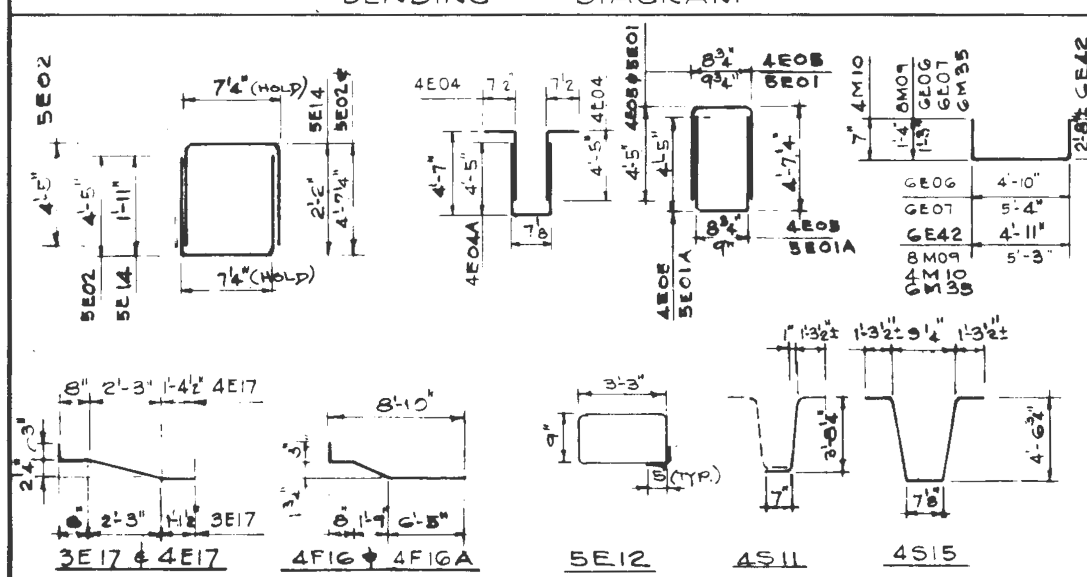

NOTE: All bars dimensions are out to out.

BENDING DIAGRAM

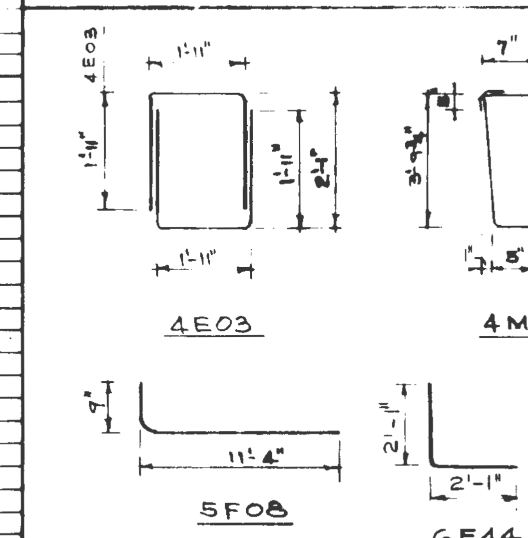

DIAMETER OF PIN FOR BENT BARS		
SIZE	STIRRUP	BAR
#3	1 1/2"	2 1/4"
#4	2"	3"
#5	2 1/2"	3 3/4"
#6	—	4 1/2"
#8	—	6"

I. Jurca / S.D. 3/30/78 DESIGNED	△ 11-6-78		NEW BARS 3E17 & 4E17, SIZE/QTY/LENGTH 4E37, 3F30, 4F29, 4M13 & 4M21
I.E. Vorena 3/30/78 DRAWN	4-14-78		NEW BARS 4S11 & 3F25A
[signature] 4/11/78 CHECKED	6-28-78		SIZE/QTY/LENGTH BARS: 4F16, 8E24, 5E1A, GE42, 4S15, 6M35, 4S11, 4E04A, 4E04, 4E05, 3F30, 4E06, 6E07, 5F08, 4E43, ... 5E18, 6E19
APPROVED [signature]	5-19-78		SIZE/QTY/LENGTH BARS: 4F39, 4F40, 4F41, 4S15, 4F26, 4S22, 4F16, 4F29, 3F30, 4M13, 4M34, 6M35
	5-11-78		4S11, 4S15 & 4M13 BAR DIMENSION
	NO. DATE BY APP.		REVISIONS

Dade County Transportation Improvement Program

THE KAISER TRANSIT GROUP a joint venture
KAISER ENGINEERS, DIVISION OF HENRY J. KAISER COMPANY
HARRY WEESE & ASSOCIATES LTD.
POST, BUCKLEY, SCHUH & JERNIGAN, INC.
CARR SMITH AND ASSOCIATES, INC.
SCHIMPELER-CORRADINO ASSOCIATES

APPROVED | DATE
APPROVED [signature] DATE 5/18/78

FULL-SIZE DOUBLE TEE TEST GIRDERS

REINFORCEMENT DETAILS & SCHEDULES

SCALE As noted | DRAWING 4 | Fig. 1d

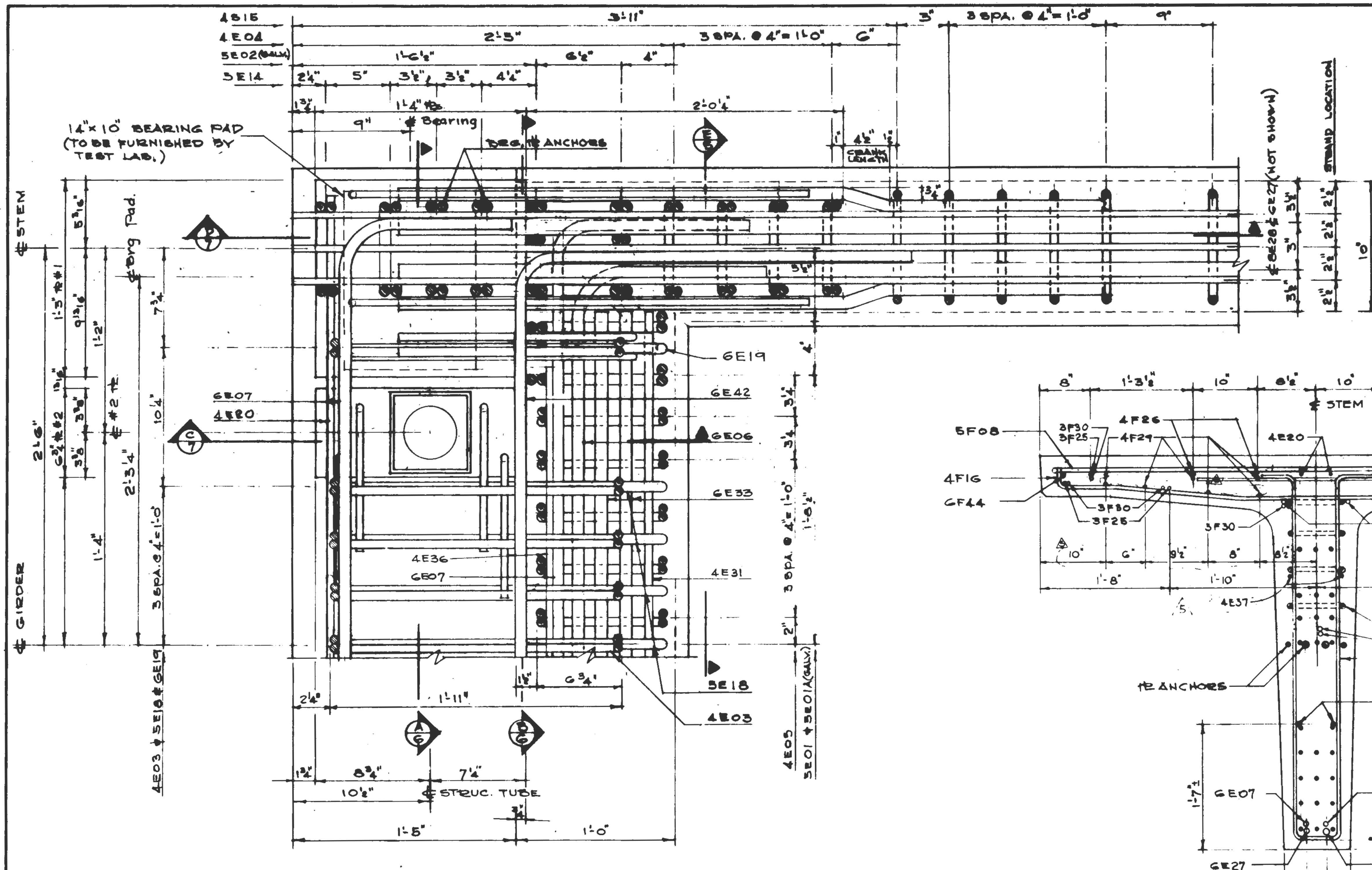

PLAN - END DIAPHRAGM

SCALE : 3" = 1'-0"

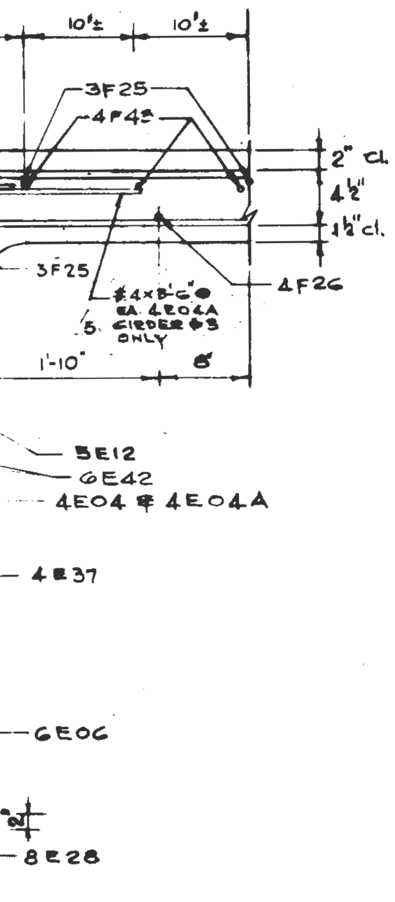

E/5 SECTION

SCALE 1½" = 1'-0"

1	11-6-78			ADDED BARS 4F29, 4E37 & #4x3'-6"
2	9-19-78			BARS 4E36, 6E07, 3F25 & 3F30
3	8-23-78			BARS: 4F45, 4E03, 5E18, 6E19, 4E05, 5E01 & 6E07
4	8-7-78			SIZE OF BARS: 3F25, 4F26, 4F29 & 3F30 (SECT. E)
5	6-5-78			TOP AND BOTT. FLANGE CLEAR COVER
NO.	DATE	BY	APP.	REVISIONS

DESIGNED: I. Jawsoui/S.D. 3/30/78
DRAWN: Perez 4/28/78
CHECKED: 5/18/78
APPROVED: H. Horowitz 5/19/78

Dade County Transportation Improvement Program

THE KAISER TRANSIT GROUP a joint venture

KAISER ENGINEERS, DIVISION OF HENRY J. KAISER COMPANY; HARRY WEESE & ASSOCIATES LTD.; POST, BUCKLEY, SCHUH & JERNIGAN, INC.; CARR SMITH AND ASSOCIATES, INC.; SCHIMPELER · CORRADINO ASSOCIATES

APPROVED | DATE 5/18/78

FULL-SIZE DOUBLE TEE TEST GIRDERS

END DETAILS - SHEET 1

SCALE | DRAWING 5 | Fig. 1e

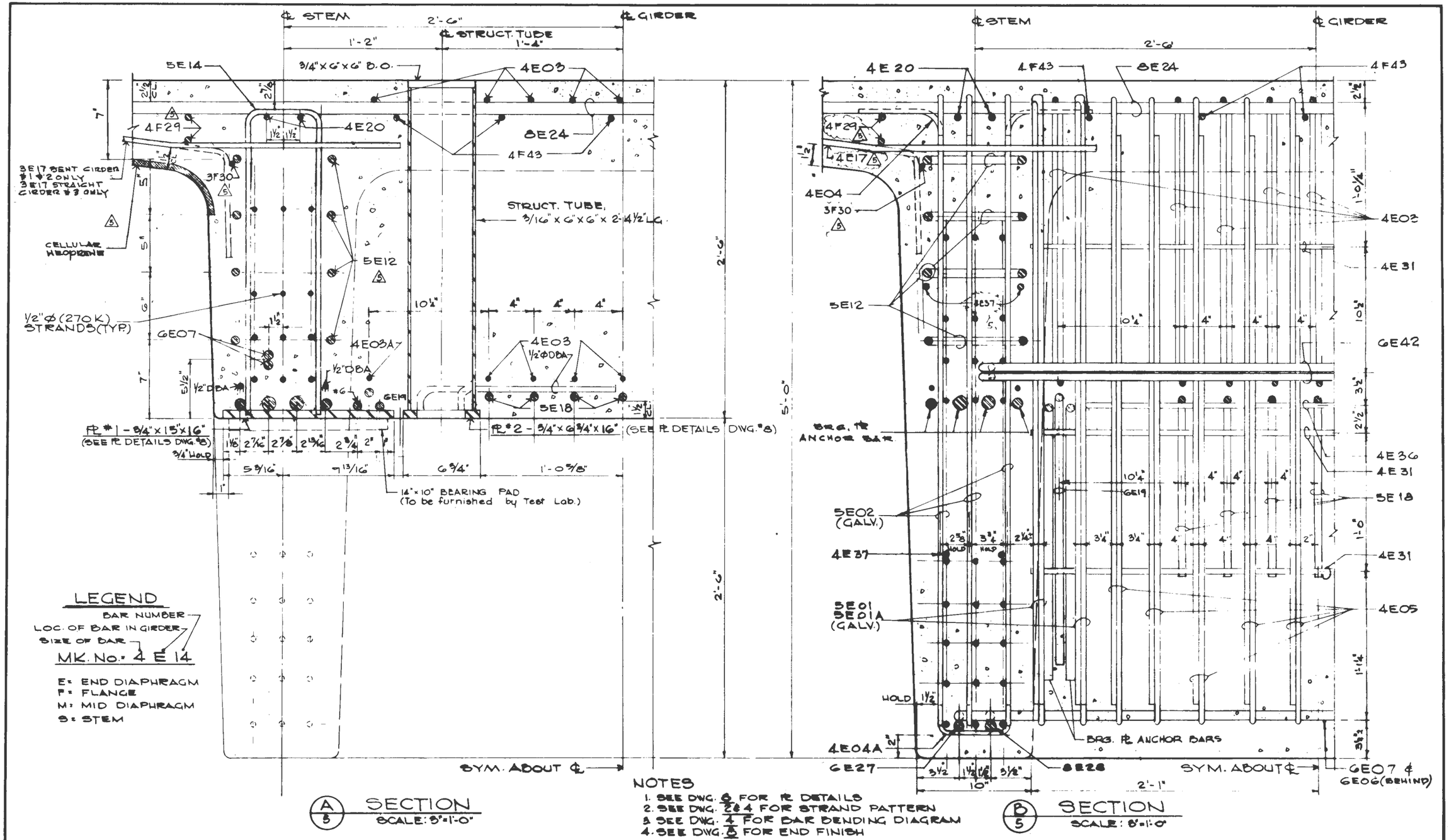

LEGEND

BAR NUMBER
LOC. OF BAR IN GIRDER
SIZE OF BAR
MK. No. = 4 E 14

E = END DIAPHRAGM
F = FLANGE
M = MID DIAPHRAGM
S = STEM

A/5 SECTION
SCALE: 3"=1'-0"

B/5 SECTION
SCALE: 3"=1'-0"

NOTES
1. SEE DWG. 5 FOR FR DETAILS
2. SEE DWG. 2 & 4 FOR STRAND PATTERN
3. SEE DWG. 4 FOR BAR BENDING DIAGRAM
4. SEE DWG. 5 FOR END FINISH

A	11-6-70	VH		CELLULAR NEOP. & BARS 4E17, 3E17, 4F29
A	7-19-71	VH	JH	LOCATION OF BAR 3F30
A	8-3-71	VH	JH	SIZE OF BARS GE19, 4F43 & GE07
A	9-17-71	VH	JH	SIZE OF GE42
				4E31 & 3F30
A	2-8-72	VH	JH	TOP CLEAR COVER
NO.	DATE	BY	APP.	REVISIONS

4E31 & 3F30

I. Jaureguy/EP 3/24/71 DESIGNED DATE
Dordelman 9/28/70 DRAWN DATE
CHECKED DATE
APPROVED DATE

Dade County Transportation Improvement Program

THE KAISER TRANSIT GROUP a joint venture
KAISER ENGINEERS, DIVISION OF HENRY J. KAISER COMPANY
HARRY WEBBE & ASSOCIATES LTD.
POST, BUCKLEY, SCHUH & JERNIGAN, INC.
CARR SMITH AND ASSOCIATES, INC.
SCHIMPELER-CORRADINO ASSOCIATES

APPROVED DATE
APPROVED DATE

FULL-SIZE DOUBLE TEE TEST GIRDERS
END DETAILS - SHEET 2

SCALE AS NOTED | DRAWING 6 | Fig. 1f

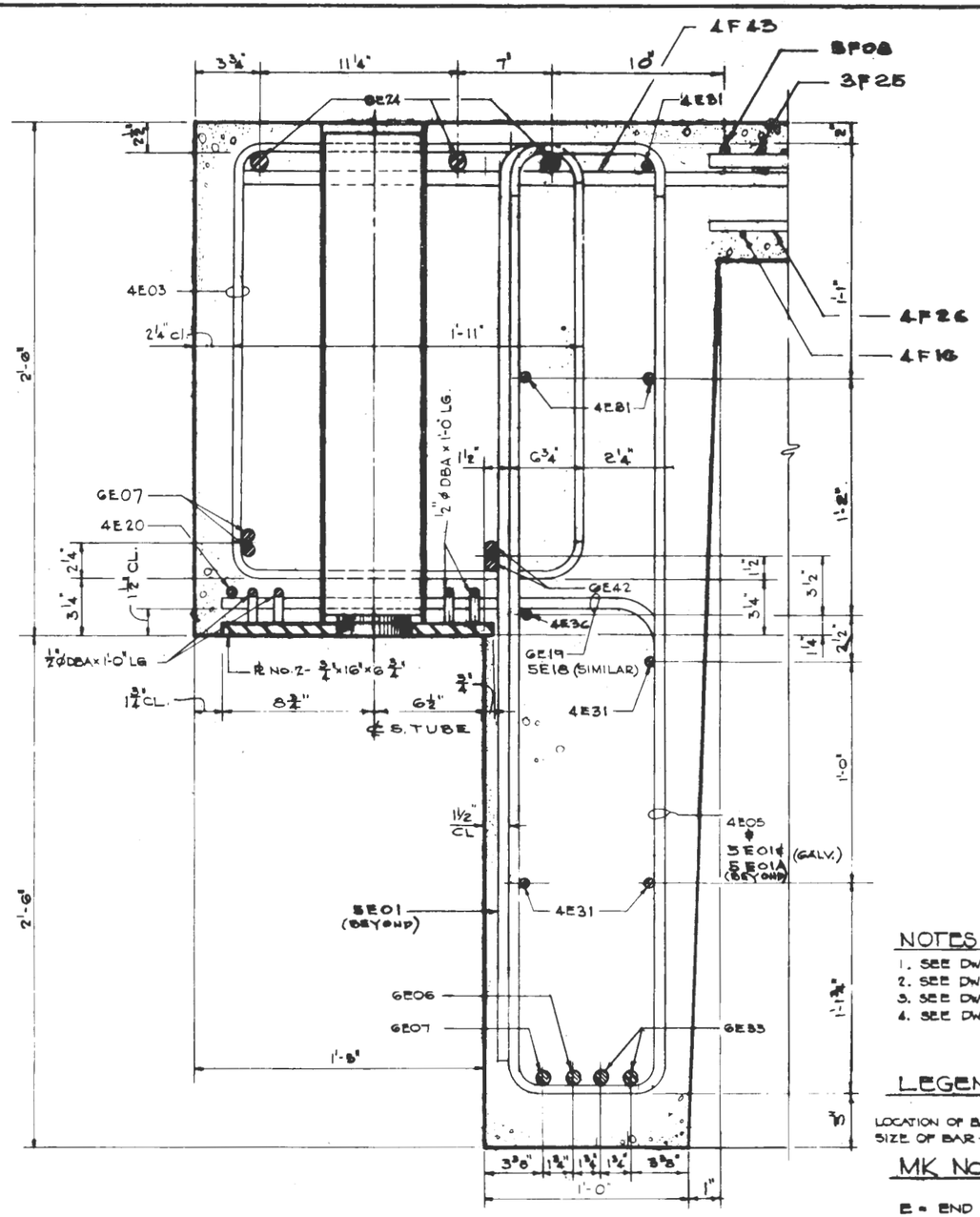

NOTES :

1. SEE DWG. 8 FOR ℄ DETAILS.
2. SEE DWG'S 2 & 4 FOR STRAND PATTERN
3. SEE DWG. 4 FOR BAR BENDING DIAGRAM
4. SEE DWG. 8 FOR END FINISH.

LEGEND

LOCATION OF BAR IN GIRDER
SIZE OF BAR — MK No. = 4E14 — BAR NUMBER

E = END DIAPHRAGM
F = FLANGE
M = MID DIAPHRAGM
B = STEM

C/5 SECTION
SCALE: 3" = 1'-0"

D/5 SECTION
SCALE: 3" = 1'-0"

I. Jauregui/S.P. 3/1/79 DESIGNED DATE
G. Fernandez 3-78 DRAWN DATE
Chung 4-79 CHECKED DATE
APPROVED DATE 4-4-79

NO.	DATE	BY	CHK.	APP.	REVISIONS
1	11-6-78	MP	SP	MF	LOCATION OF BARS 4E17, 3E17, 5E12
2	8-19-78	MP	SP	MF	LOCATION OF BARS 4F16, 4F26 & 4F43
3	8-24-78	MP	SP	MF	SIZE OF BARS GE07, GE42
4	8-7-78	MP	SP	MF	SIZE OF BARS : 3F25 ¢ 5F08
5	5-5-78	MP	SP	MF	TOP CLEAR COVER

Dade County Transportation Improvement Program

APPROVED DATE

THE KAISER TRANSIT GROUP a joint venture
KAISER ENGINEERS — DIVISION OF HENRY J. KAISER COMPANY
HARRY WEESE & ASSOCIATES LTD.
POST, BUCKLEY, SCHUH & JERNIGAN, INC.
CARR SMITH AND ASSOCIATES, INC.
SCHIMPELER · CORRADINO ASSOCIATES

APPROVED D. Wallauer DATE 5/18/78

FULL-SIZE DOUBLE TEE TEST GIRDERS
END DETAILS - SHEET 3

SCALE AS NOTED | DRAWING 7 | Fig. 19

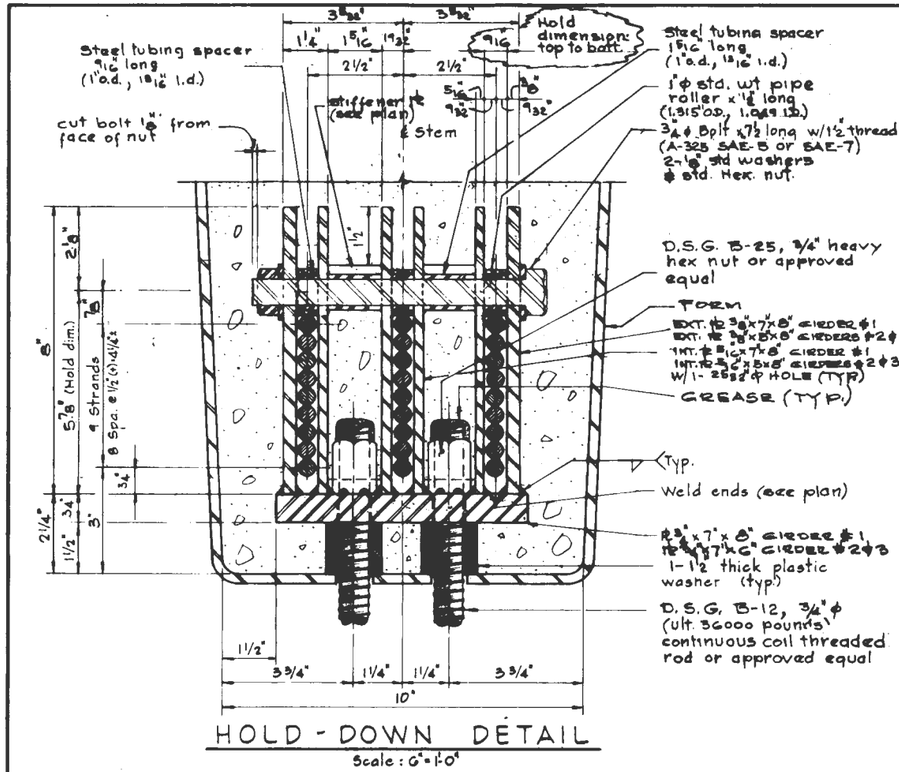

HOLD-DOWN DETAIL

Scale: 6"=1'-0"

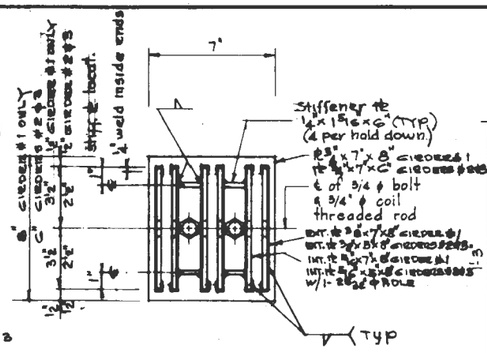

PLAN
HOLD DOWN PL

Scale: 3"=1'-0"

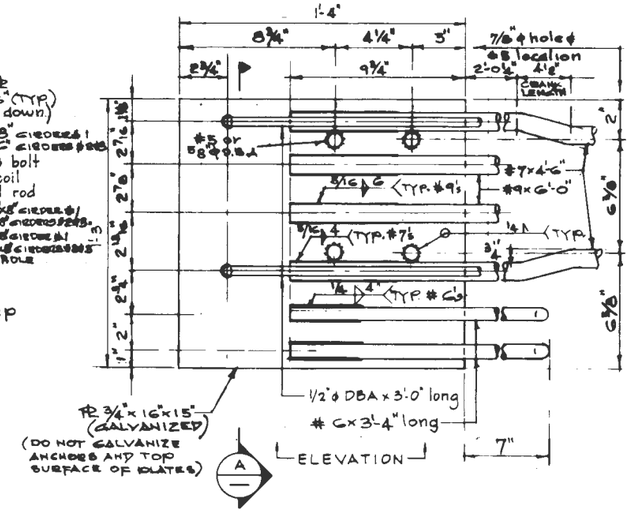

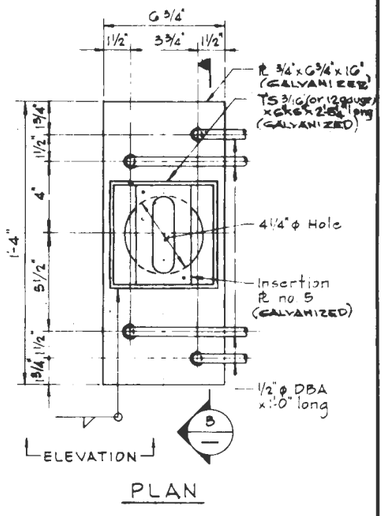

PLAN

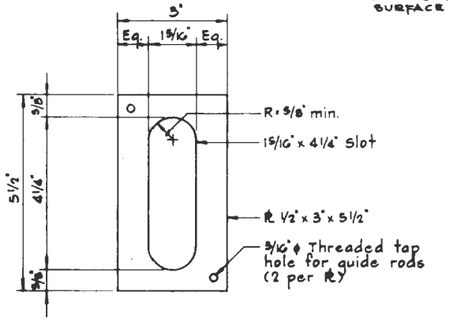

PLAN
INSERTION PL N° 5 (GALVANIZED)

Scale: 6"=1'-0"

(REQ'D: 4 PER GIRDER)

(3 Insertion PL's No.5 for Test Girders Nos. 2 & 3 shall be shipped loose to test laboratory)

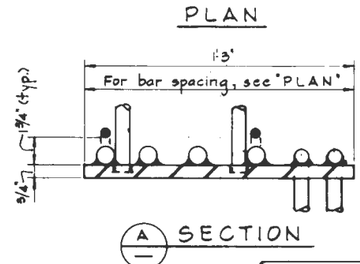

PLAN

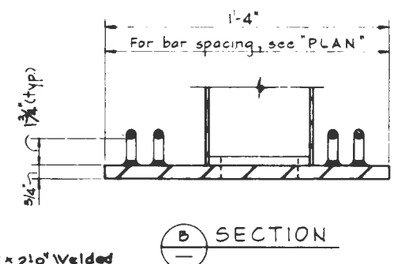

A SECTION

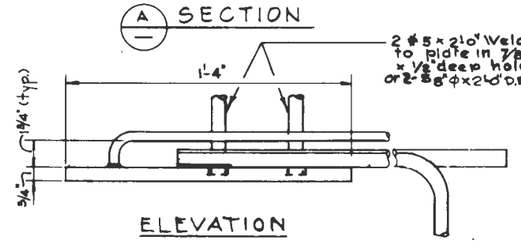

ELEVATION
PLATE N° 1 (AS SHOWN)
PLATE N° 1A (OPP. HAND)

Scale: 3"=1'-0"

(REQ'D: 2 OF EACH PER GIRDER)

B SECTION

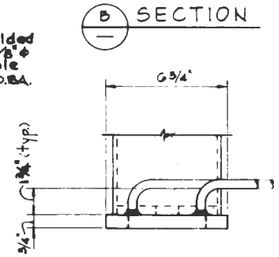

ELEVATION
PLATE N°2 (AS SHOWN)
PLATE N°2A (OPP. HAND)

Scale: 3"=1'-0"

(REQ'D: 2 OF EACH PER GIRDER)

* NOTE: Refer to note no. 6 for detensioning/stripping procedure. Release hold-downs in two operations: first two hold-downs on one side of mid-span in one simultaneous operation, and then the remaining two hold-downs so as to eliminate twisting of the girder during release. Also, both coil rods of any one hold-down should be removed as nearly simultaneously as possible.

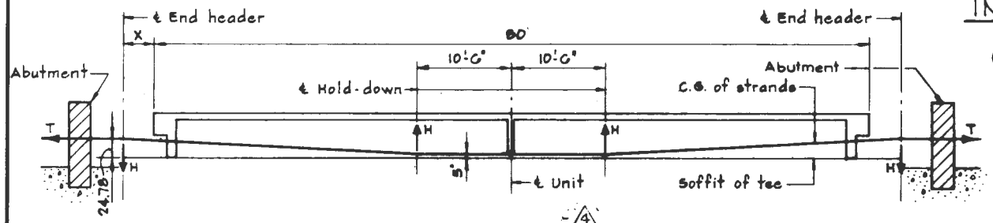

1. The three test girders shall be cast individually.
2. See "TABLE" on dwg. no. 2 for required design initial pull Pi at mid-span of unit. Tensioning pull at abutments shall be increased to account for friction loss thru hold-downs and headers; however, the maximum pull at abutments shall not exceed 32.5 kips for any strand. (31.5 kips average)
3. Friction losses thru hold-down and headers shall be determined by tests on two representative strands (top row and second row) prior to stressing of first unit. This data shall be interpolated to determine the required jacking force for each strand.
4. Stressing of three test units shall be done from one end only.
   Stress strands progressively from top to bottom with center strand of each horizontal row being stressed first.
   Max. "H" = 47.0 kips ± per stem per hold-down for Unit N° 1.
   Max. "T" = 850 kips per abutment per stem for Unit N° 1 applied 24.78" above bottom of stem.
5. Drape of strands as shown on drawings and pattern at ℄ roller of end header assumes that dimension "X" between end of unit and ℄ of header = 9". For significant variations in dimension "X," adjust strand pattern at headers to maintain the same drape of strands.
6. Detension/burn top 18 strands (9 per stem) before releasing hold-downs. Detension/burn remaining strands after releasing hold-down. Detensioning/burning shall be done simultaneously at both end headers; also, progress symmetrically about ℄ double tee and from top to bottom. Eccentricity of prestress about ℄ double tee shall not exceed that due to three strands (one row) at any time.
7. Screed finish top of flanges as smooth as possible. All other portions of flanges and stems shall have a smooth form finish. All ends of all units (flanges and stems) shall also be finished smooth. In general, after detensioning, recess strands 1" cover recess with epoxy and then finish stems and flanges.
8. Spray top of flange with liquid membrane forming compound conforming to ASTM C309, Type II. Keep top of flange covered until release of member.
9. Refer to dwg. no. 1 for locations of handling lift points, dunnage points for storage in yard, and dunnage points during transfer by rail/truck. Lifting embed items (number, diameter, shape and length of strands) shall be approved by the engineer before production commences.
10. Girders shall be at least 15 days old when they are loaded on rail cars for shipment to test laboratory at Skokie, Illinois.

PRODUCTION • DATA

Unit Drawing Scale: ⅛"=1'-0"

I. Tavangar S.P. 3/27/78 DESIGNED DATE					
M.N. BURCH 3-27-78 DRAWN DATE	4	11-6-78	MM		NOTE No 4
CHECKED 4-11-78 DATE	3	9-19-78	MM	MM	HOLD DOWN; NO.2 PROD. DATA NOTE
	2	9-29-78	MM	MM	HOLD DOWN, PLATE N°1 & 2
	1	2-1-78	MM	MM	NOTES FOR GALV. PL 1, 2 & 5 ADDED
APPROVED DATE 4.11.78	NO.	DATE	BY	APP.	REVISIONS

Dade County Transportation Improvement Program

THE KAISER TRANSIT GROUP a joint venture

KAISER ENGINEERS, DIVISION OF HENRY J. KAISER COMPANY; HARRY WEESE & ASSOCIATES LTD.; POST, BUCKLEY, SCHUH & JERNIGAN, INC.; CARR SMITH AND ASSOCIATES, INC.; SCHNEIDLER-CORRADINO ASSOCIATES

APPROVED DATE

APPROVED DATE 5/10/78

FULL-SIZE DOUBLE TEE TEST GIRDERS
MISCELLANEOUS DETAILS AND PRODUCTION DATA

SCALE AS NOTED | DRAWING 8 | Fig. 1h

Fig. 2a Form for Manufacture of Girders

Fig. 2b Manufacture of Girders

Fig. 3 Transportation of Girders by Railroad

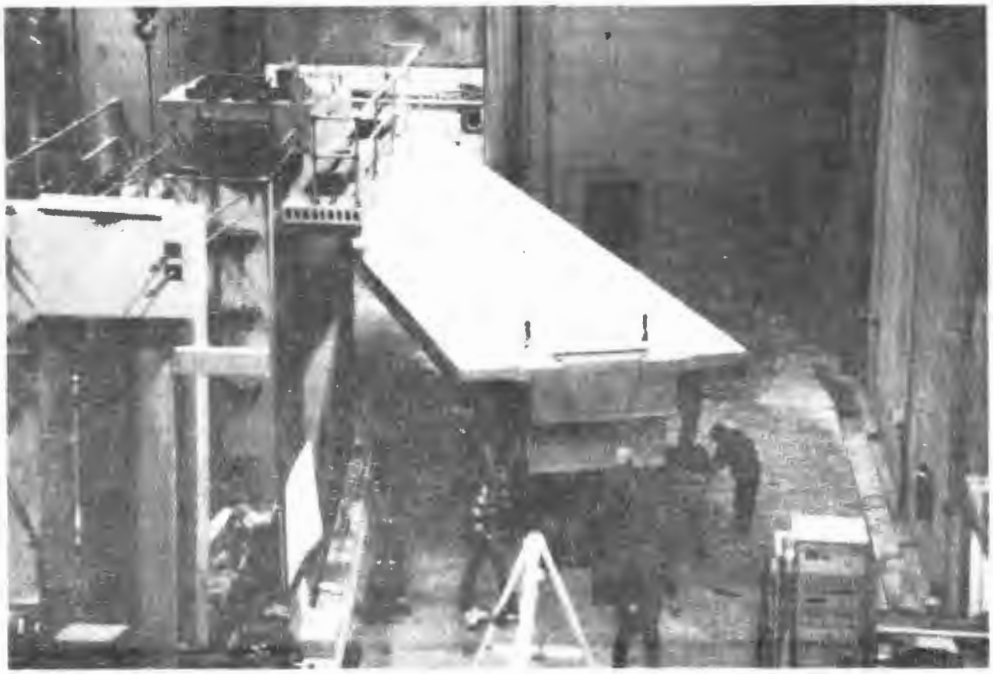

Fig 4 Hauling Girders Into Laboratory

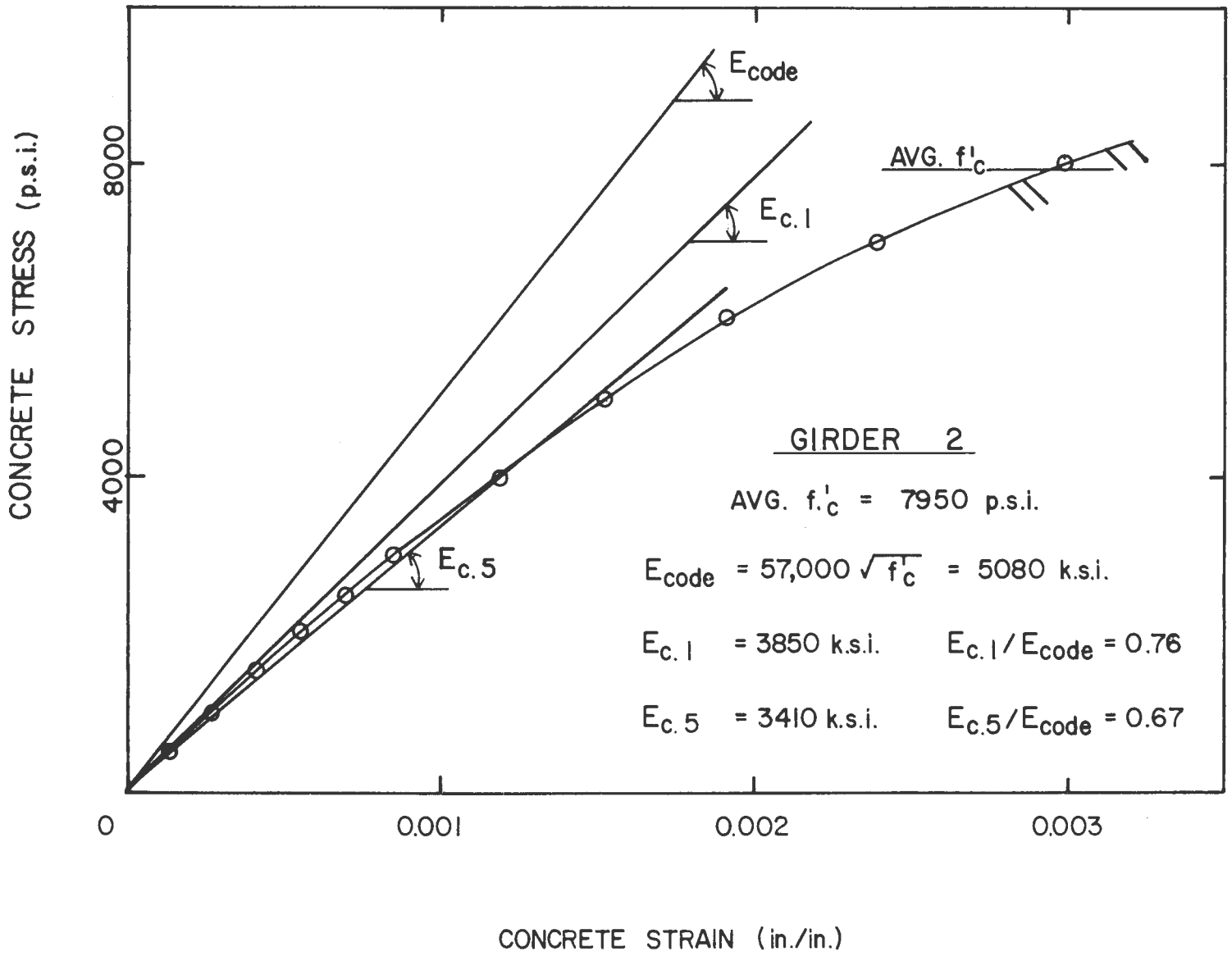

Fig. 5. Stress-Strain Curve of Florida-Oolite Concrete

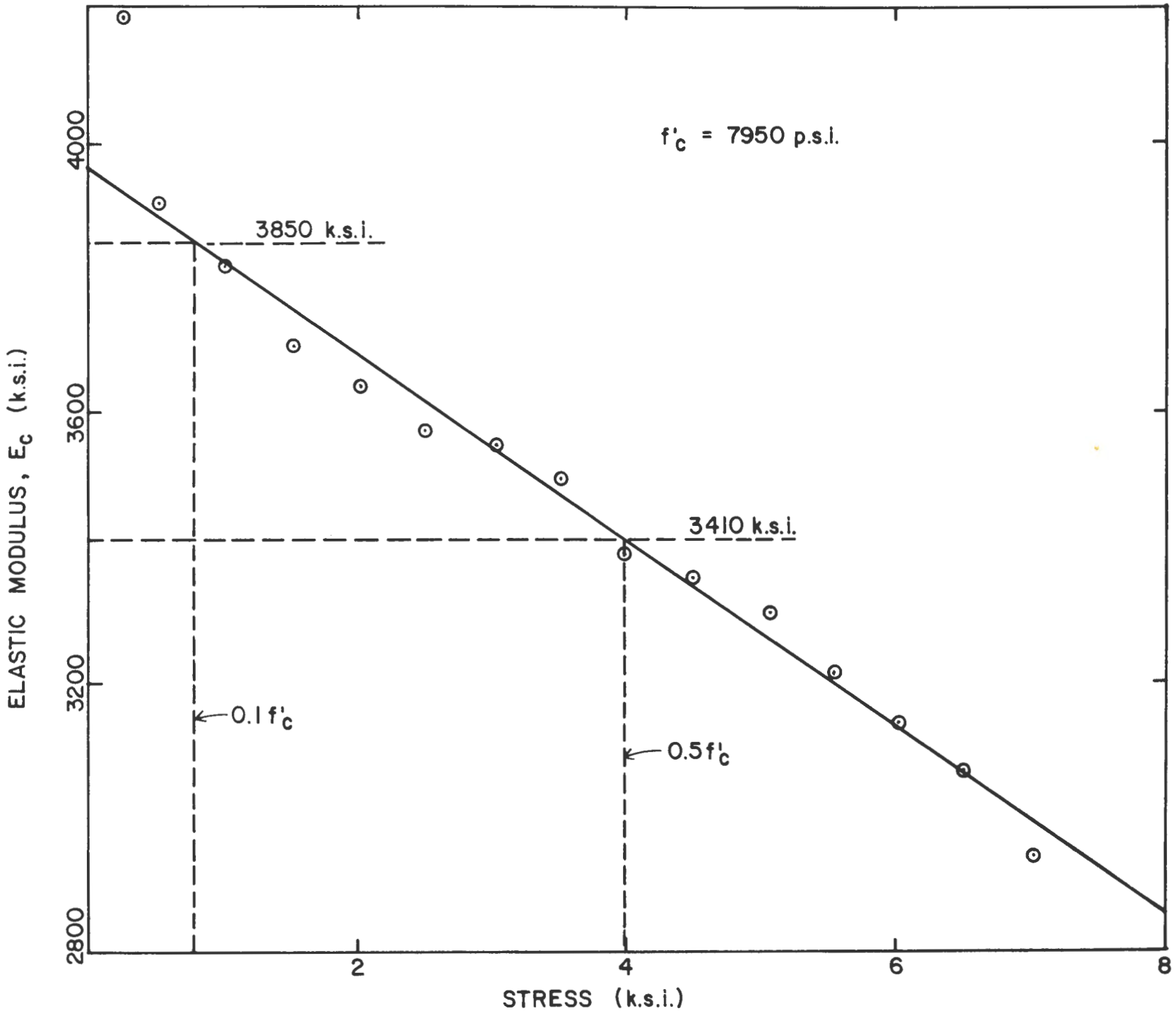

Fig. 6. Secant Modulus of Elasticity As Function of Stress Levels.

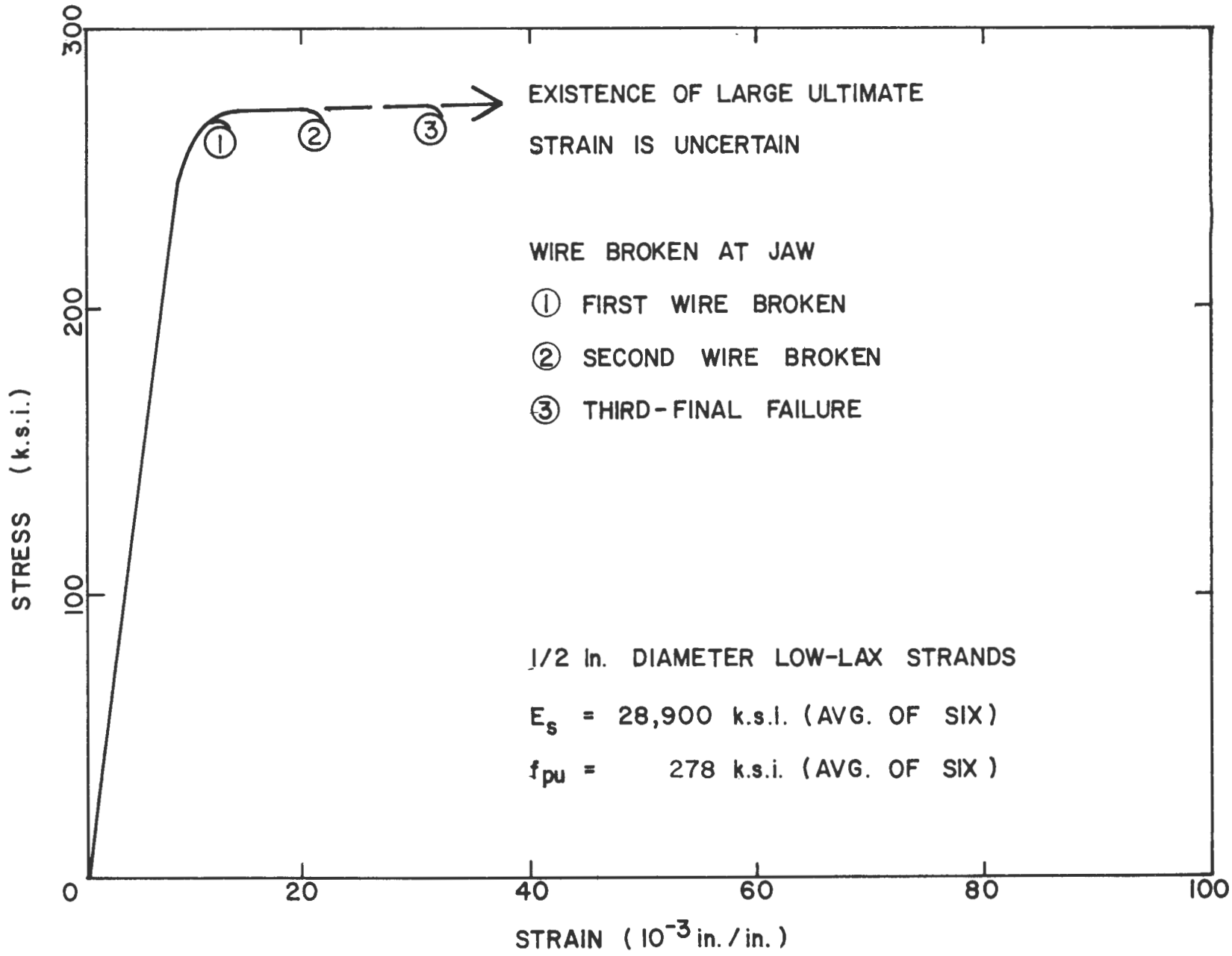

Fig. 7. Stress-Strain Curve of Prestress Strands

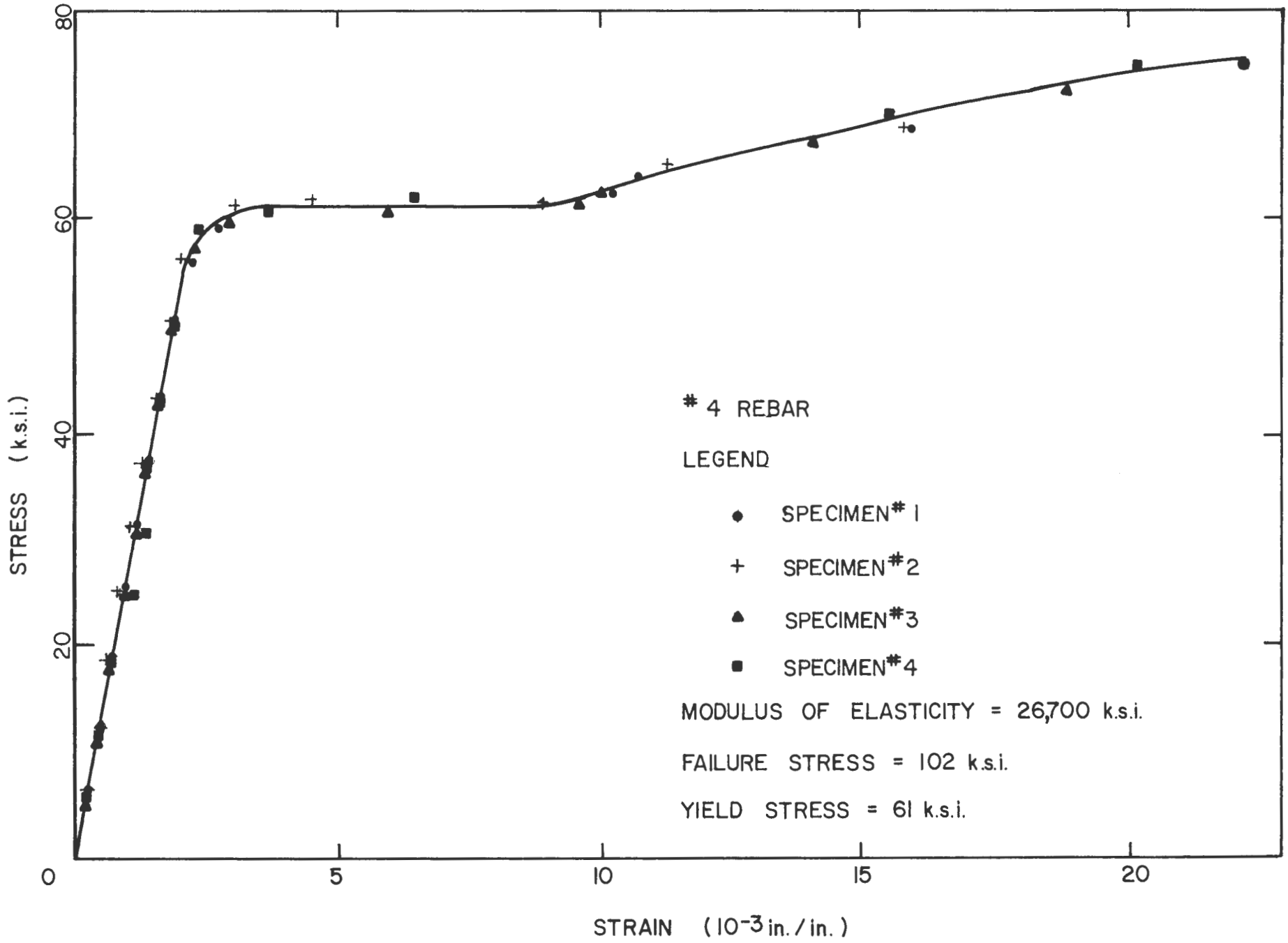

Fig. 8. Stress-Strain Curve of Mild Steel Reinforcement.

Fig. 9 General View of Initial Static Test - Girder 2

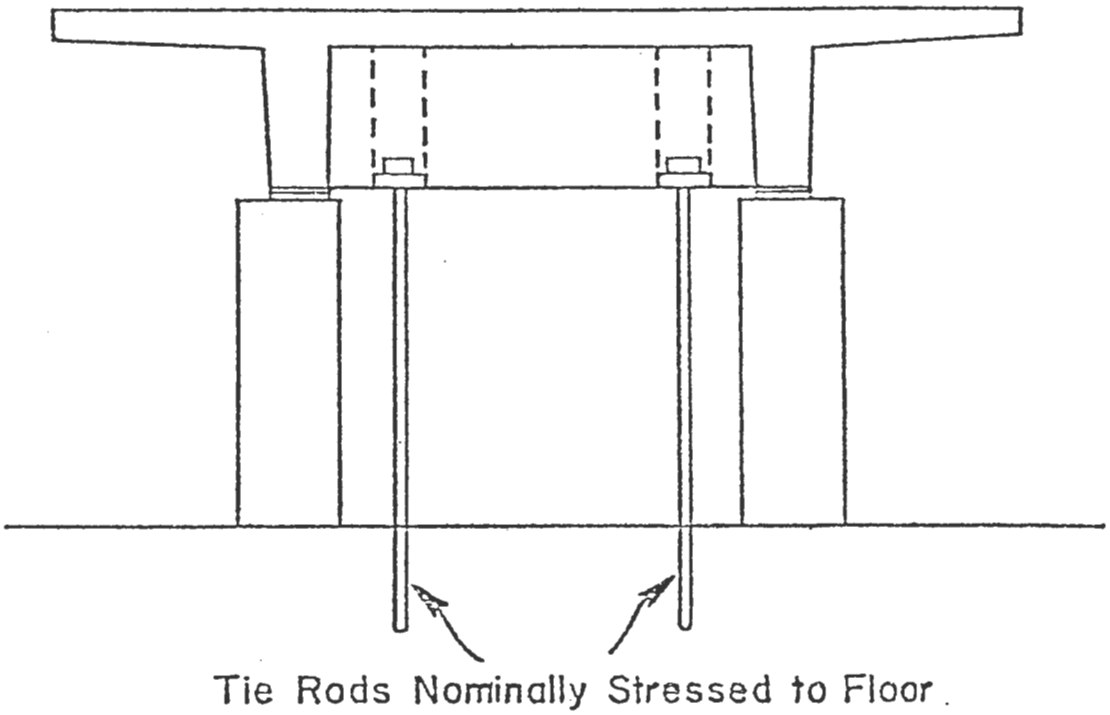

Fig. 10 Hold-Down at End Supports

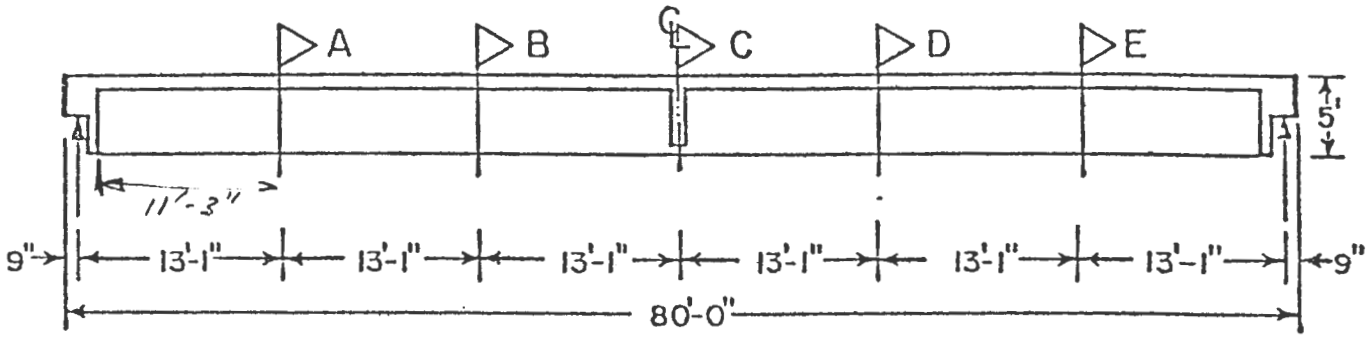

a. Longitudinal Section

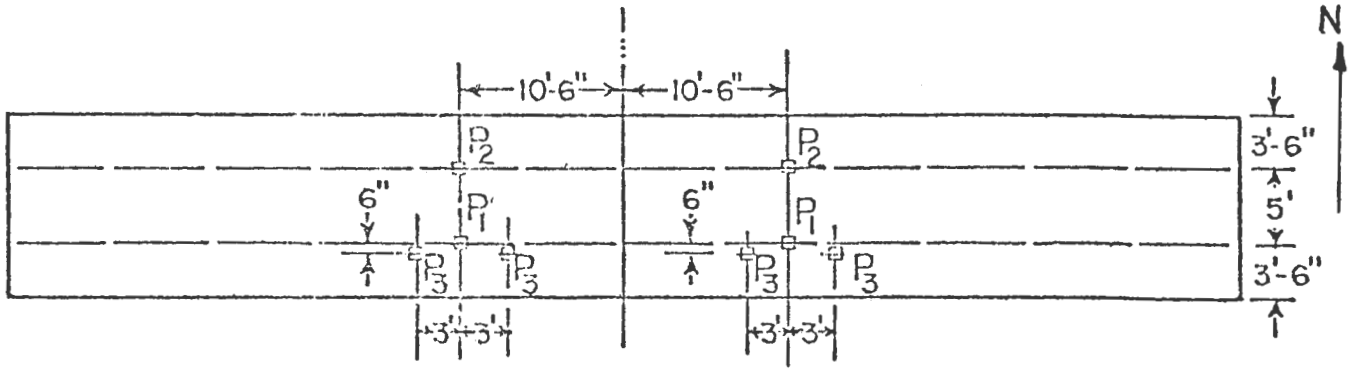

b. Plan — Girder 2

Fig. 11 Loading Locations - Girder 2

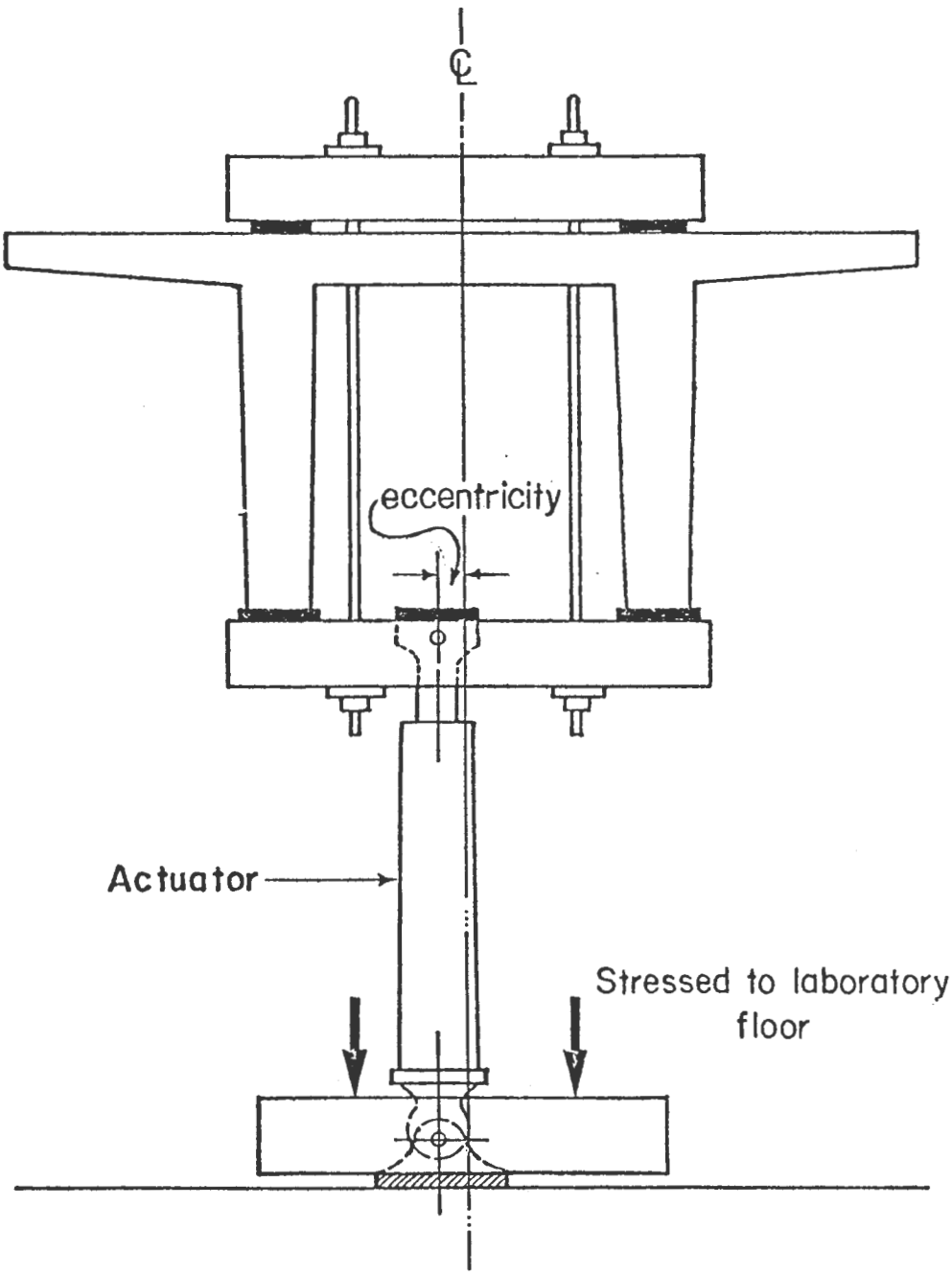

Fig. 12 Fatigue Test Set-Up

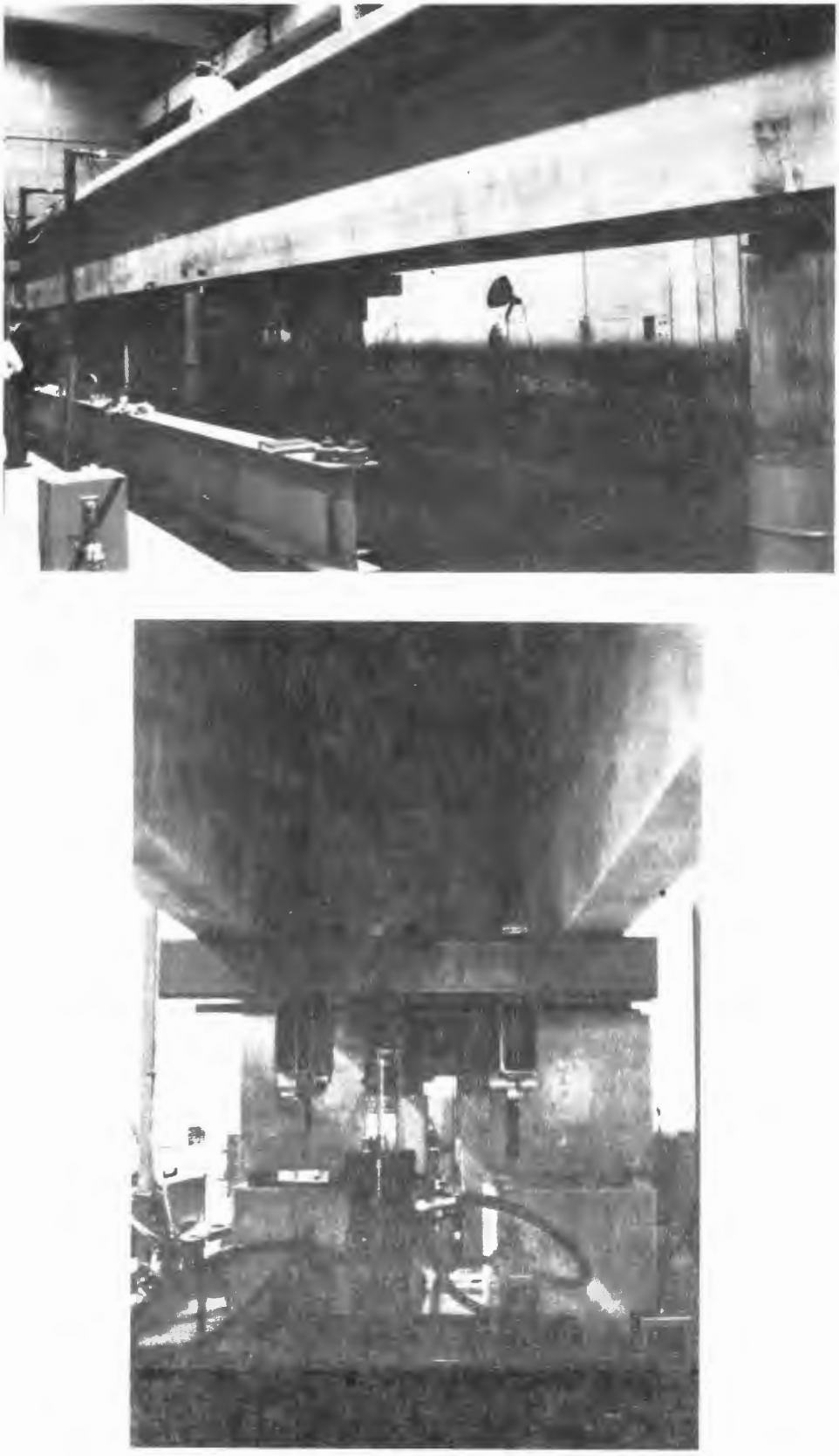

Fig. 13 General View of Fatigue Test - Girder 2

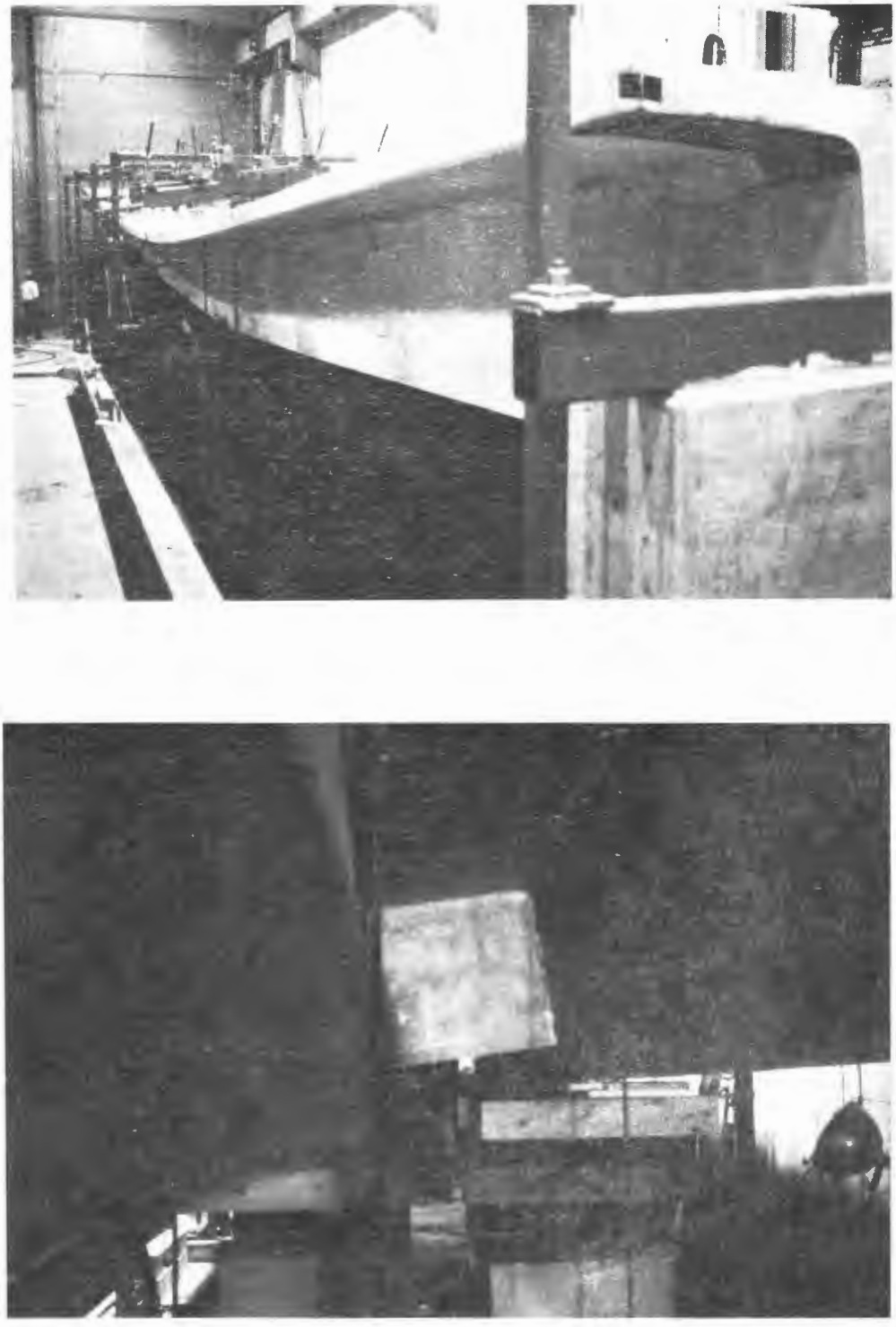

Fig. 14 General View of Derailment Test - Girder 2

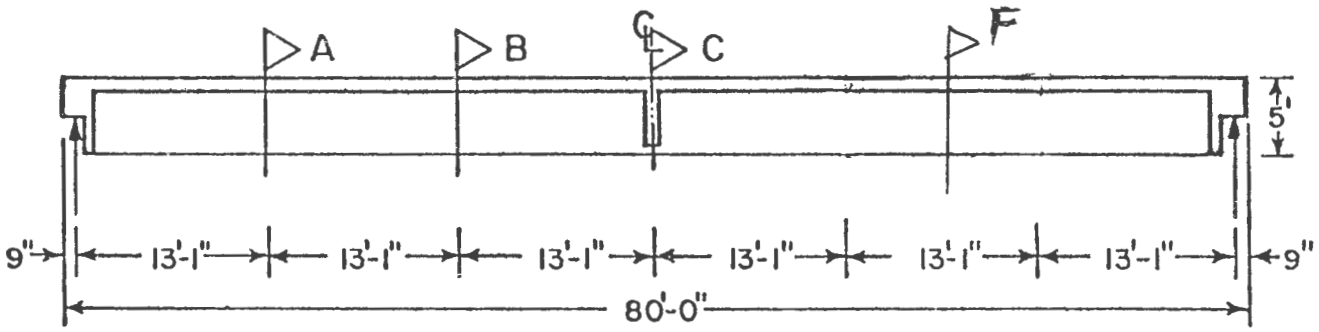

a. Longitudinal Section

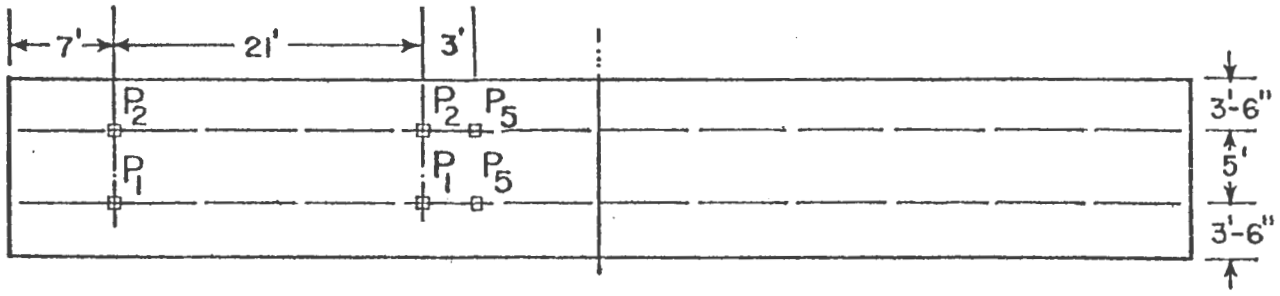

b. Plan , Fatigue Tests

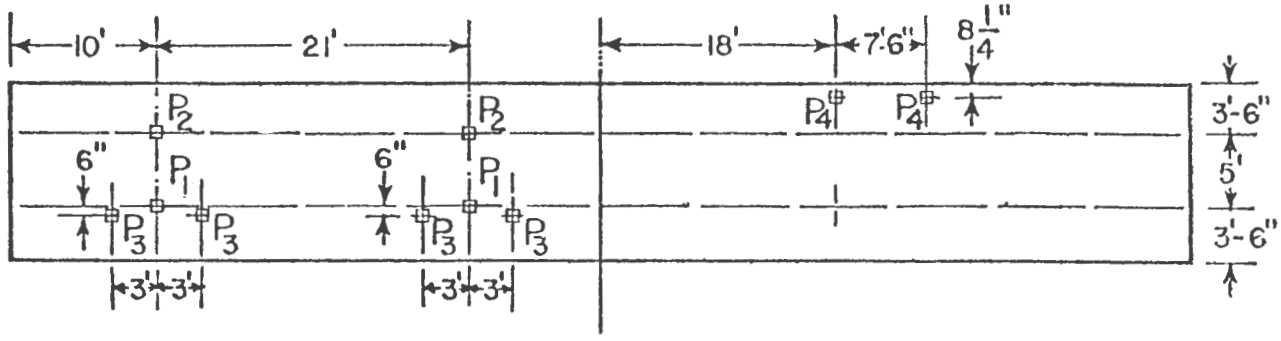

c. Plan , Derailment Tests

Fig. 15 Loading Locations - Girder 3

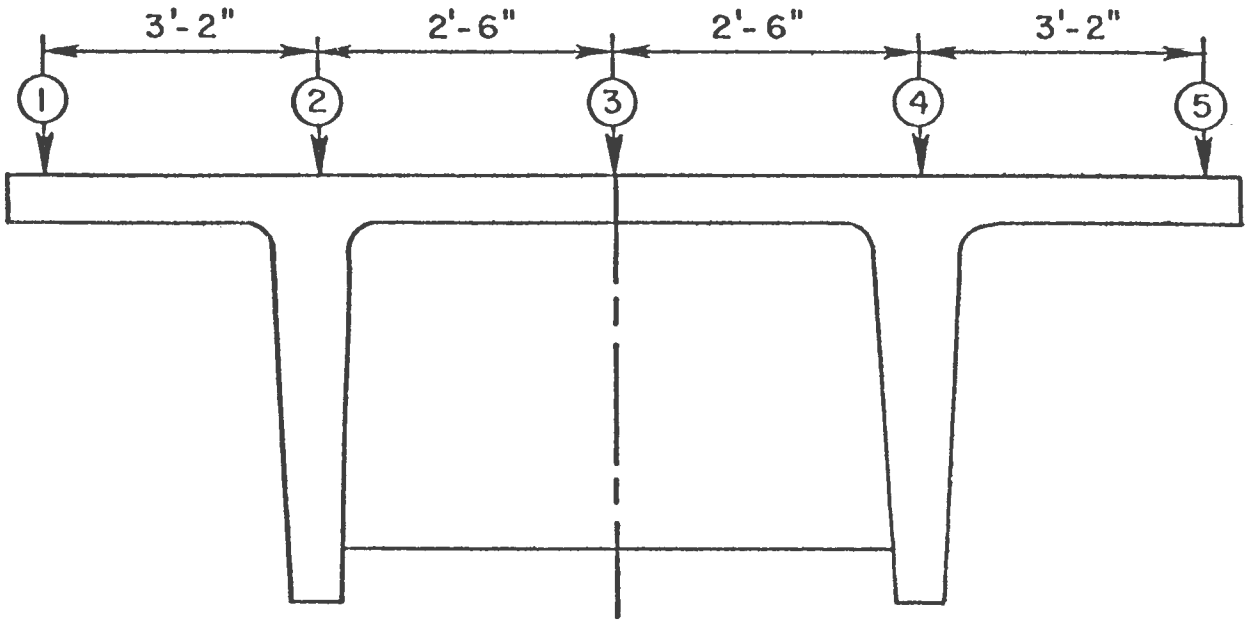

a Vertical Translation

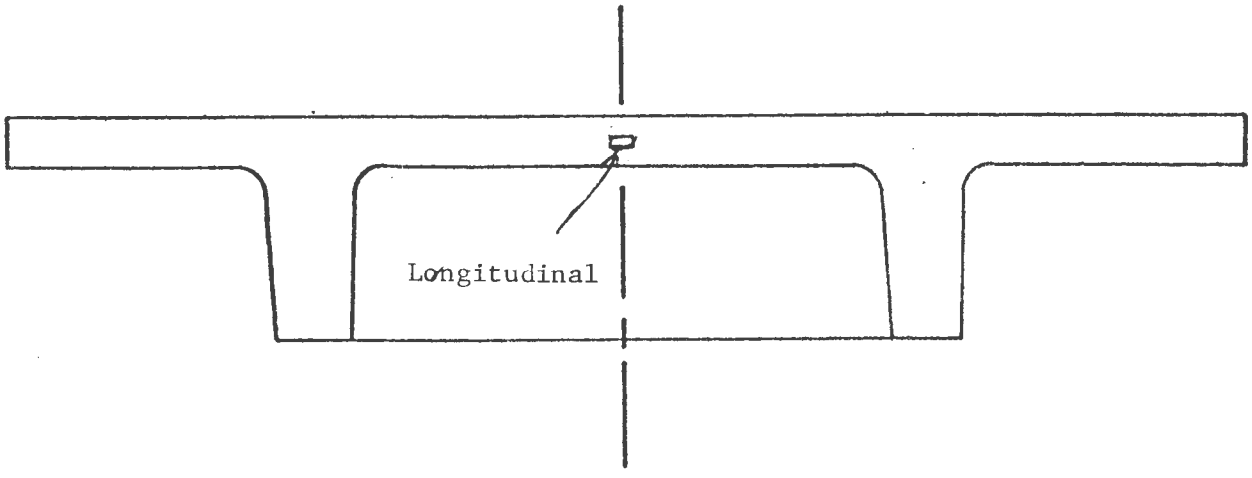

b. Longitudinal Translation at End Diaphragm

Fig. 16 Locations of Translation Measurements

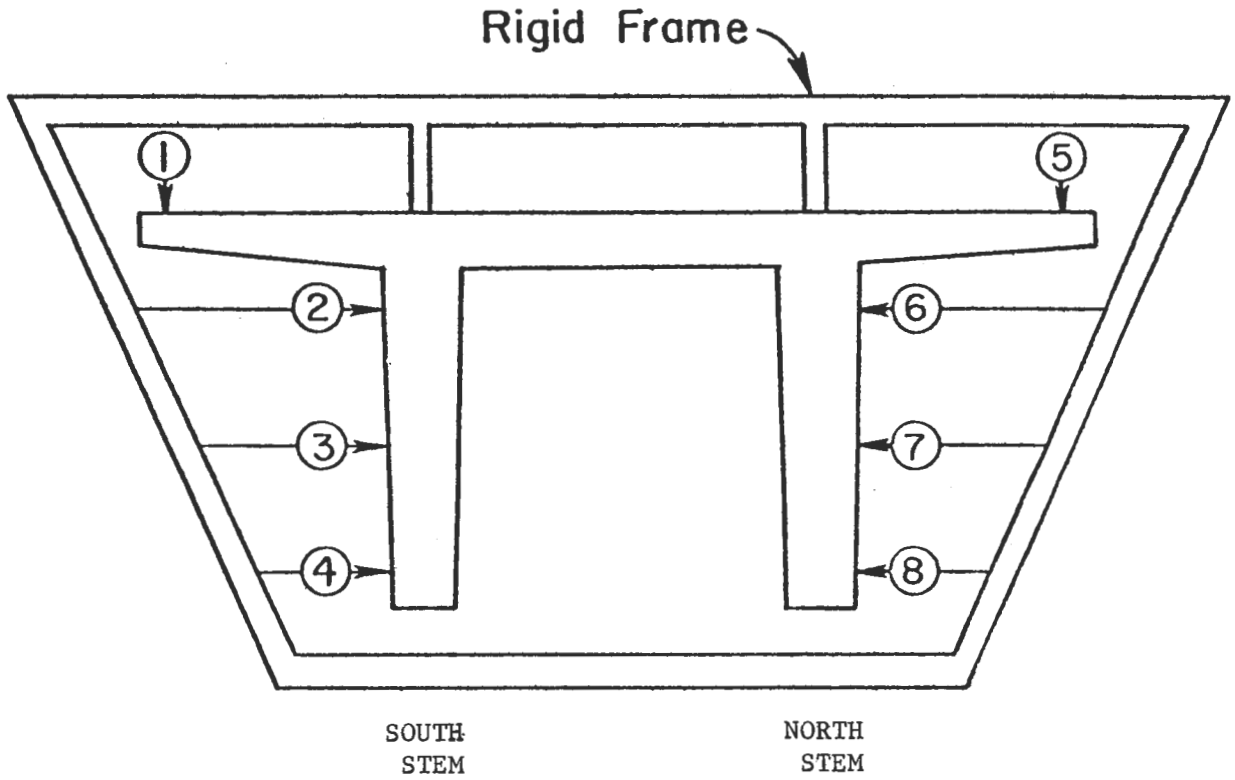

Fig. 17 Measurement of Deformation of Cross Section

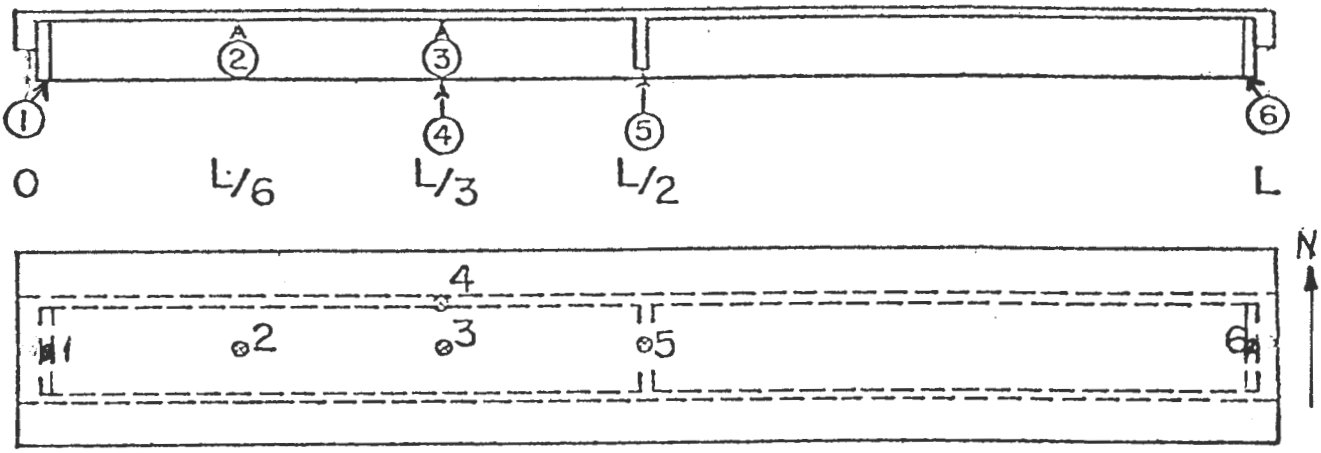

(a) Girder 2

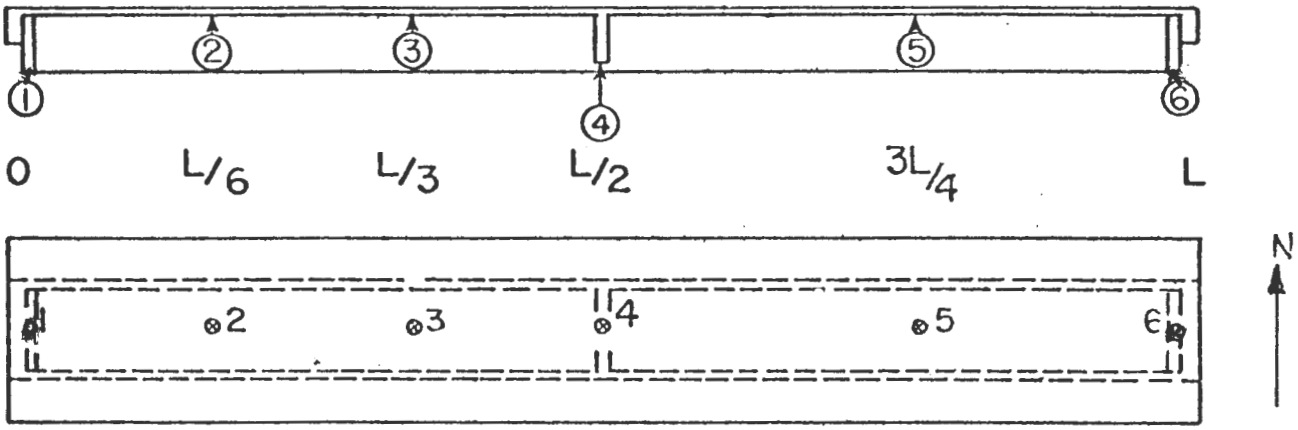

(b) Girder 3

Fig. 18 Locations of Rotation Measurements

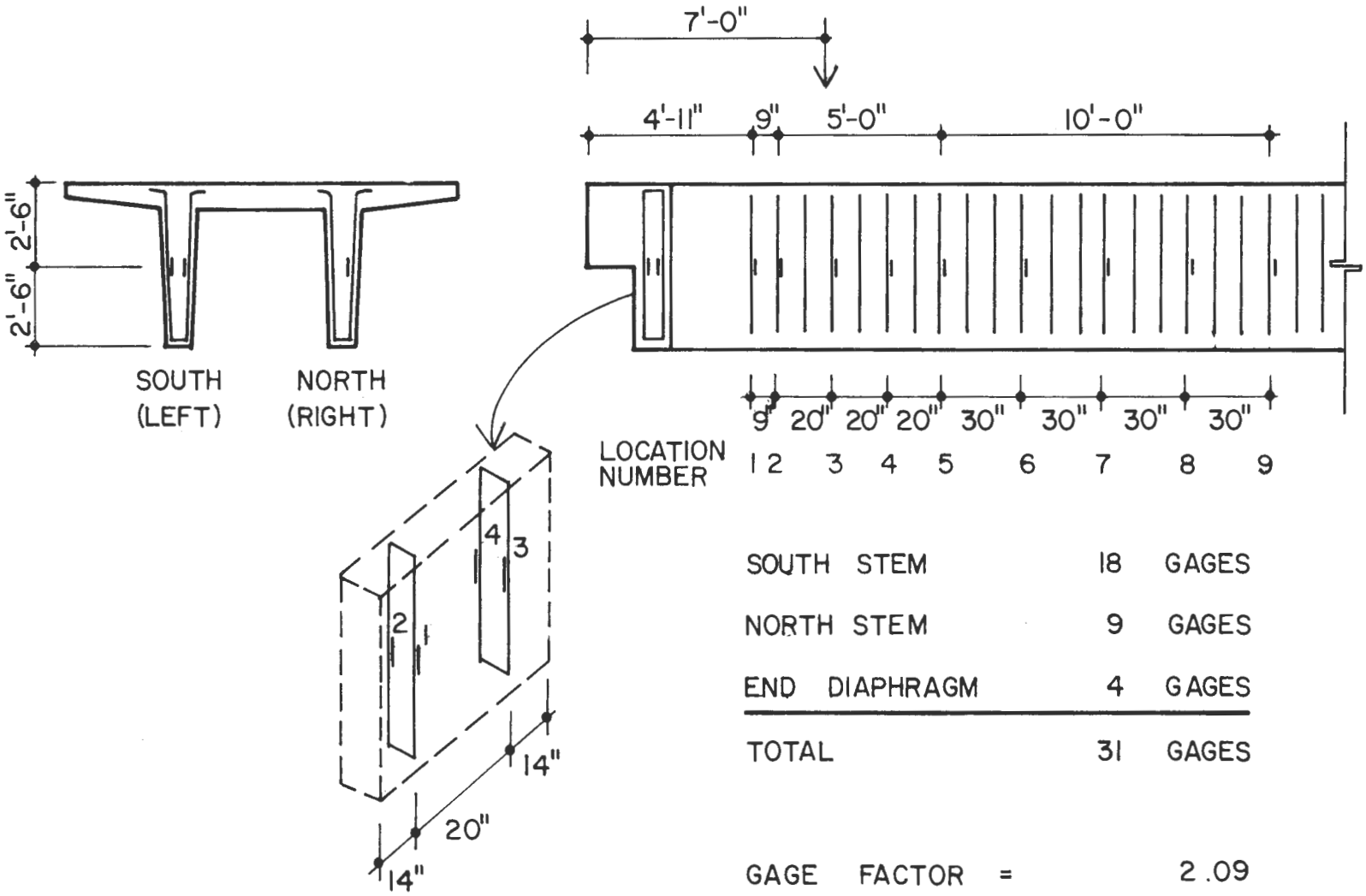

Fig. 19. SR4 Gage Locations in Girder 3

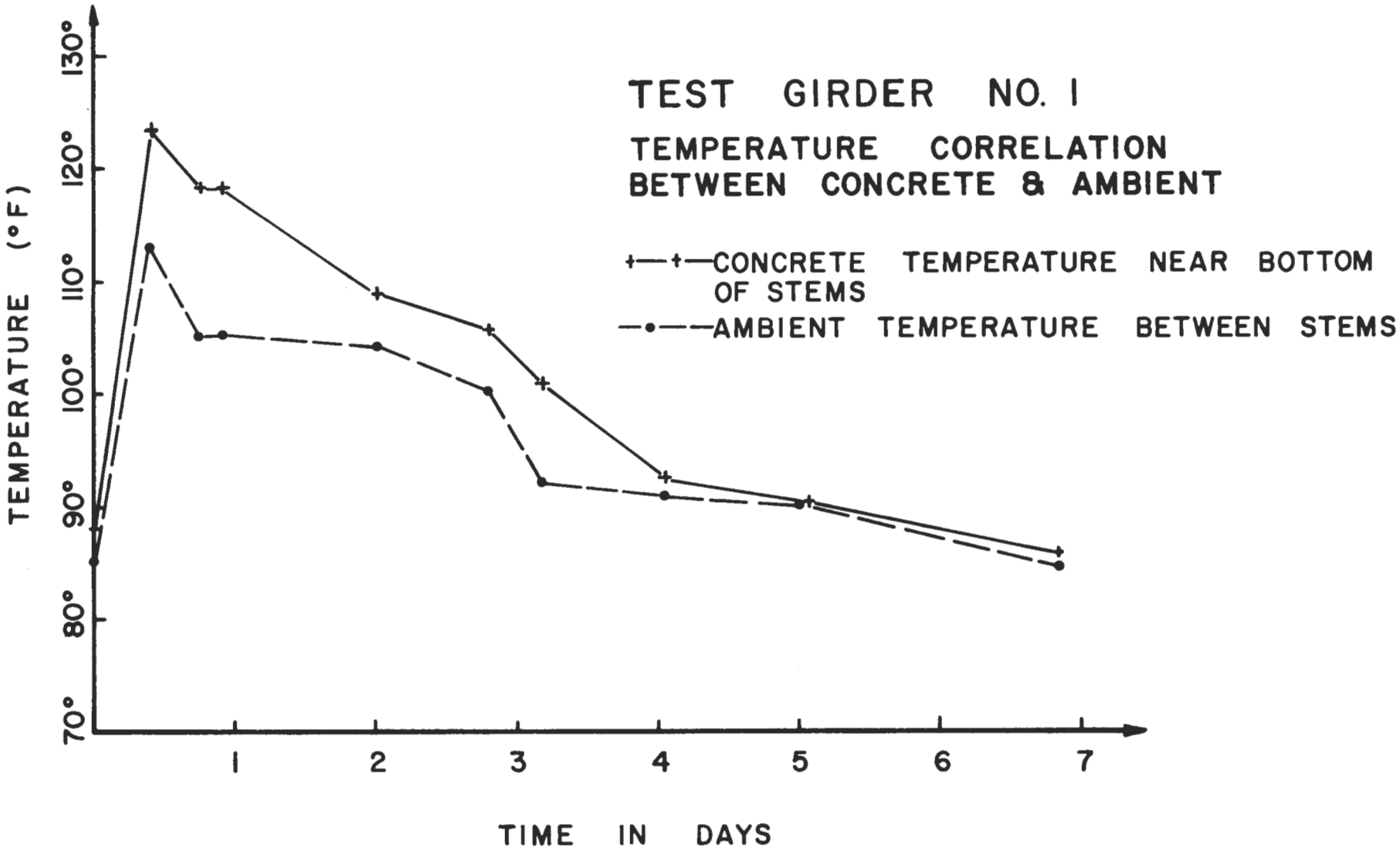

Fig. 20. Temperature Change of Concrete at Early Age

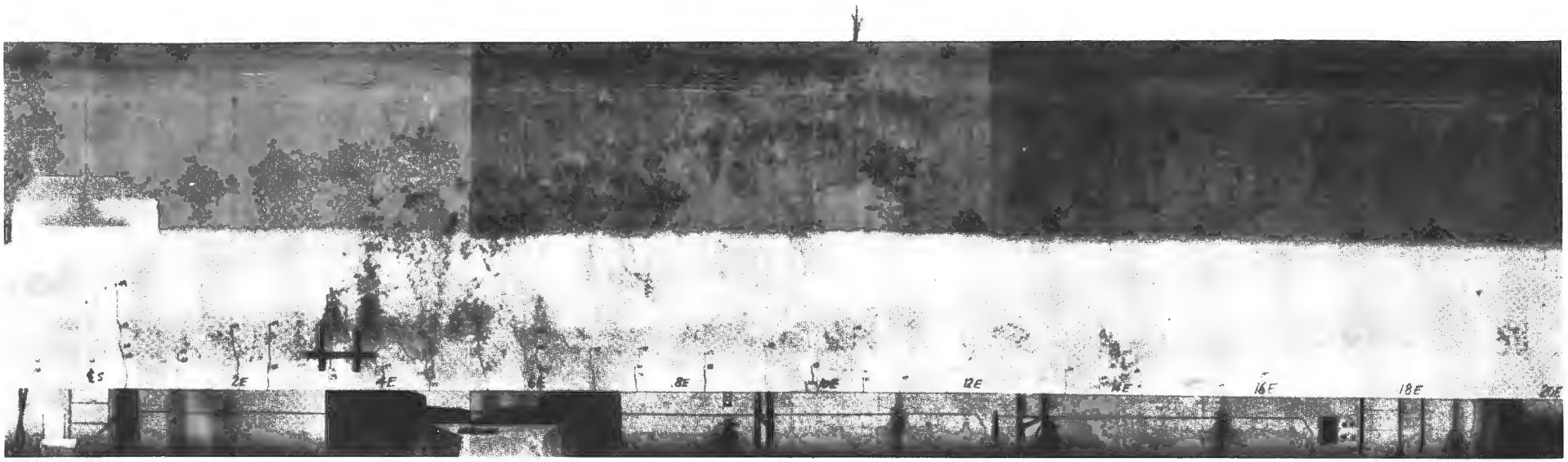

Fig. 21a Crack Pattern for Initial Static Test of Girder 2 (Center Line to 20 Ft. East)

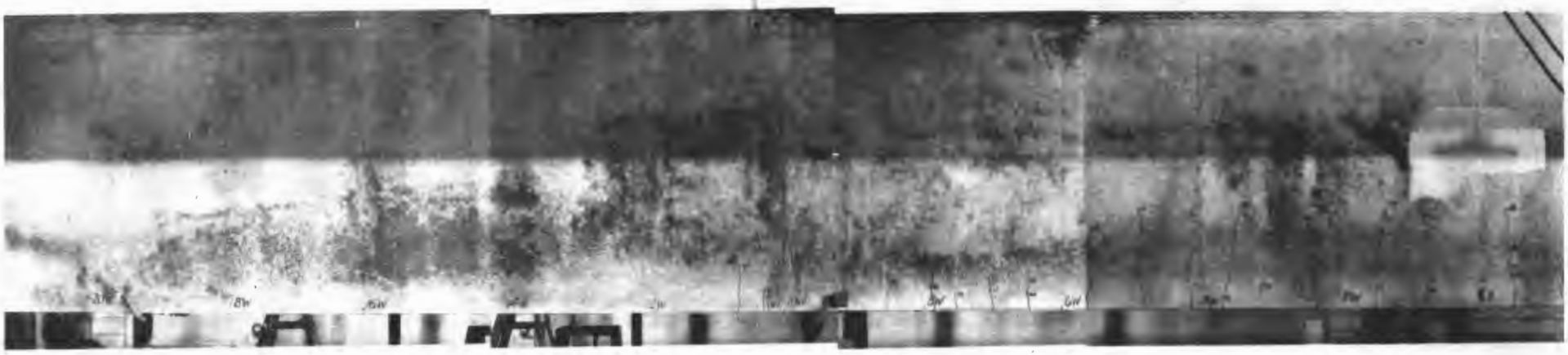

Fig. 21 b Crack Pattern for Initial Static Test of Girder 2 (Center Line to 20 Ft. West)

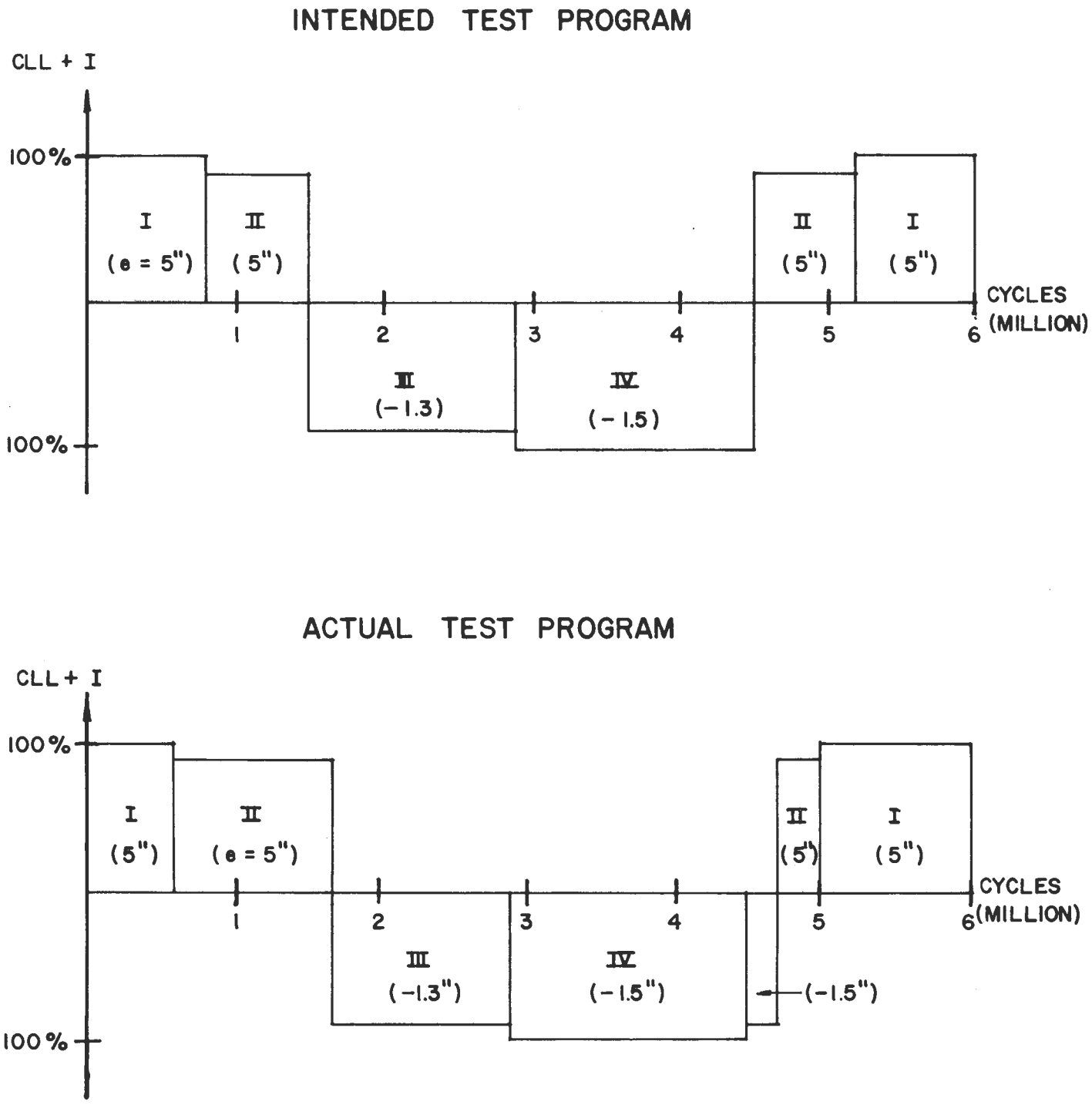

Fig. 22 Fatigue Test Program - Girder 2

Fig. 22A. Cracking Pattern prior to Fatigue Test - Girder 3.

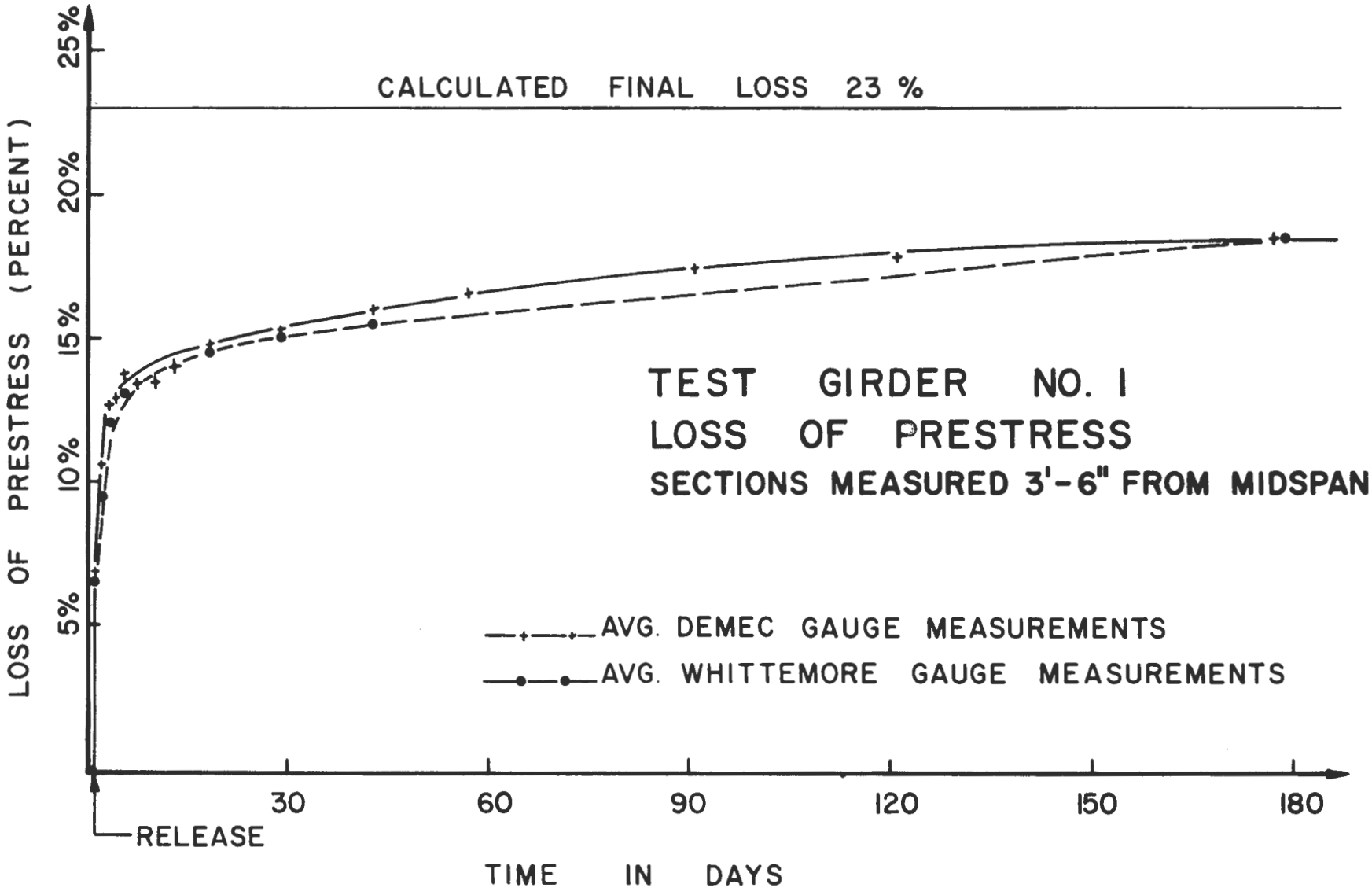

Fig. 23. Loss of Prestress - Girder I

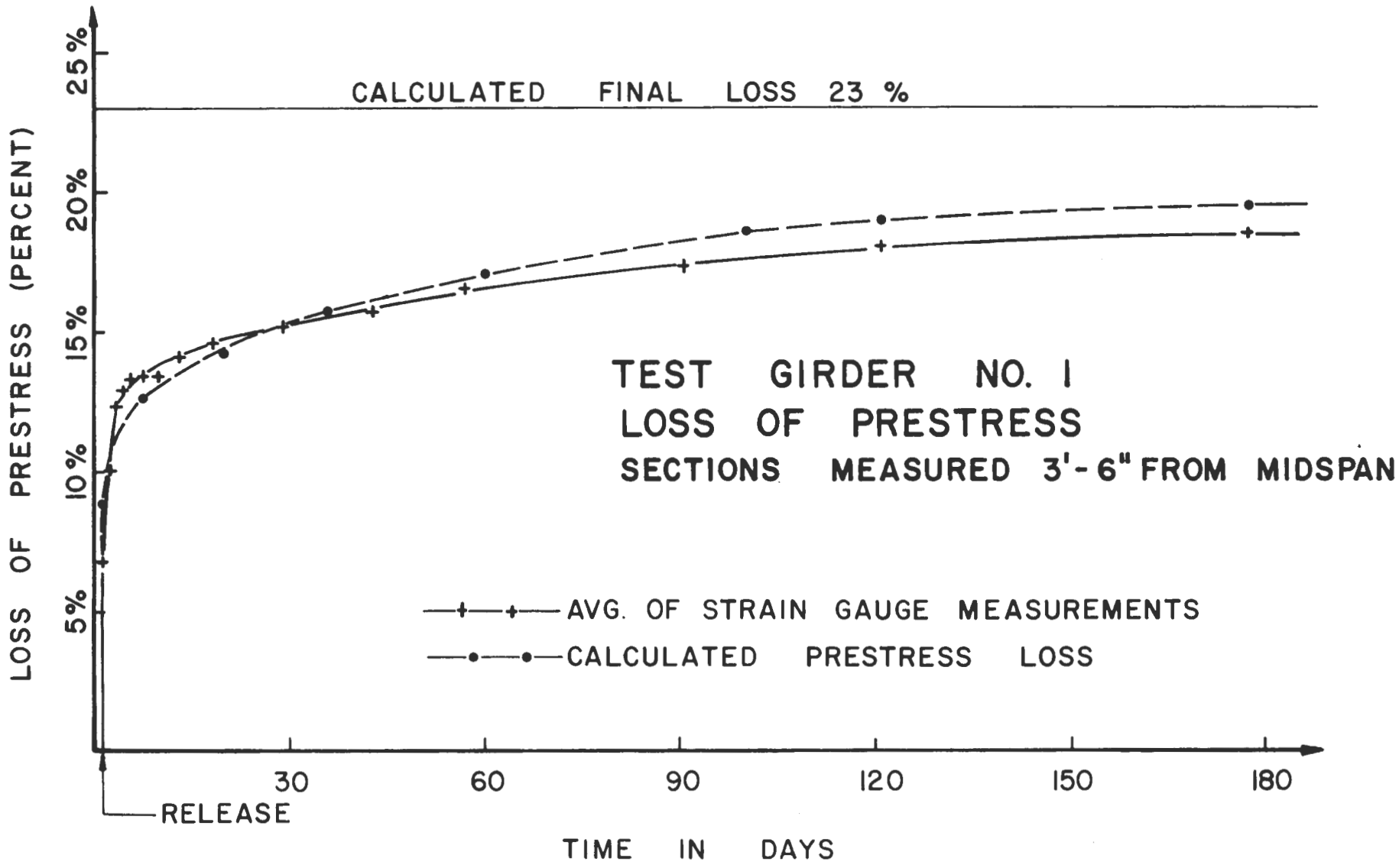

Fig. 24. Comparison of Experimental and Theoretical Prestress Losses - Girder 1

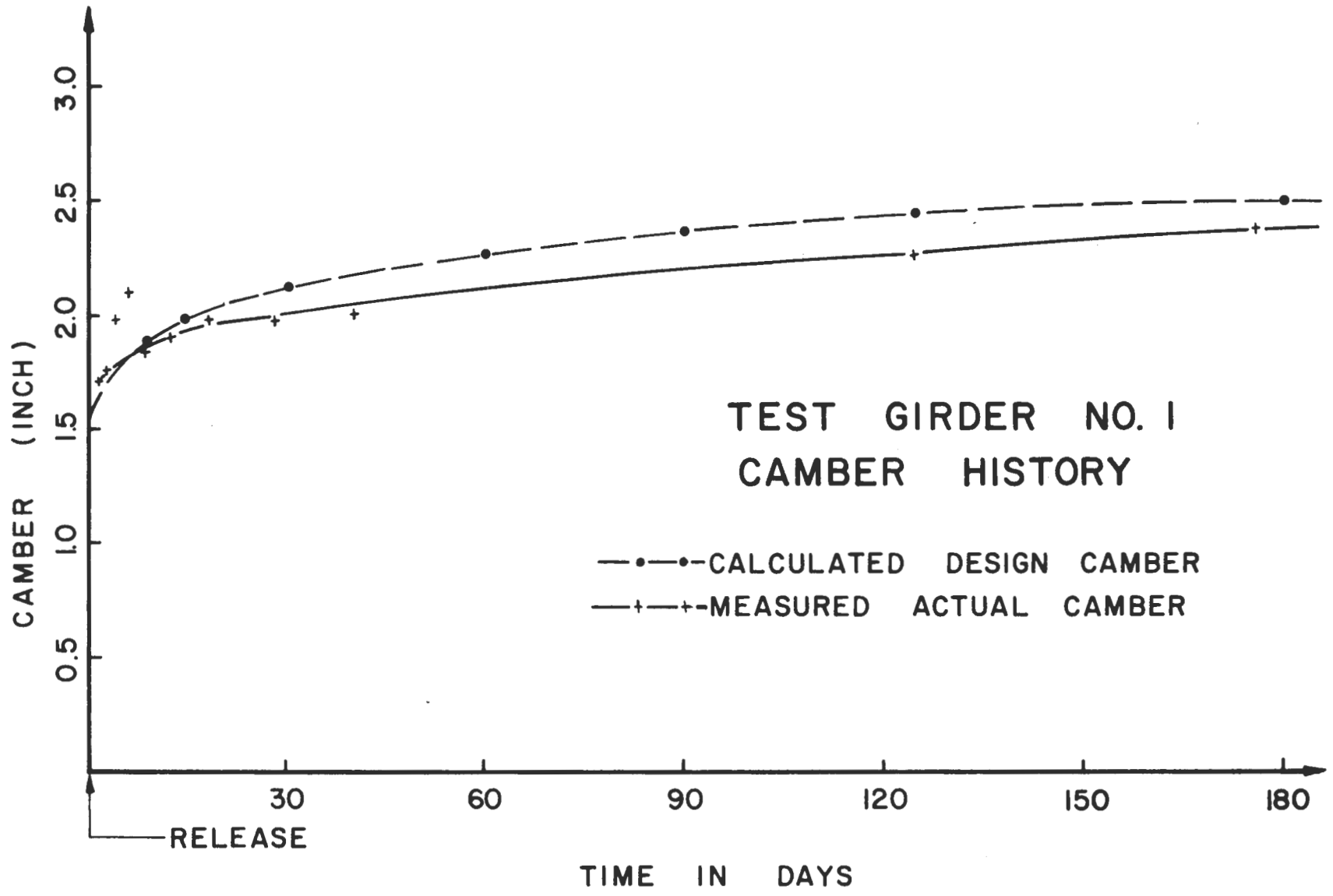

Fig. 25. Camber Growth - Girder 1

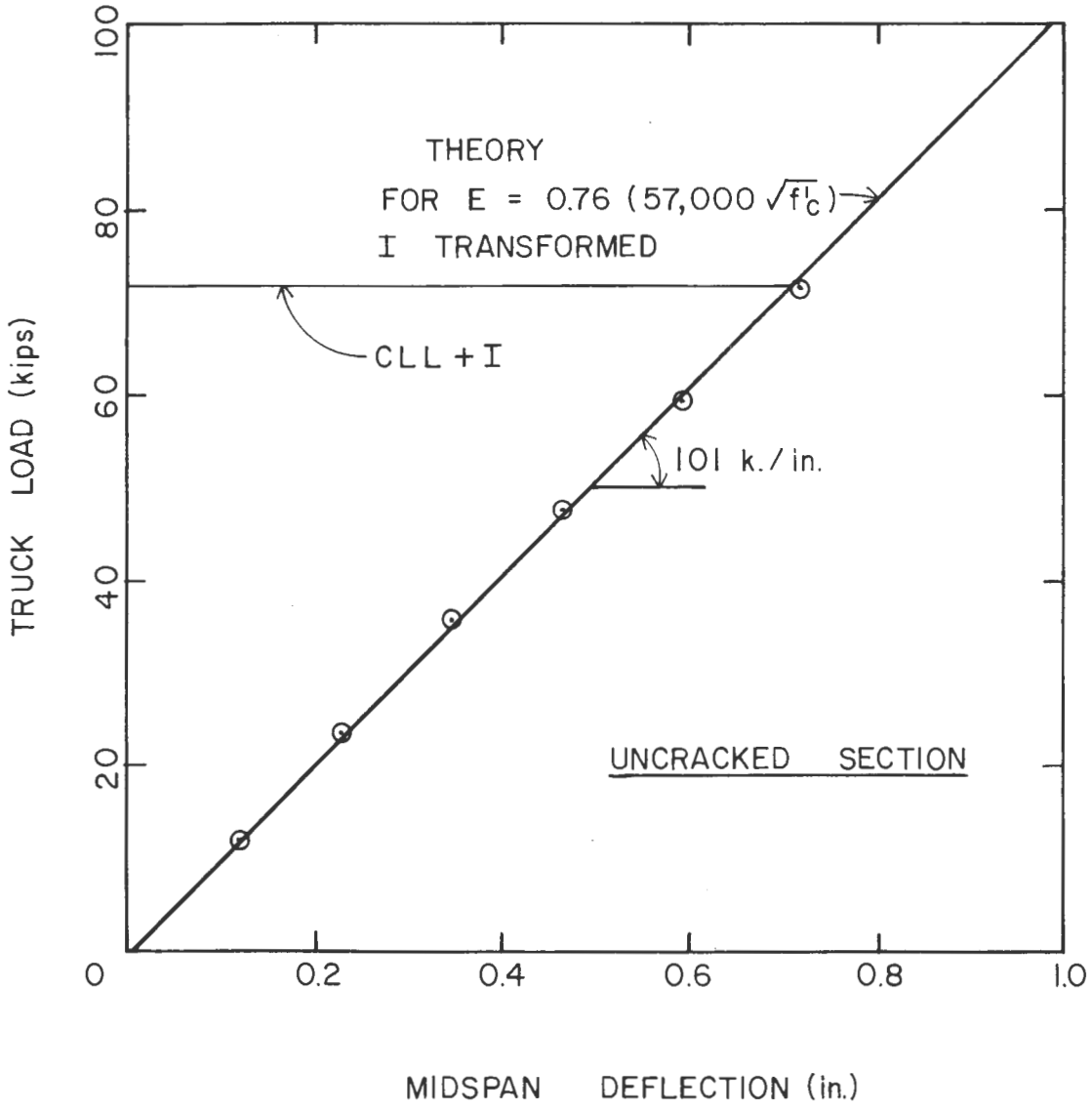

Fig. 26. Loads vs. Midspan Deflections (Uncracked) - Girder 2, Initial Static Test.

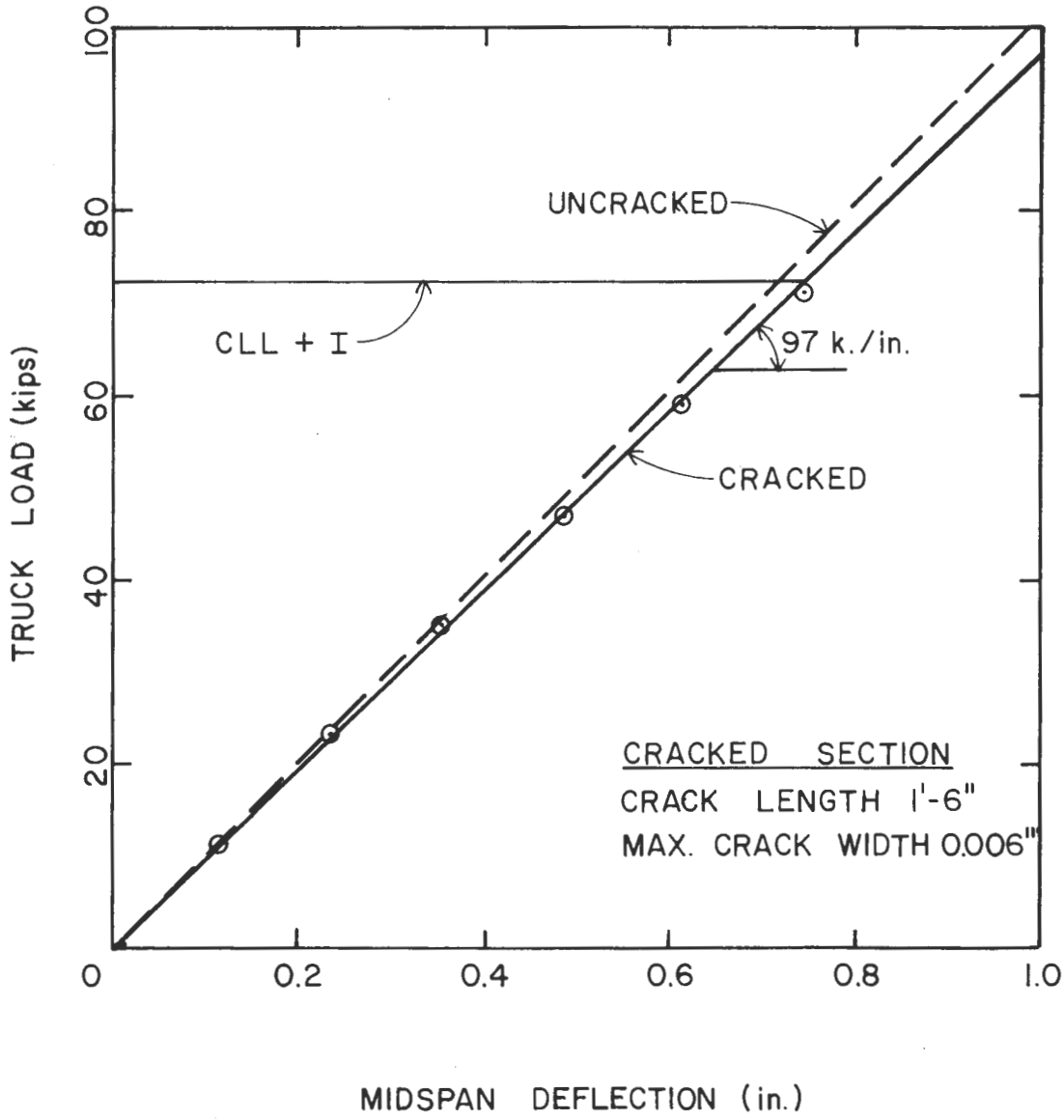

Fig. 27. Load vs. Midspan Deflections (Cracked) - Girder 2, Initial Static Test.

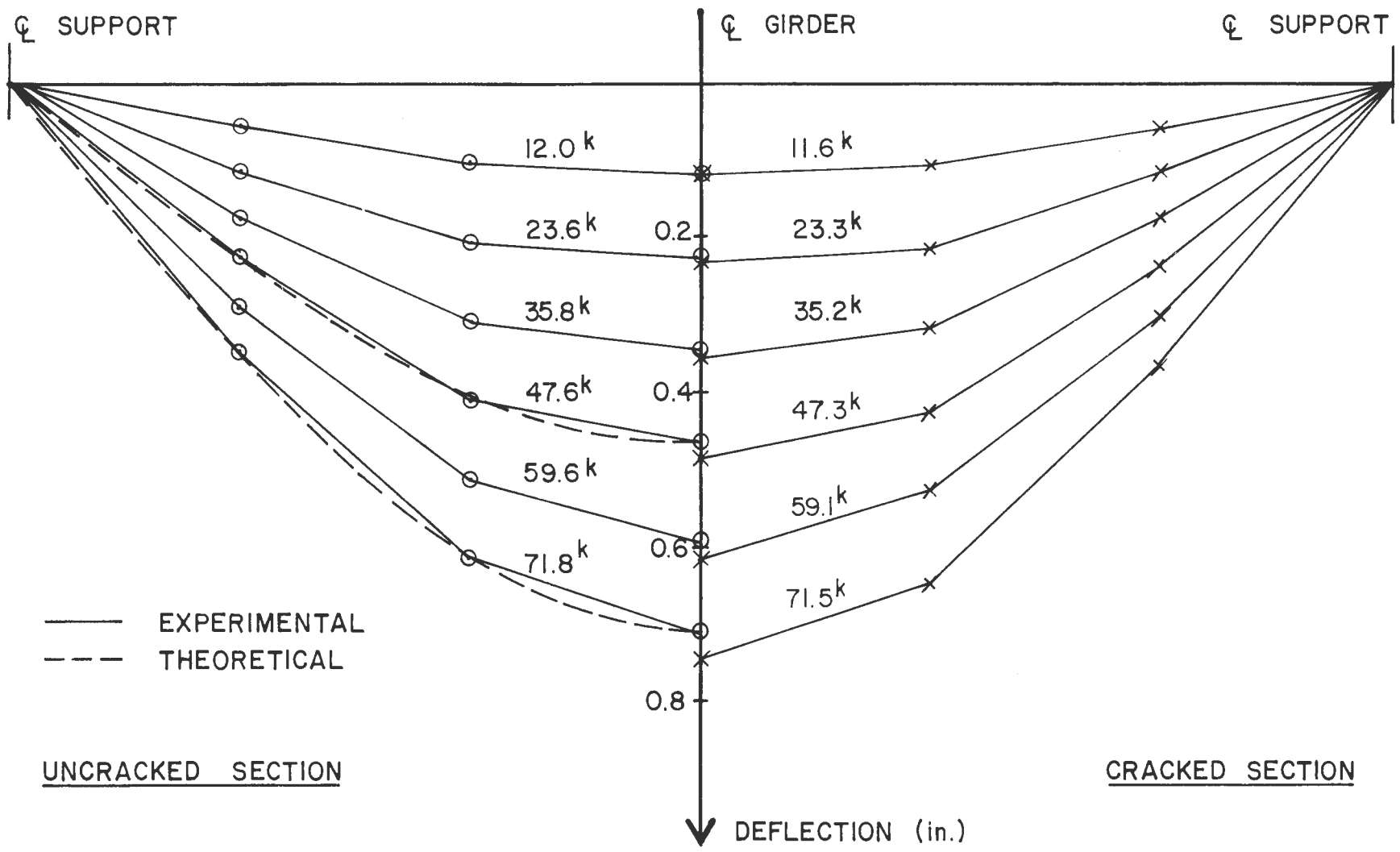

Fig. 28. Deflections Along Girder Axis - Girder 2, Initial Static Test.

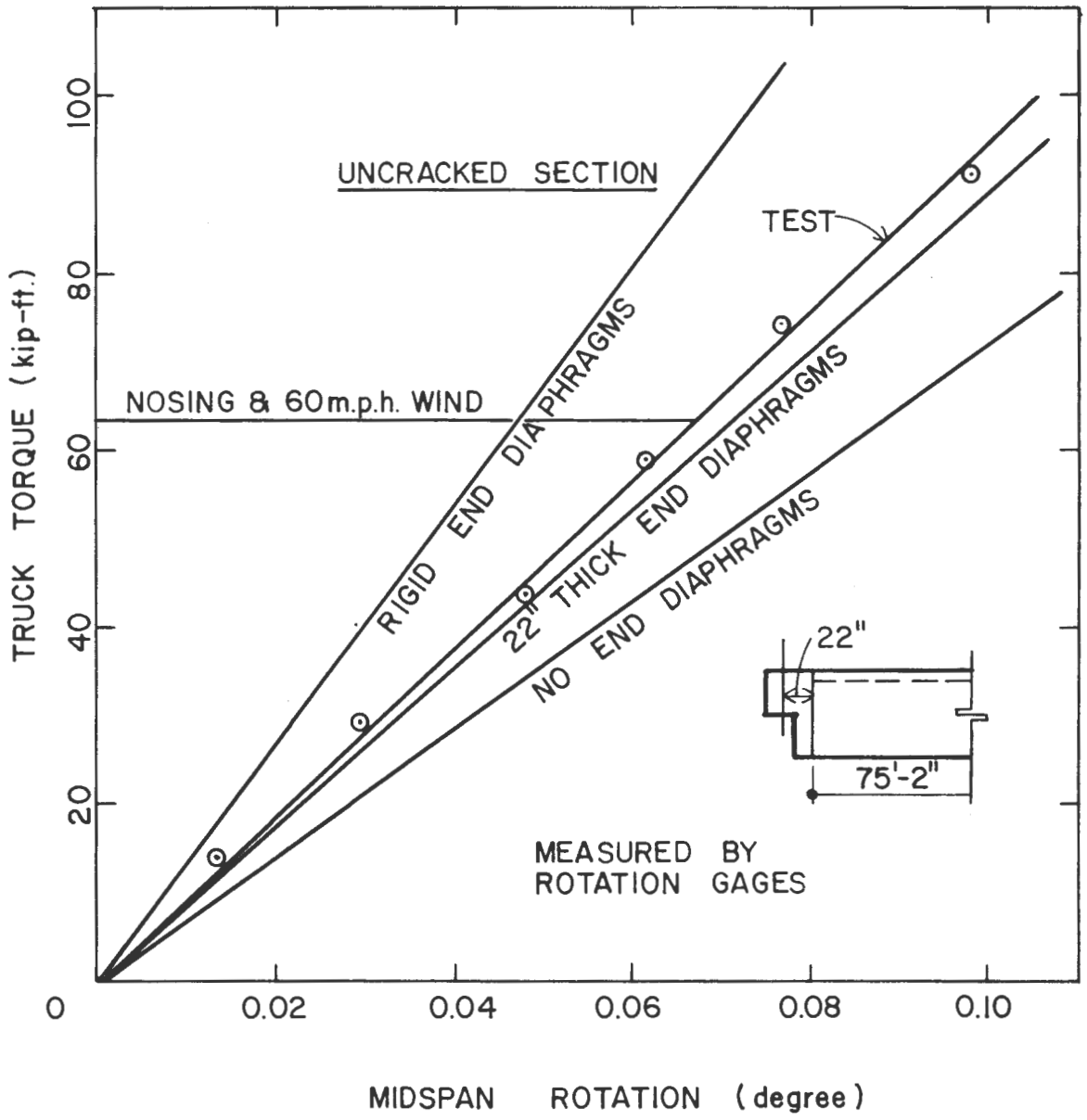

Fig. 29. Torque vs. Midspan Rotation (Uncracked)

- Girder 2, Initial Static Test.

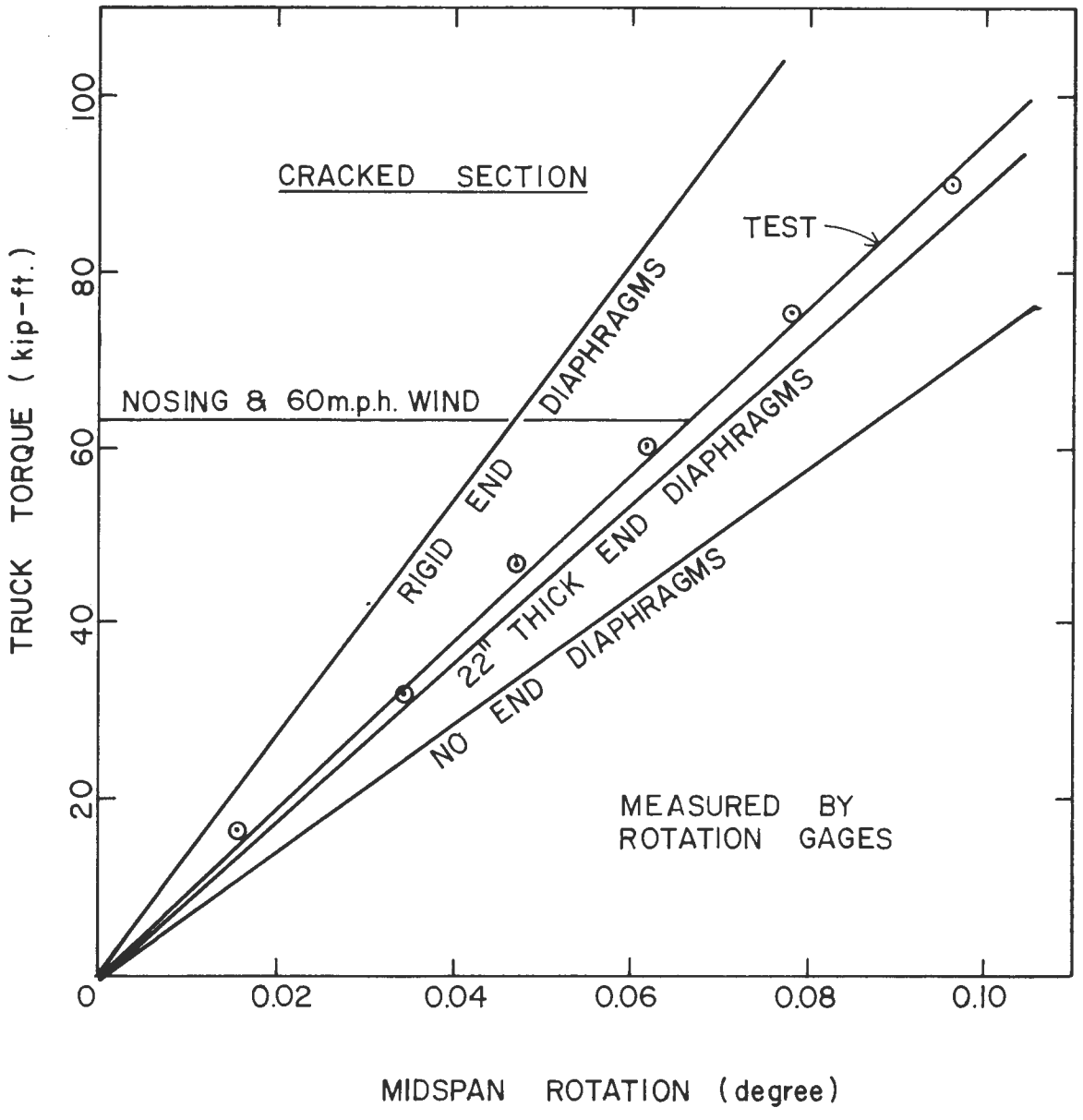

Fig. 30. Torque vs. Midspan Rotation (Cracked)

- Girder 2, Initial Static Test.

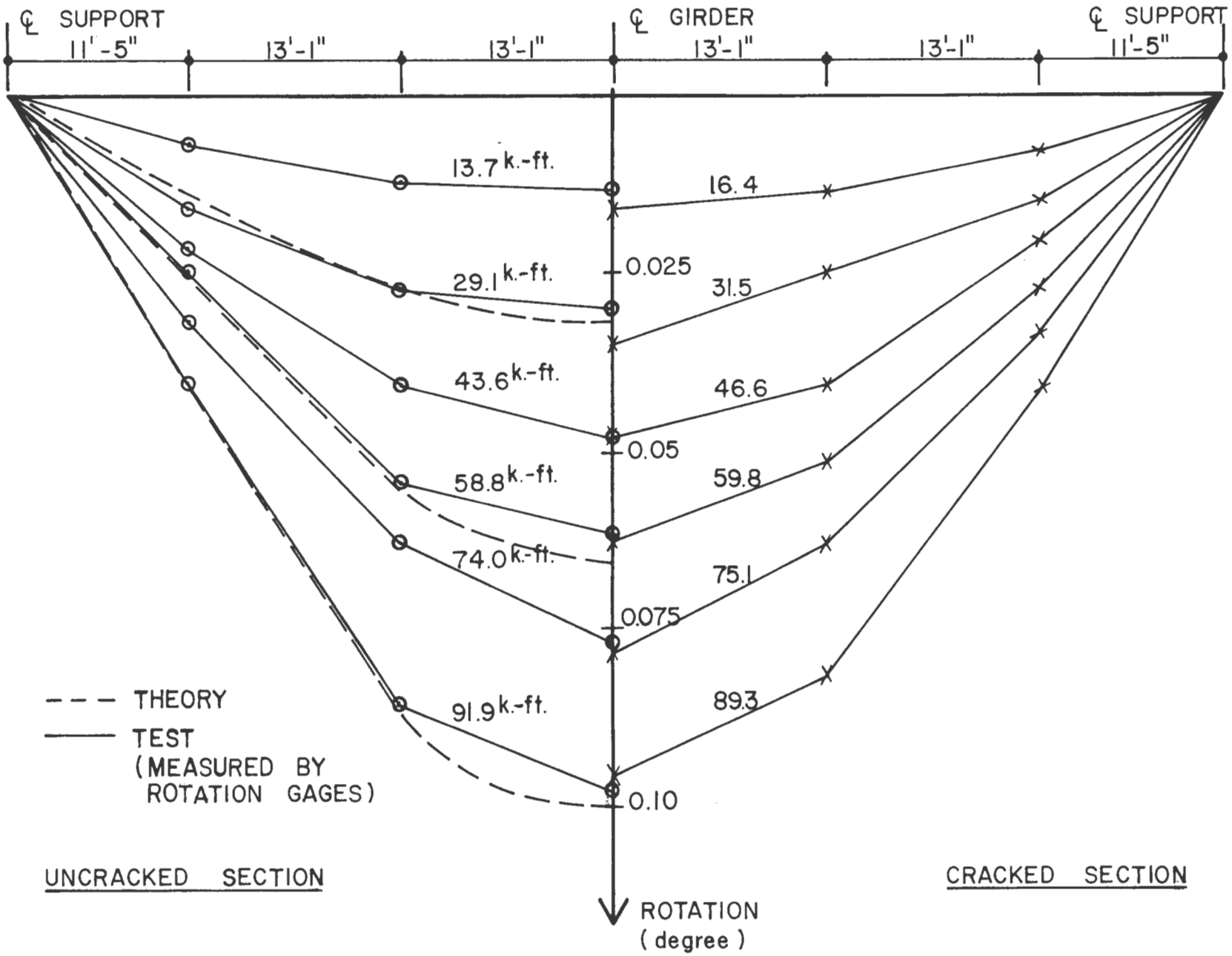

Fig. 31. Rotations Along Girder Axis - Girder 2, Initial Static Test.

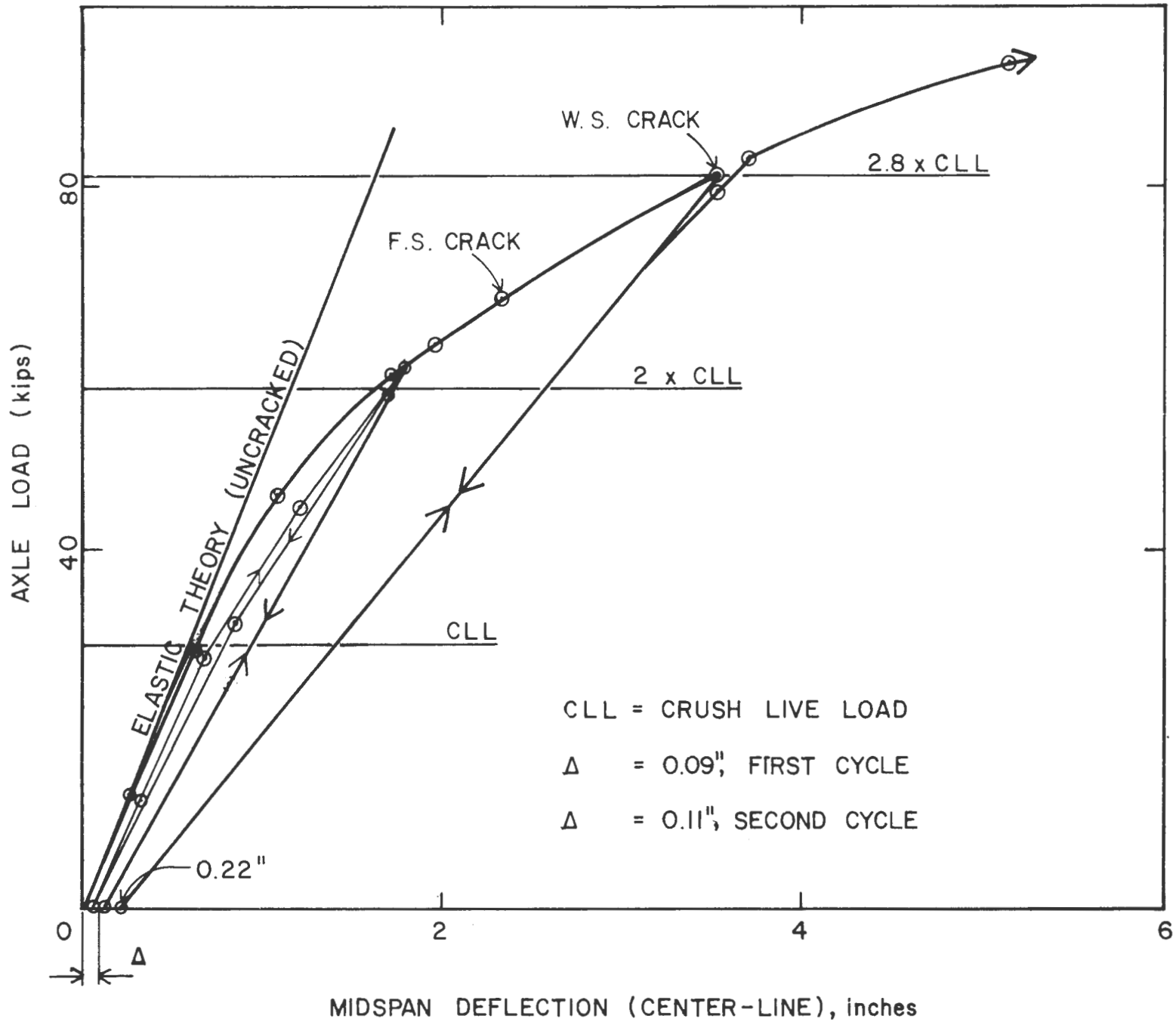

Fig. 32a. Load vs. Midspan Deflection (Center Line) - Girder 2, Derailment Test.

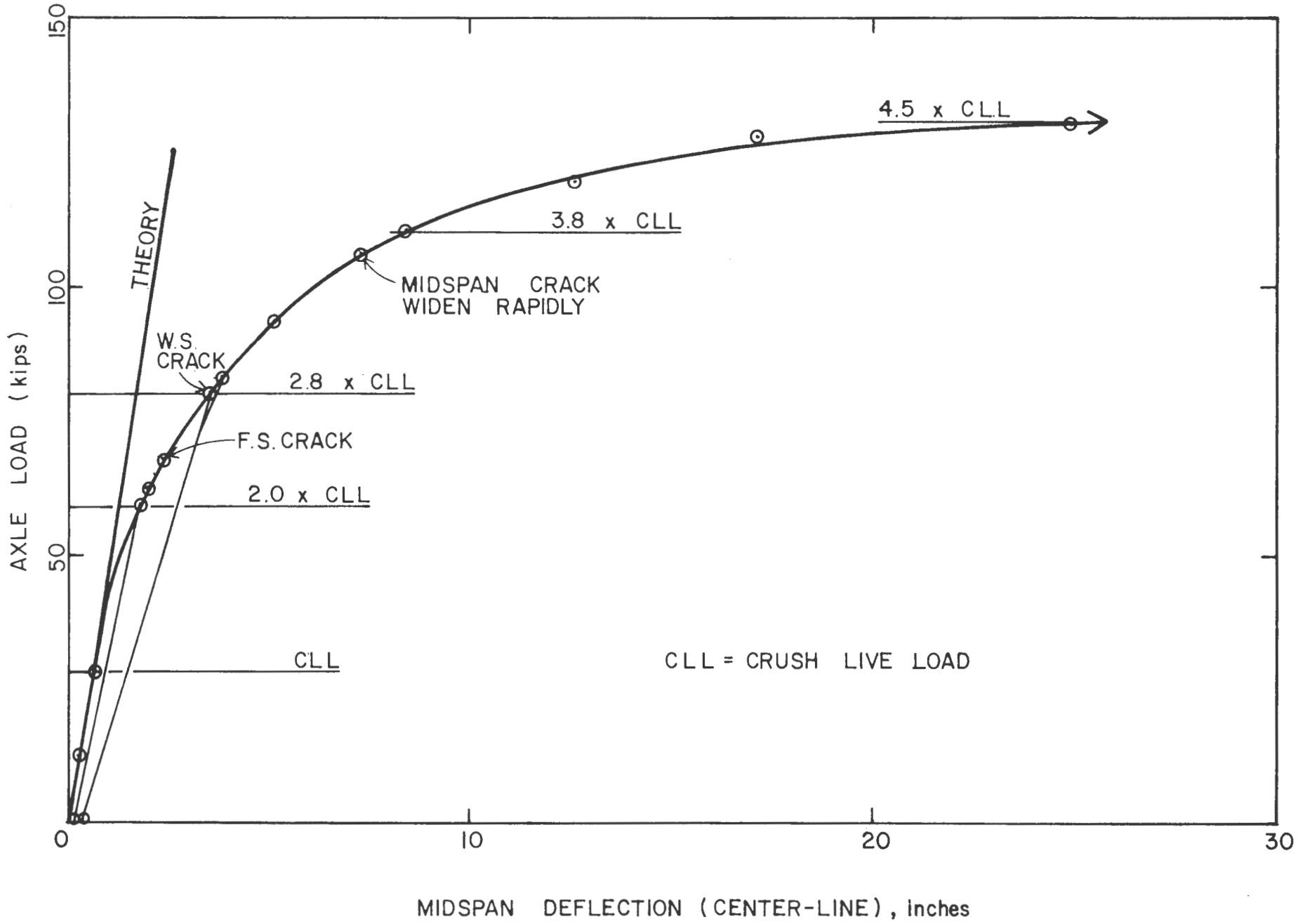

Fig. 32b. Load vs. Midspan Deflection (Center Line) - Girder 2, Derailment Test.

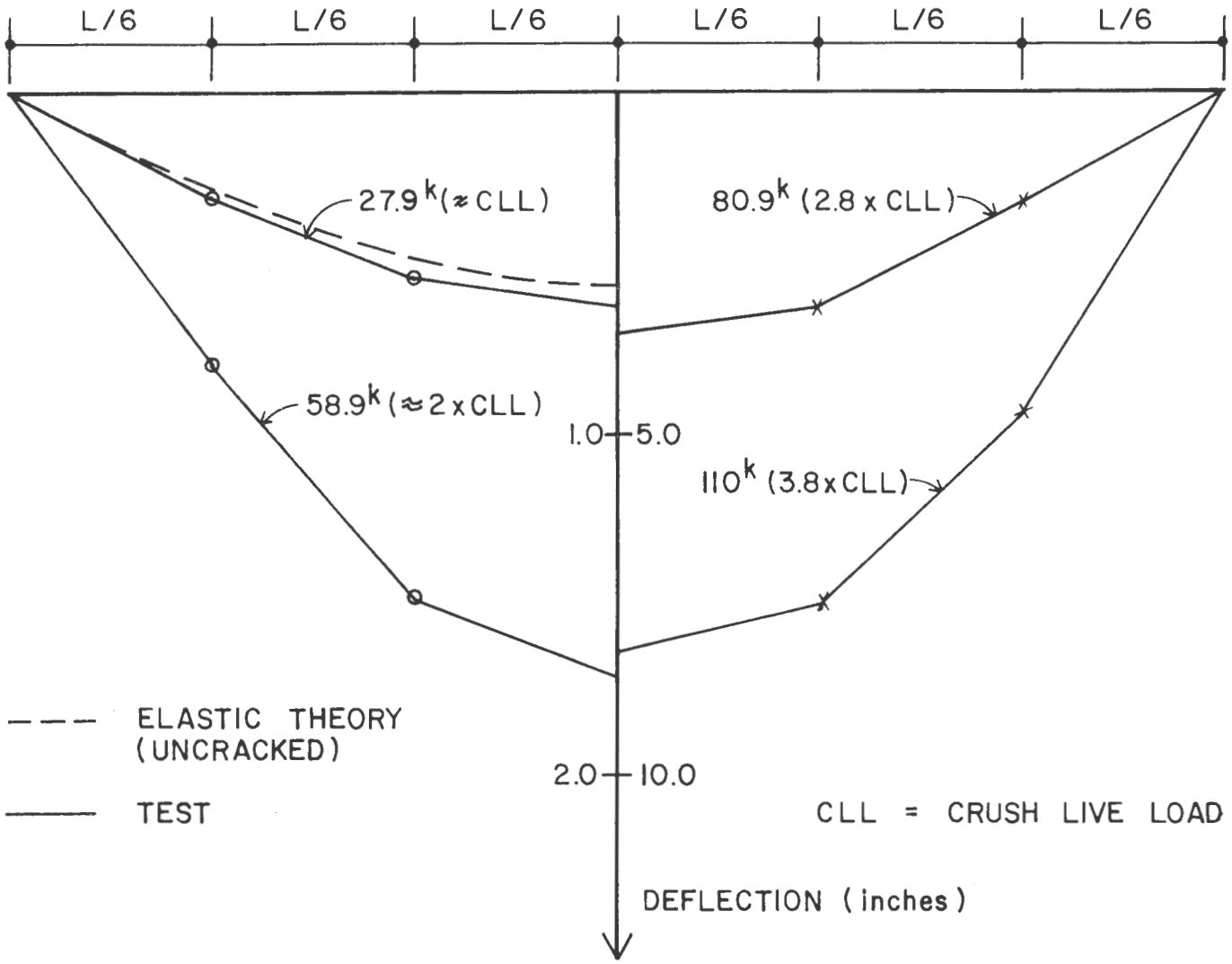

Fig. 33. Deflection Along Center-Line Axis - Girder 2, Derailment Test.

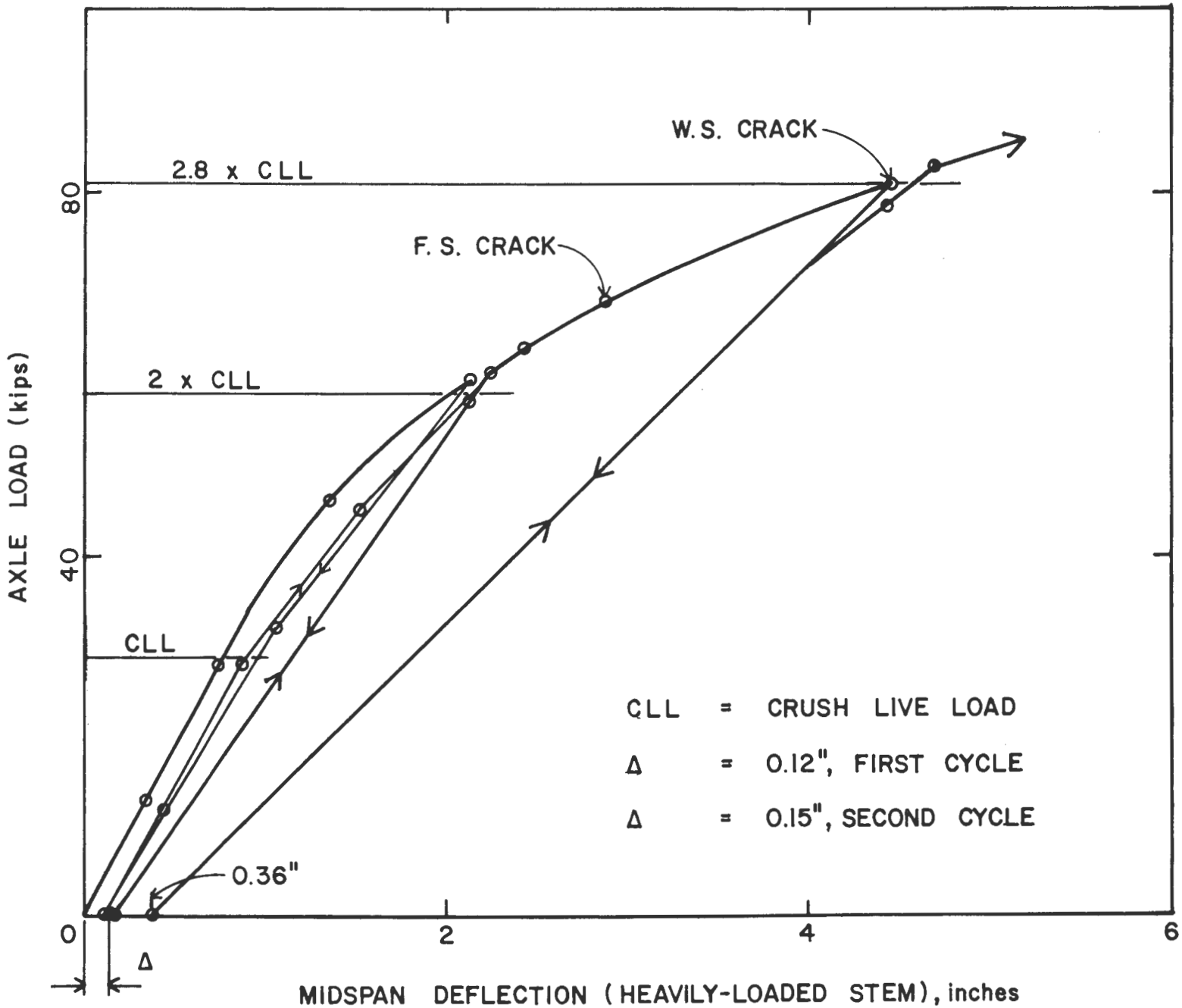

Fig. 34. Load vs. Midspan Deflection (Heavily-Loaded Stem) - Girder 2, Derailment Test.

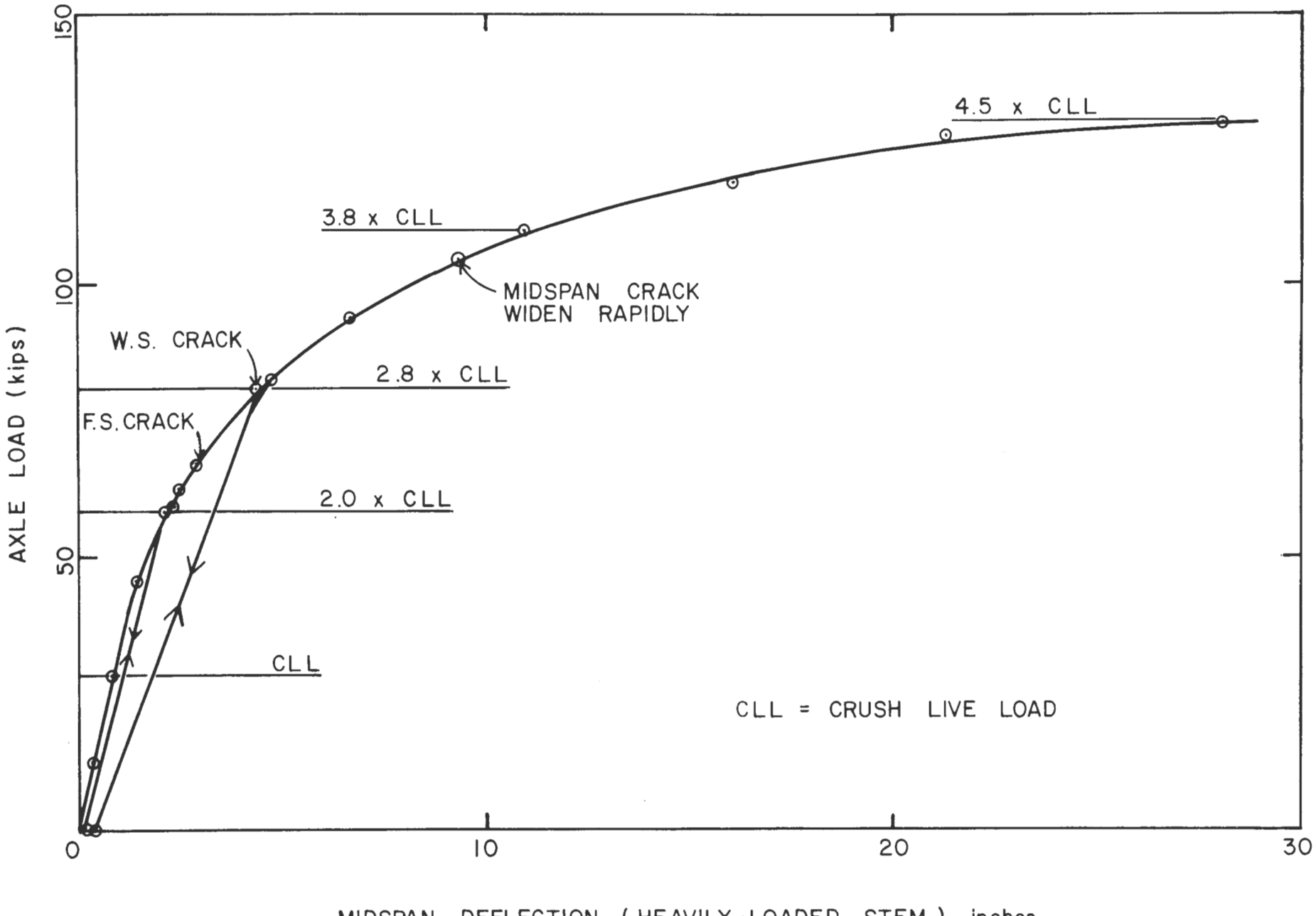

Fig. 35. Load vs. Midspan Deflection (Heavily-Loaded Stem) - Girder 2, Derailment Test.

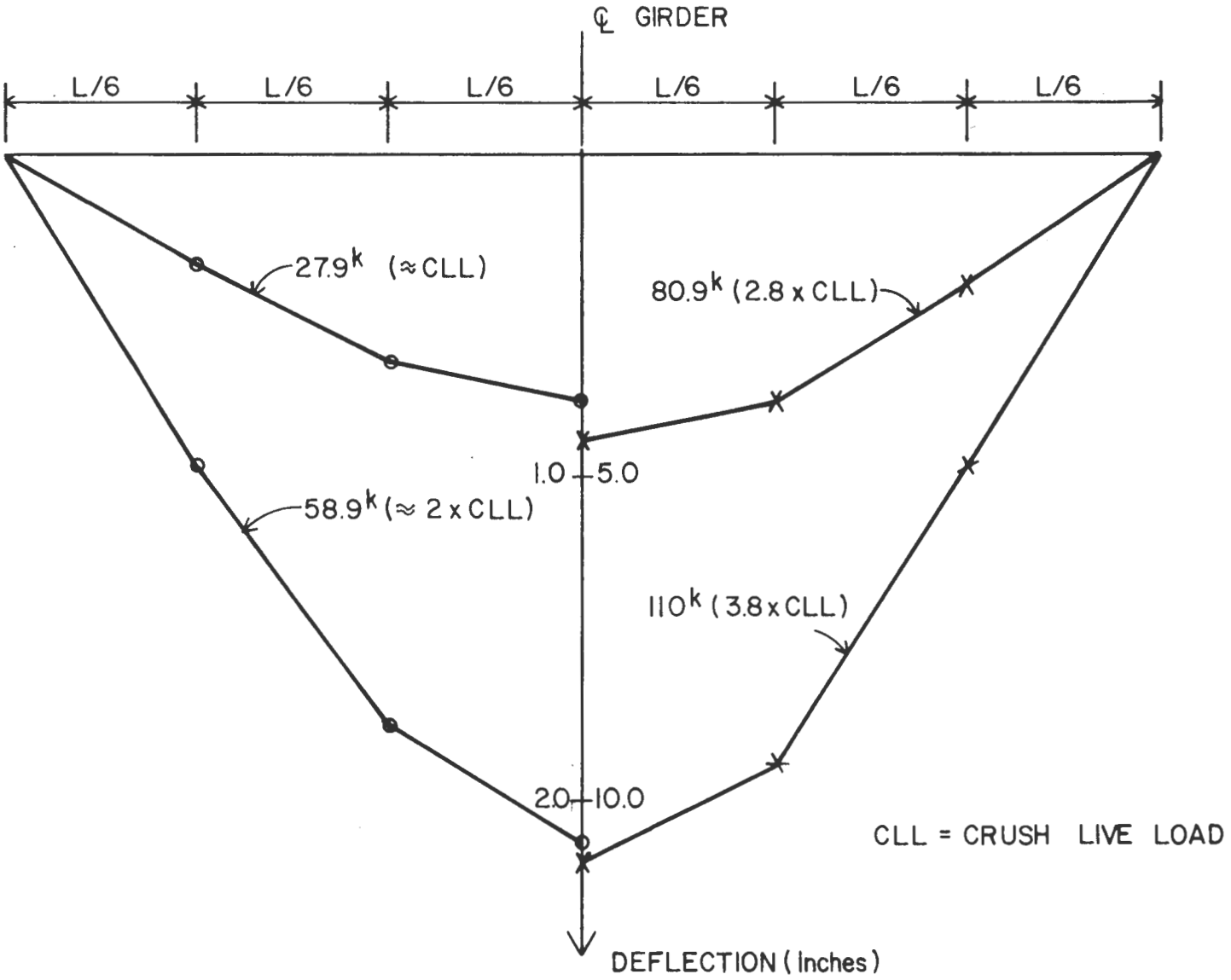

Fig. 36. Deflection Along Heavily-Loaded Stem - Girder 2, Derailment Test.

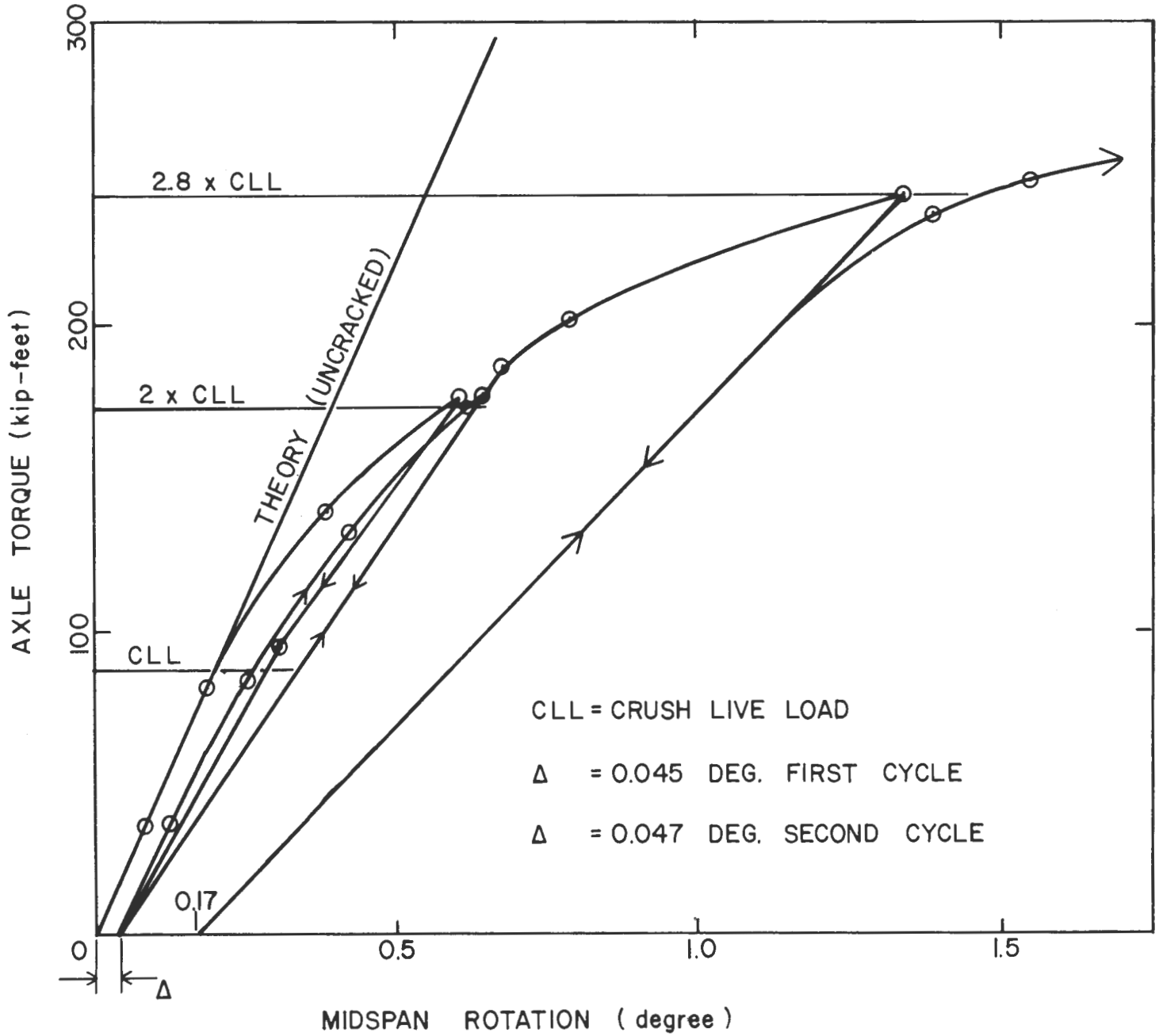

Fig. 37. Torque vs. Midspan Rotation - Girder 2, Derailment Test.

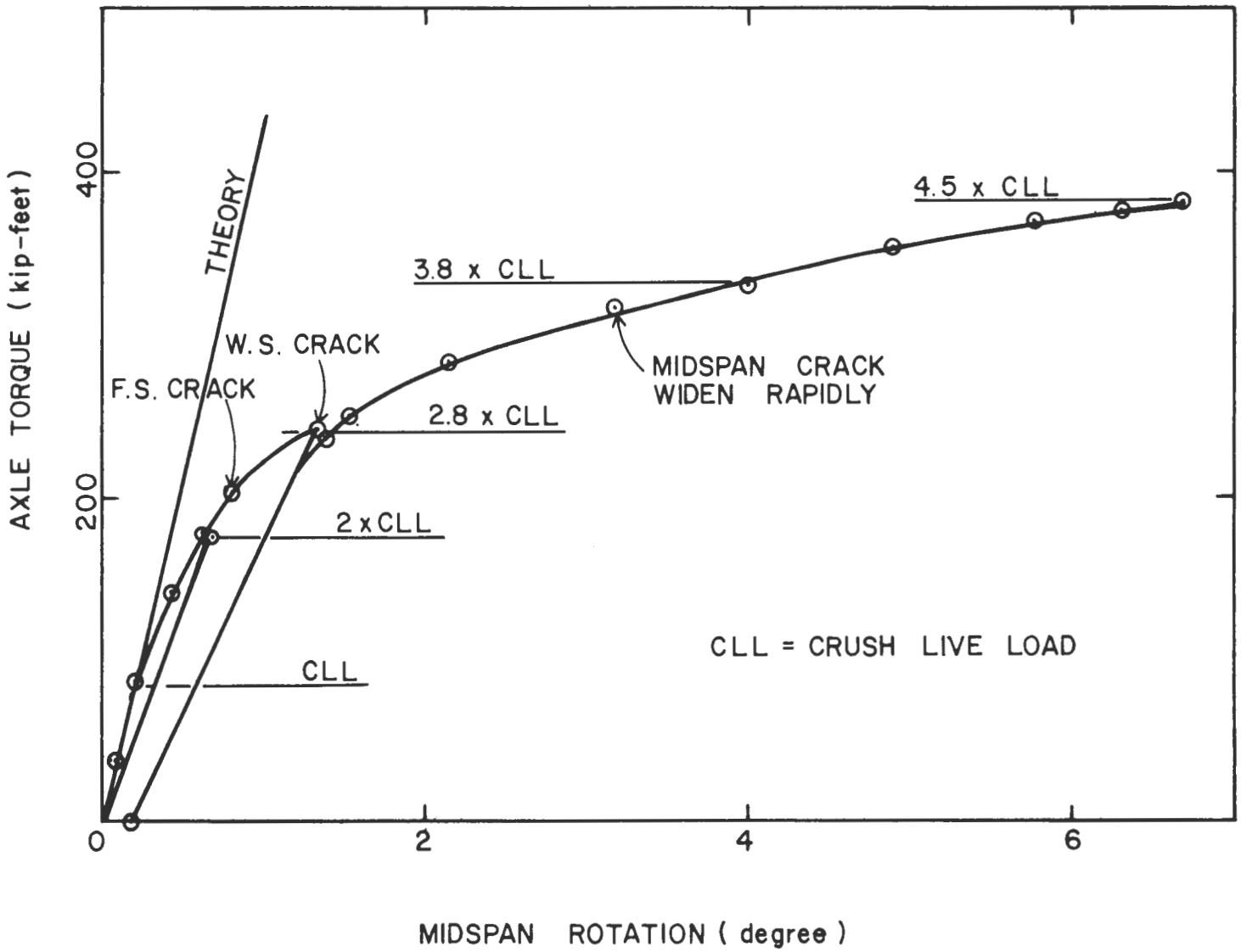

Fig. 38. Torque vs. Midspan Rotation - Girder 2, Derailment Test.

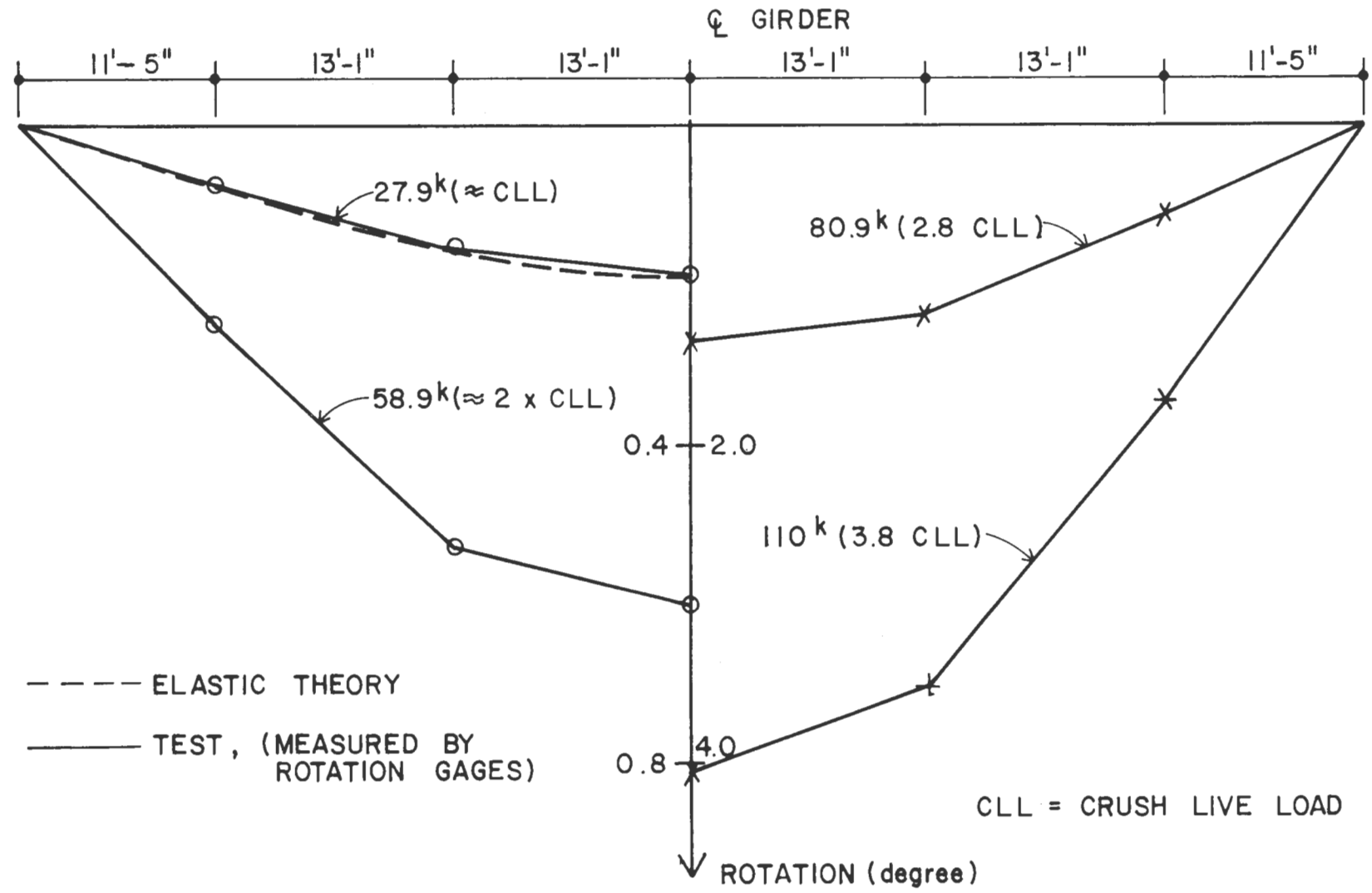

Fig. 39. Torsional Rotation Along Girder 2, Derailment Test.

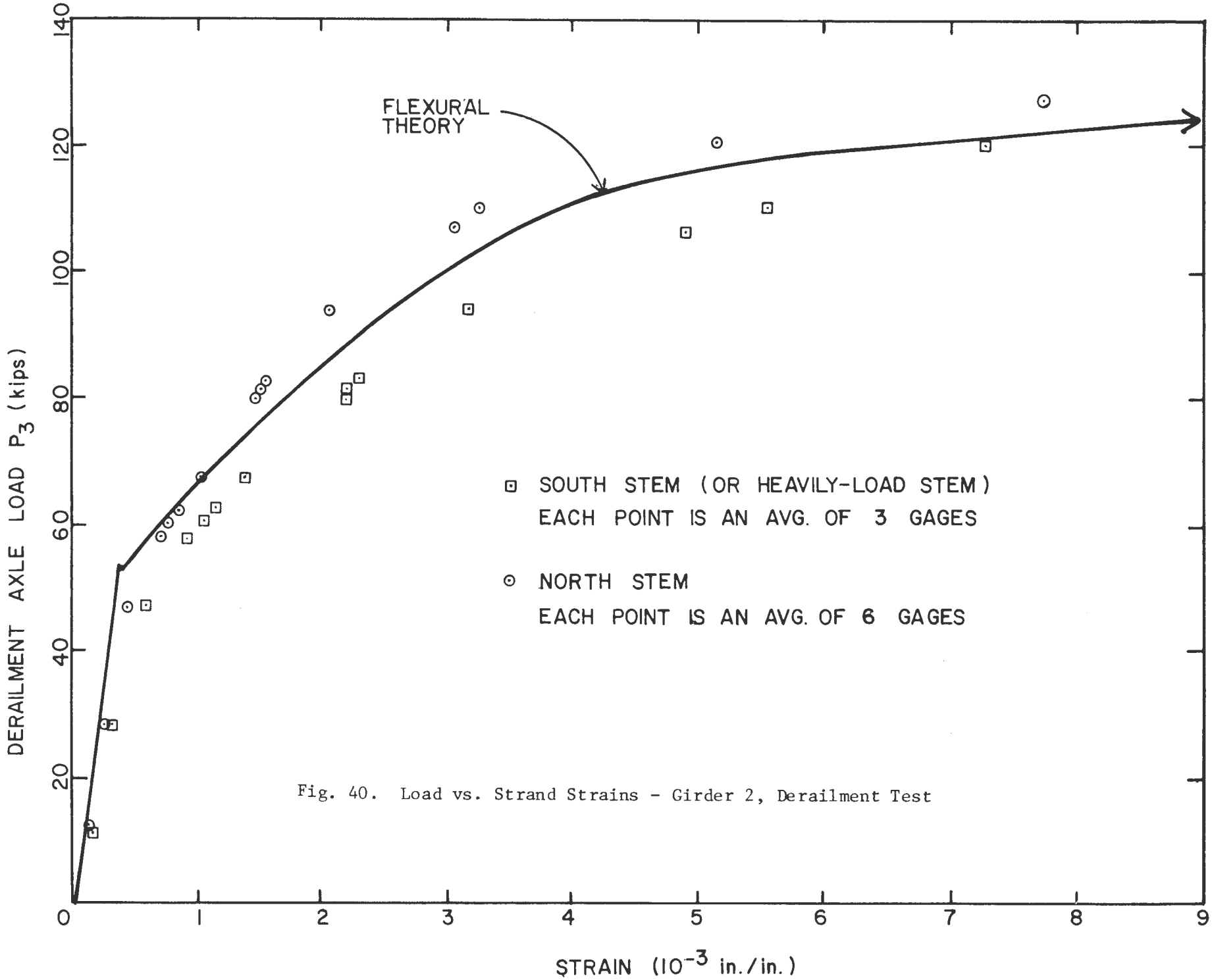

Fig. 40. Load vs. Strand Strains - Girder 2, Derailment Test

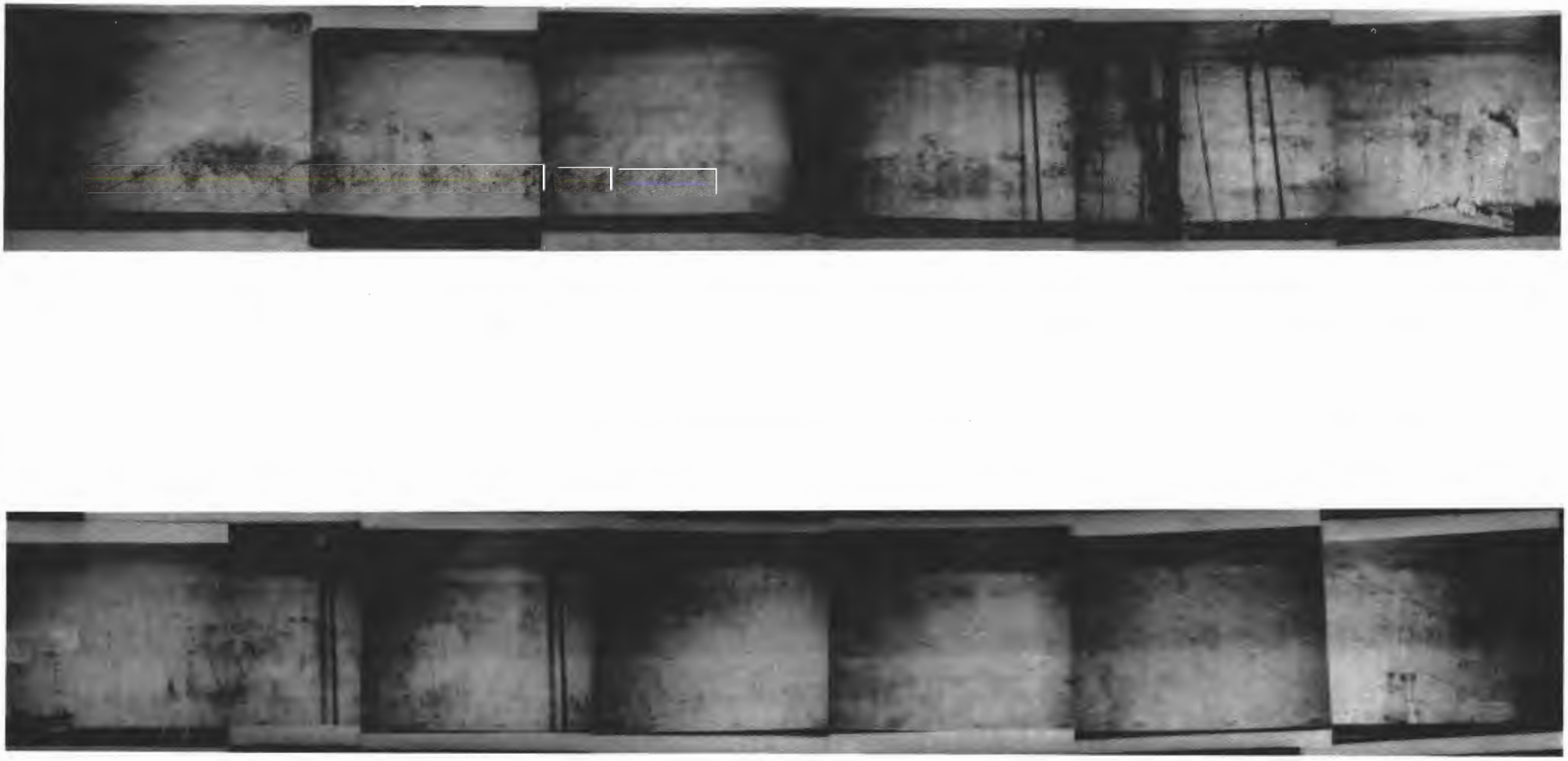

Fig 41 Crack Pattern of Girder 2 After Derailment Test

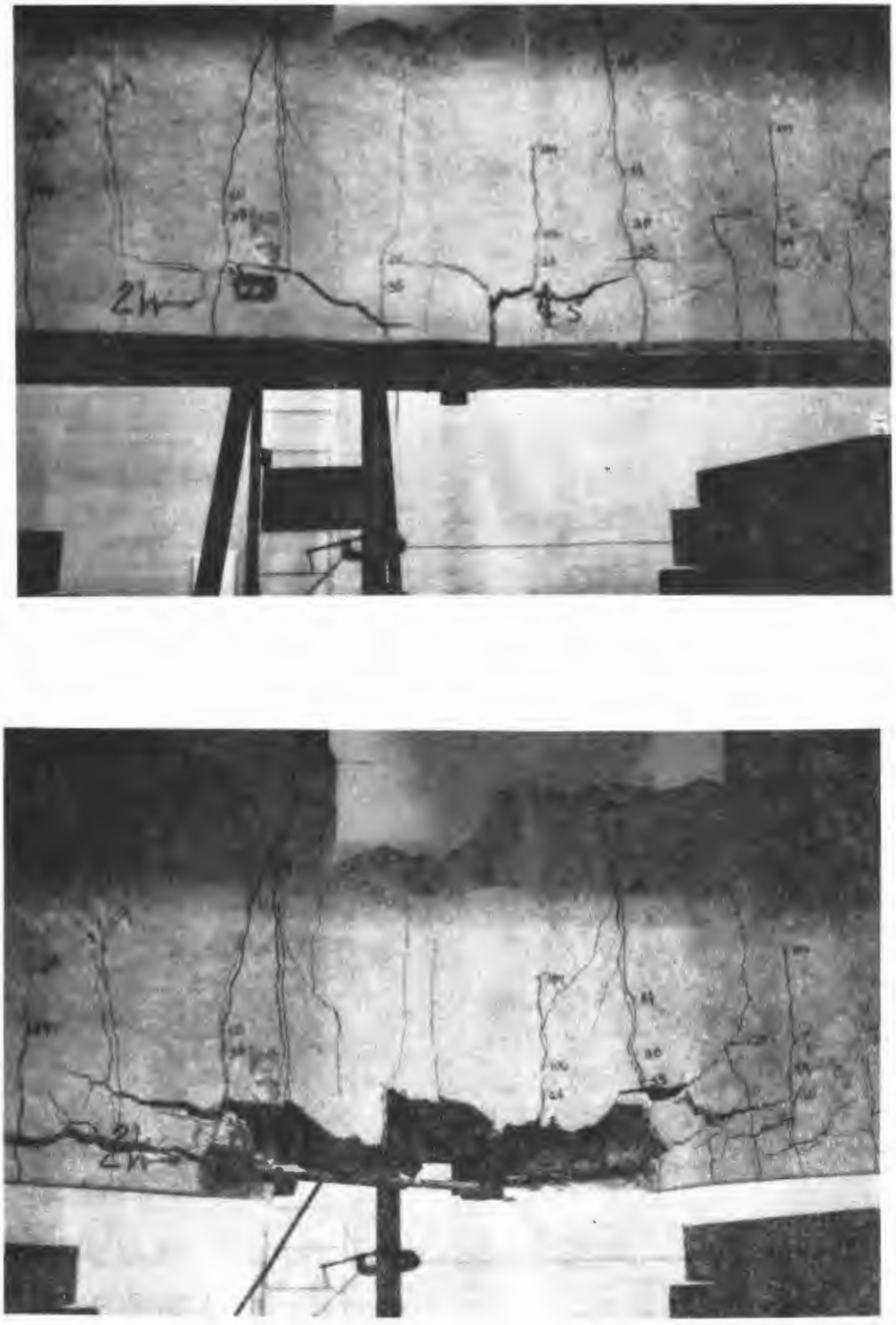

Fig. 42a Development of Cracks at Midspan
- Girder 2, Derailment Test

Fig. 42b Development of Cracks at Midspan
- Girder 2 Derailment Test

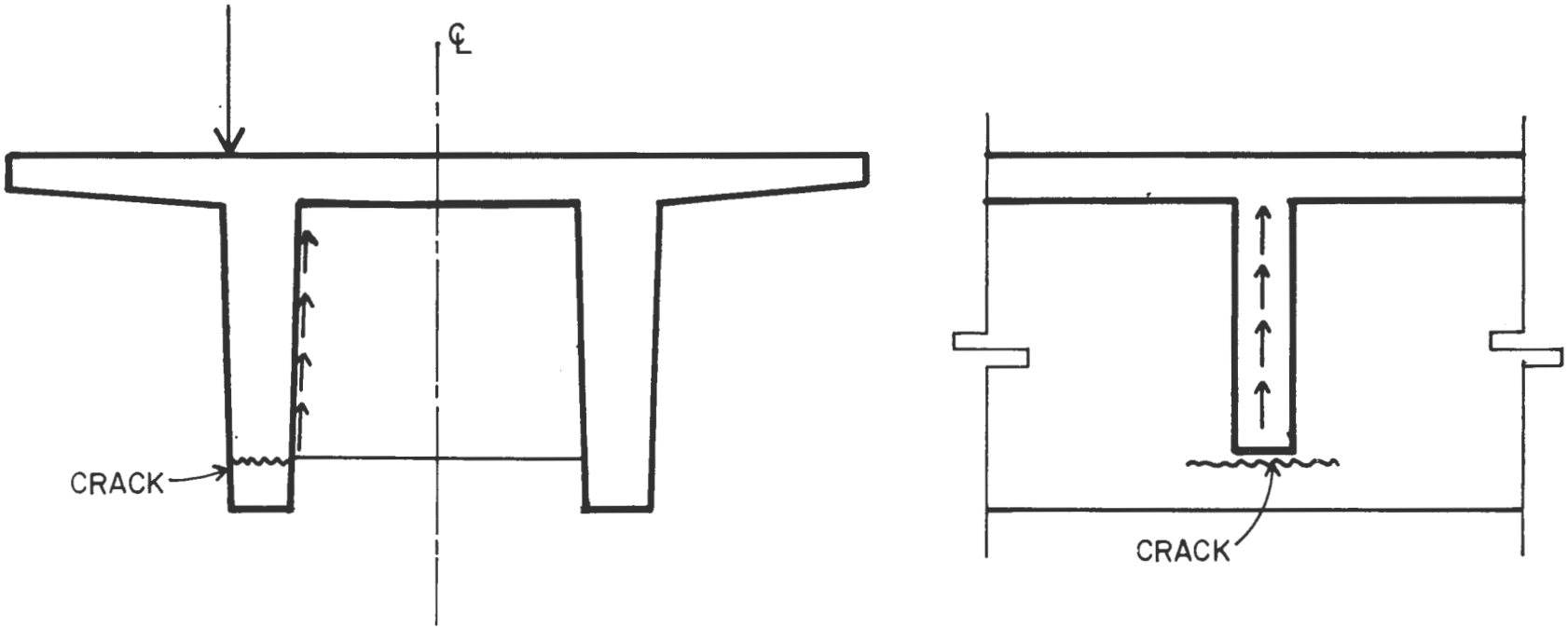

Fig. 43. Mechanism Creating Horizontal Cracks at Midspan.

Fig. 44 Diagonal Cracking of End Diaphragm

- Girder 2, Derailment Test

Fig. 45 Cracking of Stem at End Diaphragm - Girder 2, Derailment Test

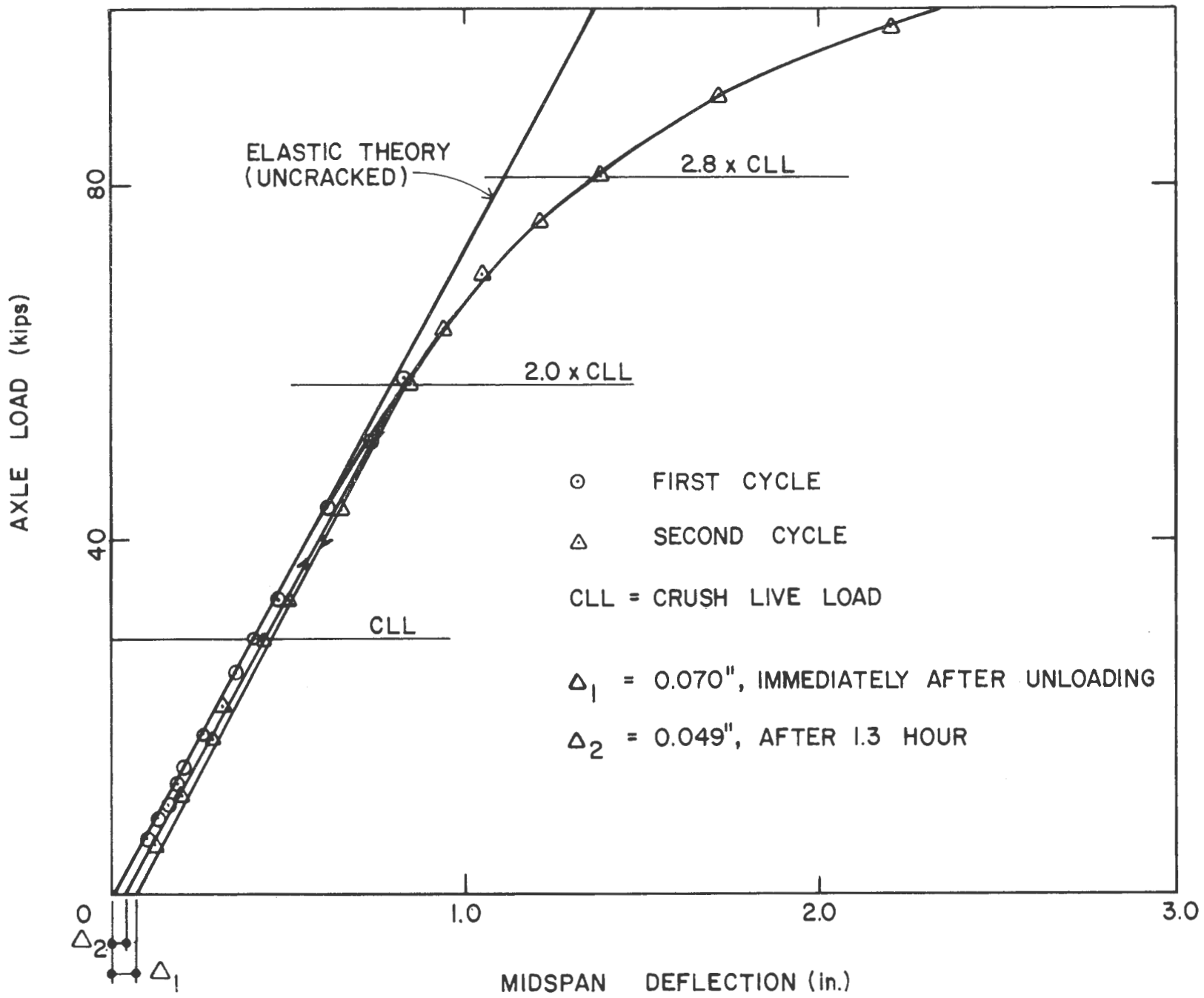

Fig. 46. Load vs. Midspan Deflection (Center Line) - Girder 3, Derailment Test.

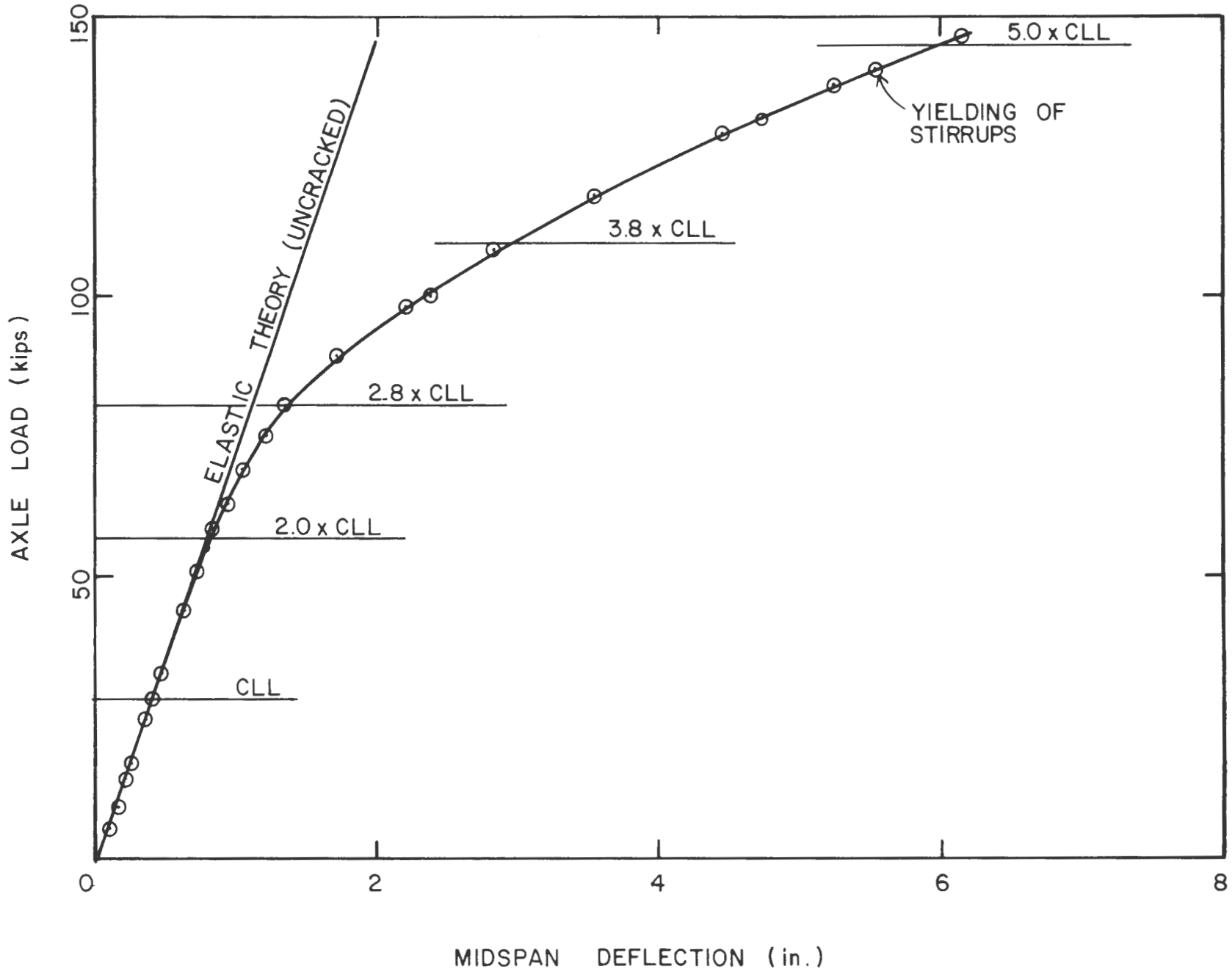

Fig. 47. Load vs. Midspan Deflection (Center-Line) - Girder 3, Derailment Test.

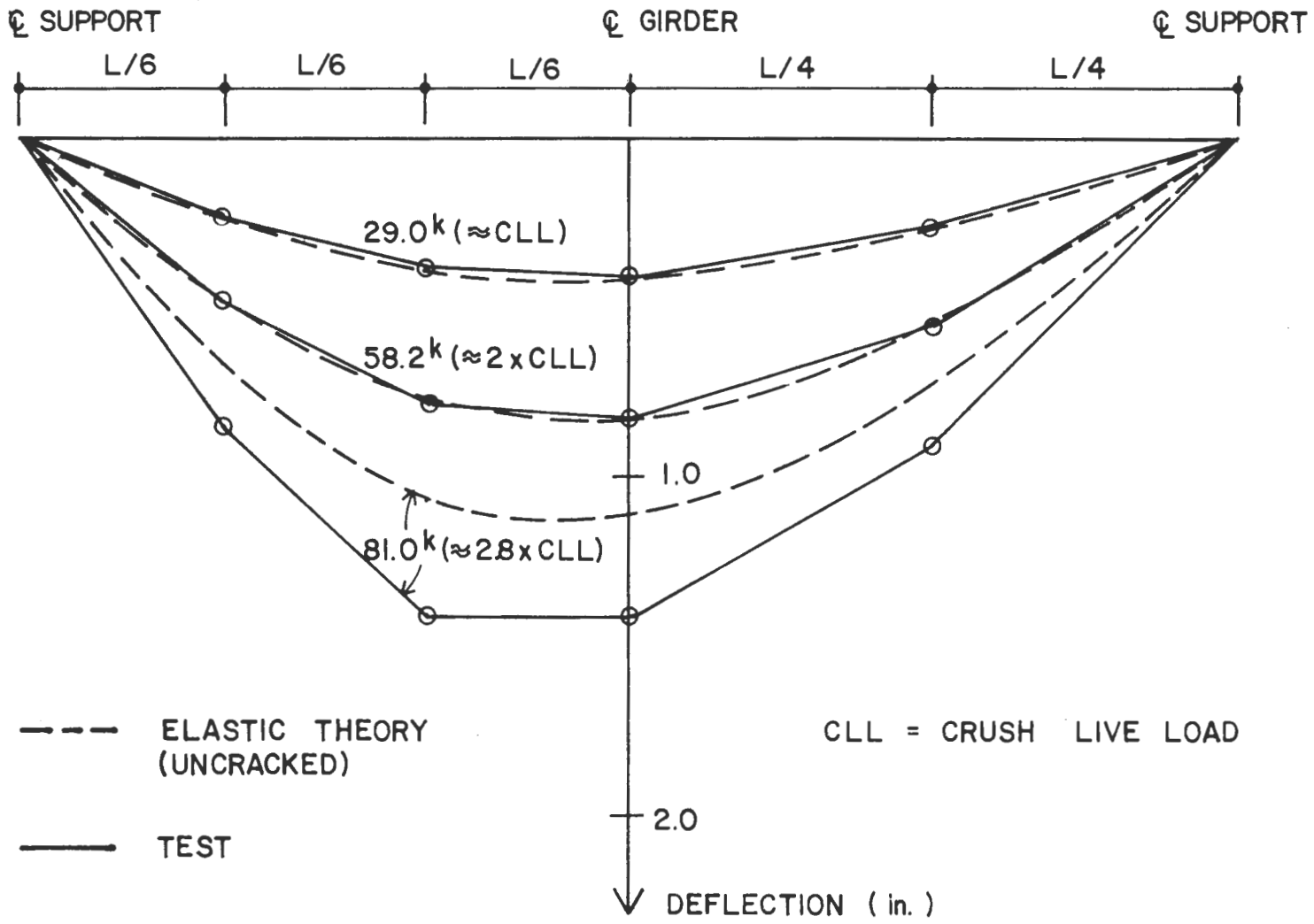

Fig. 48. Deflection Along Center-Line Axis - Girder 3, Derailment Test.

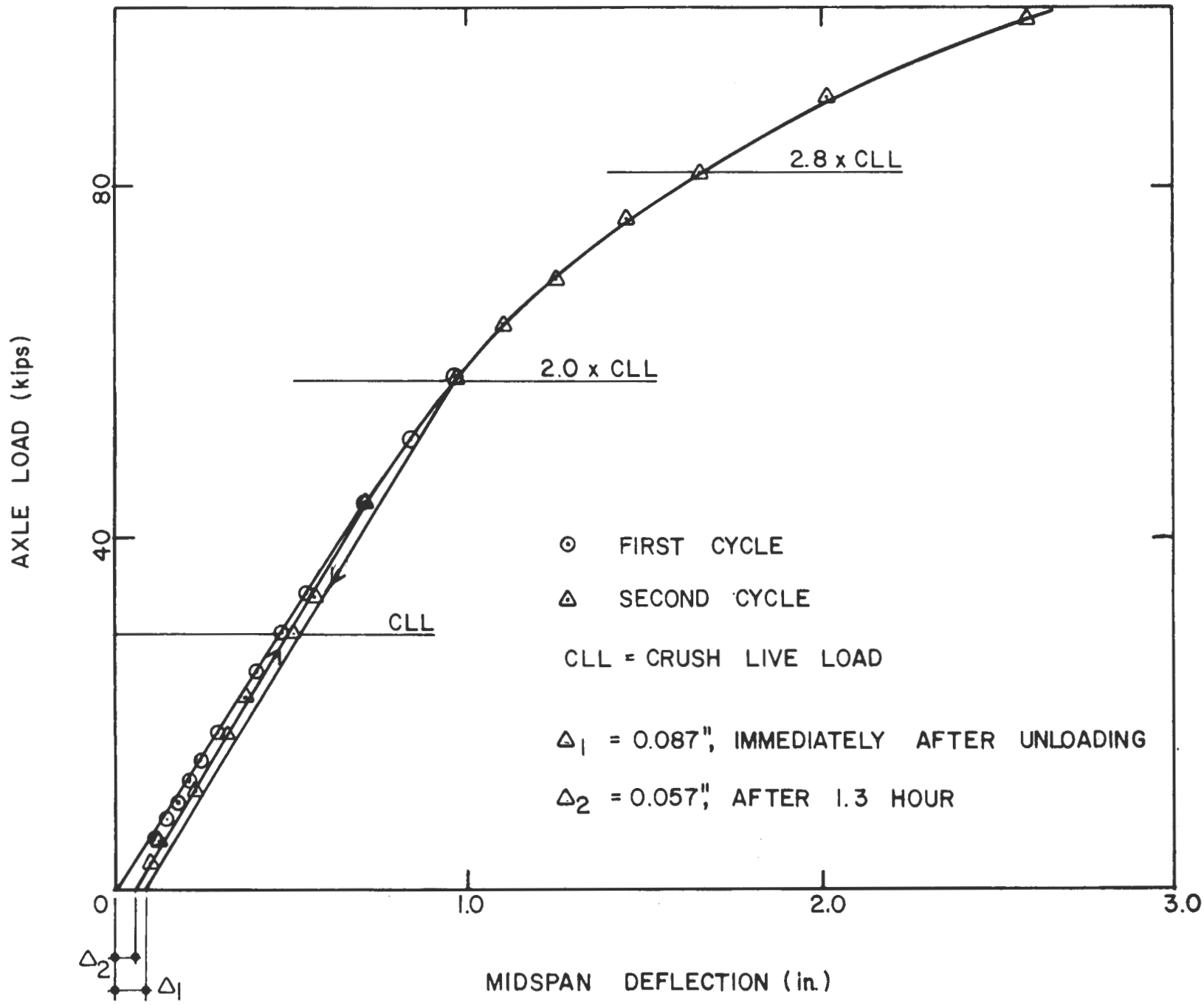

Fig. 49. Load vs. Midspan Deflection (Heavily-Loaded Stem) - Girder 3, Derailment Test.

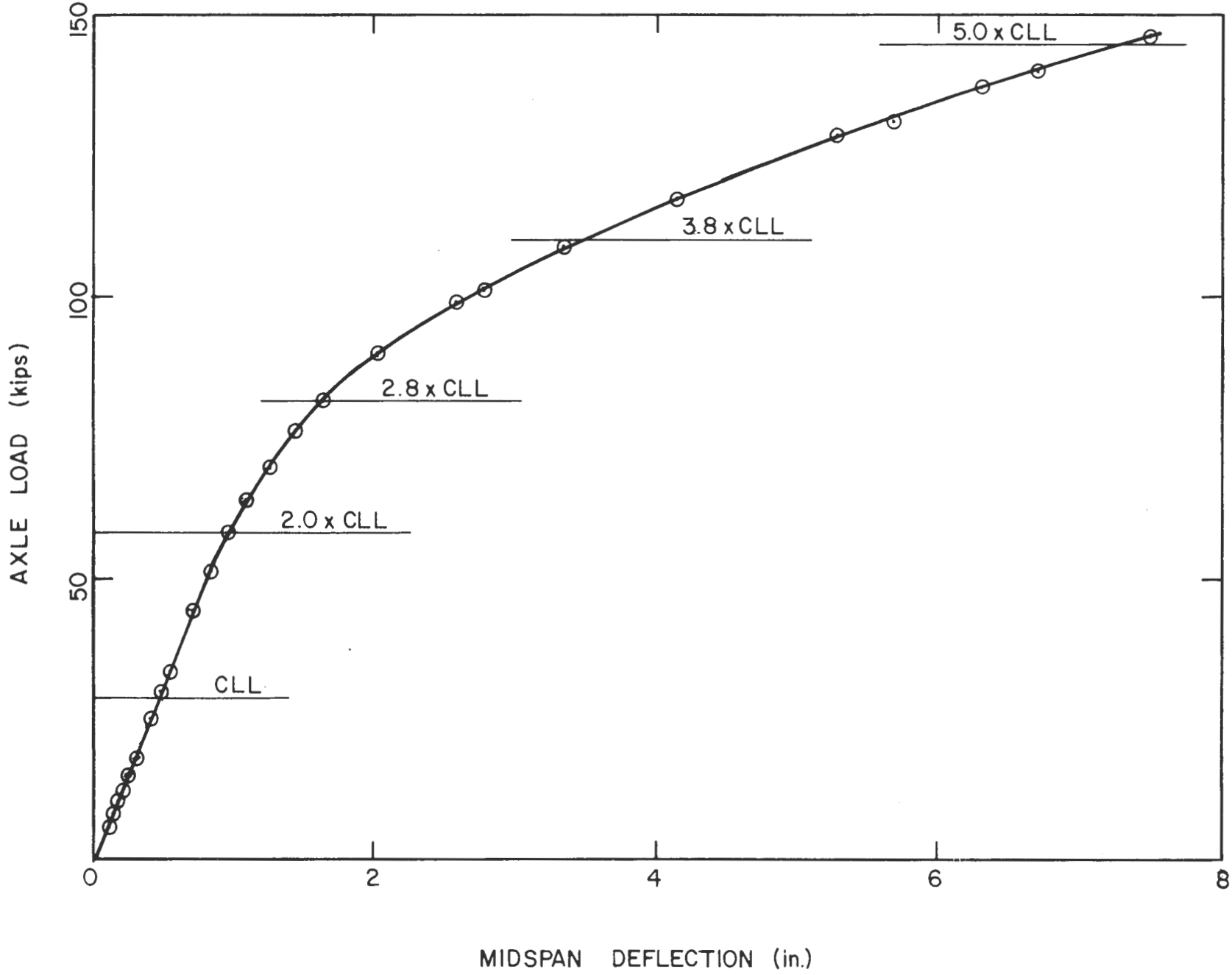

Fig. 50, Load vs. Midspan Deflection (Heavily-Loaded Stem) - Girder 3, Derailment Test.

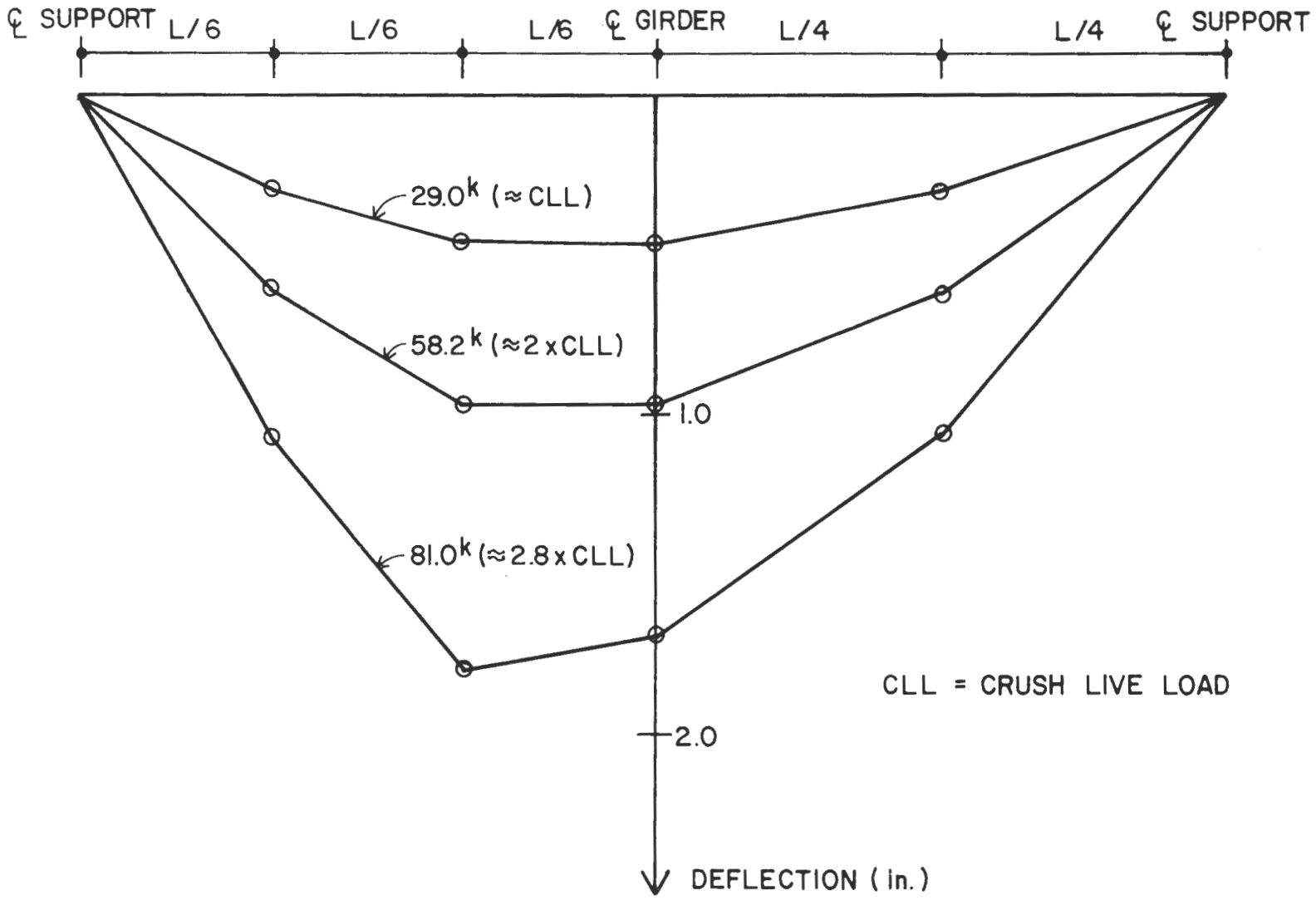

Fig. 51. Deflection Along Heavily-Loaded Stem - Girder 3, Derailment Test.

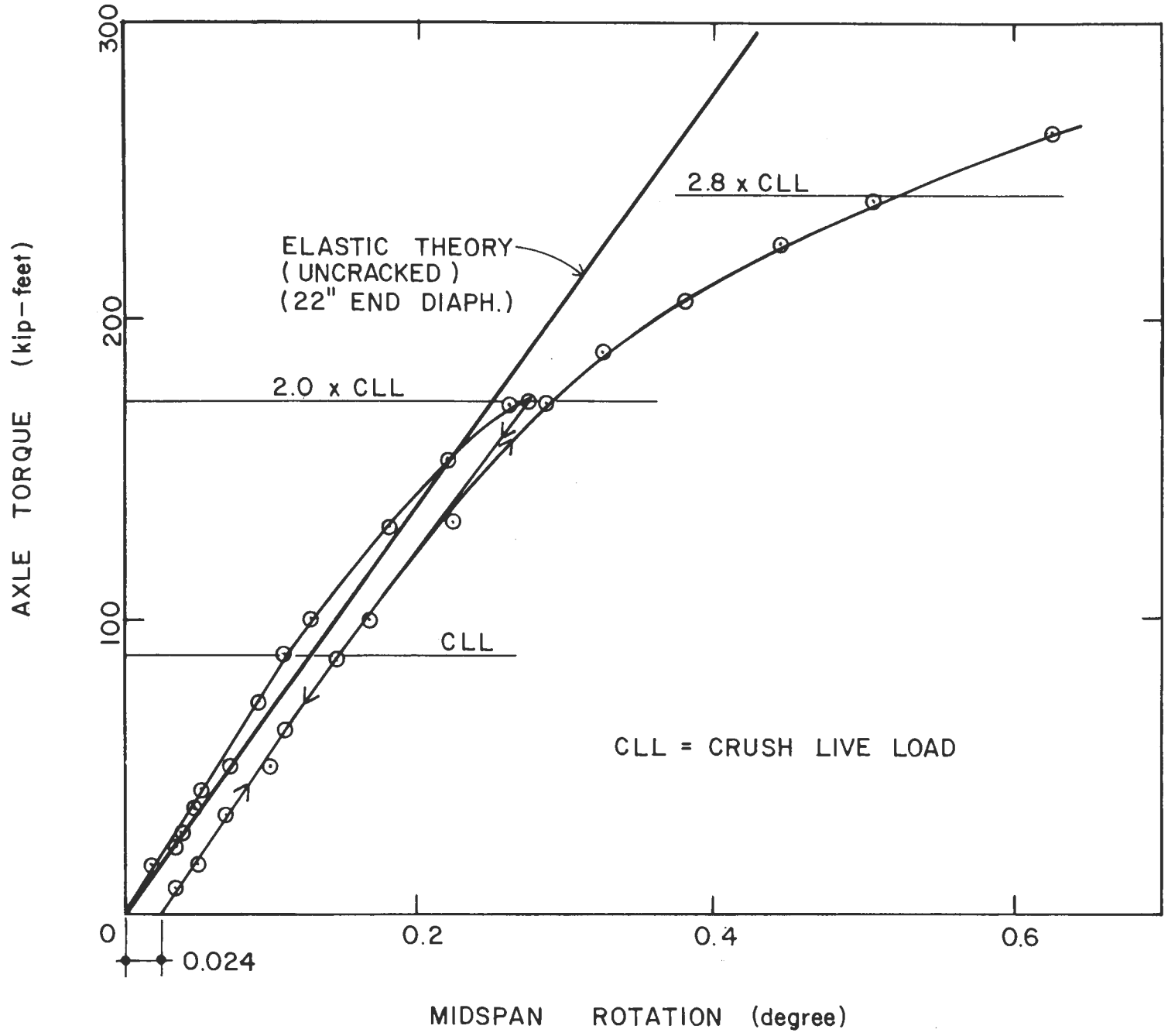

Fig. 52. Torque vs. Midspan Rotation - Girder 3, Derailment Test

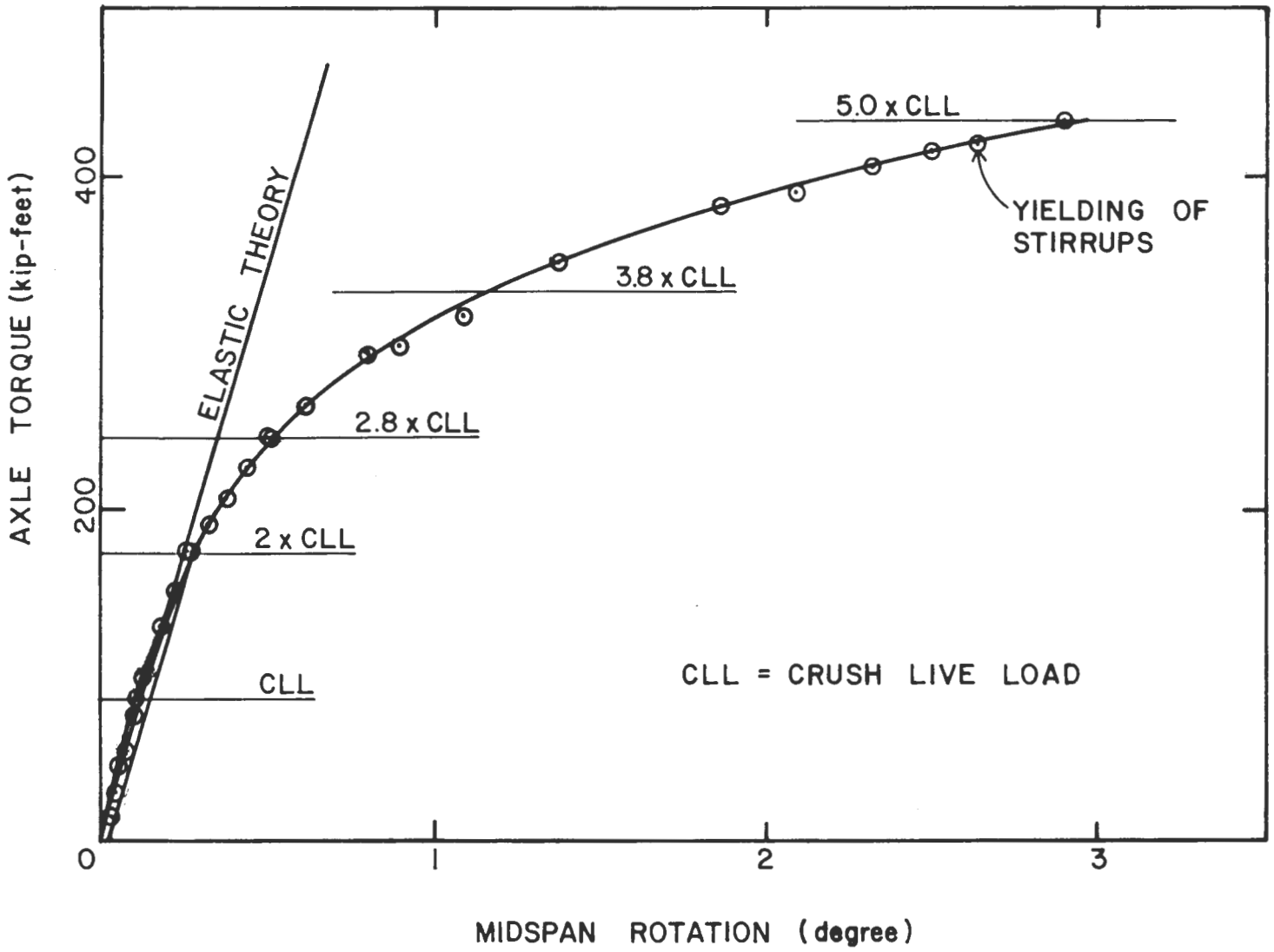

Fig. 53 Torque vs. Midspan Rotation - Girder 3, Derailment Test.

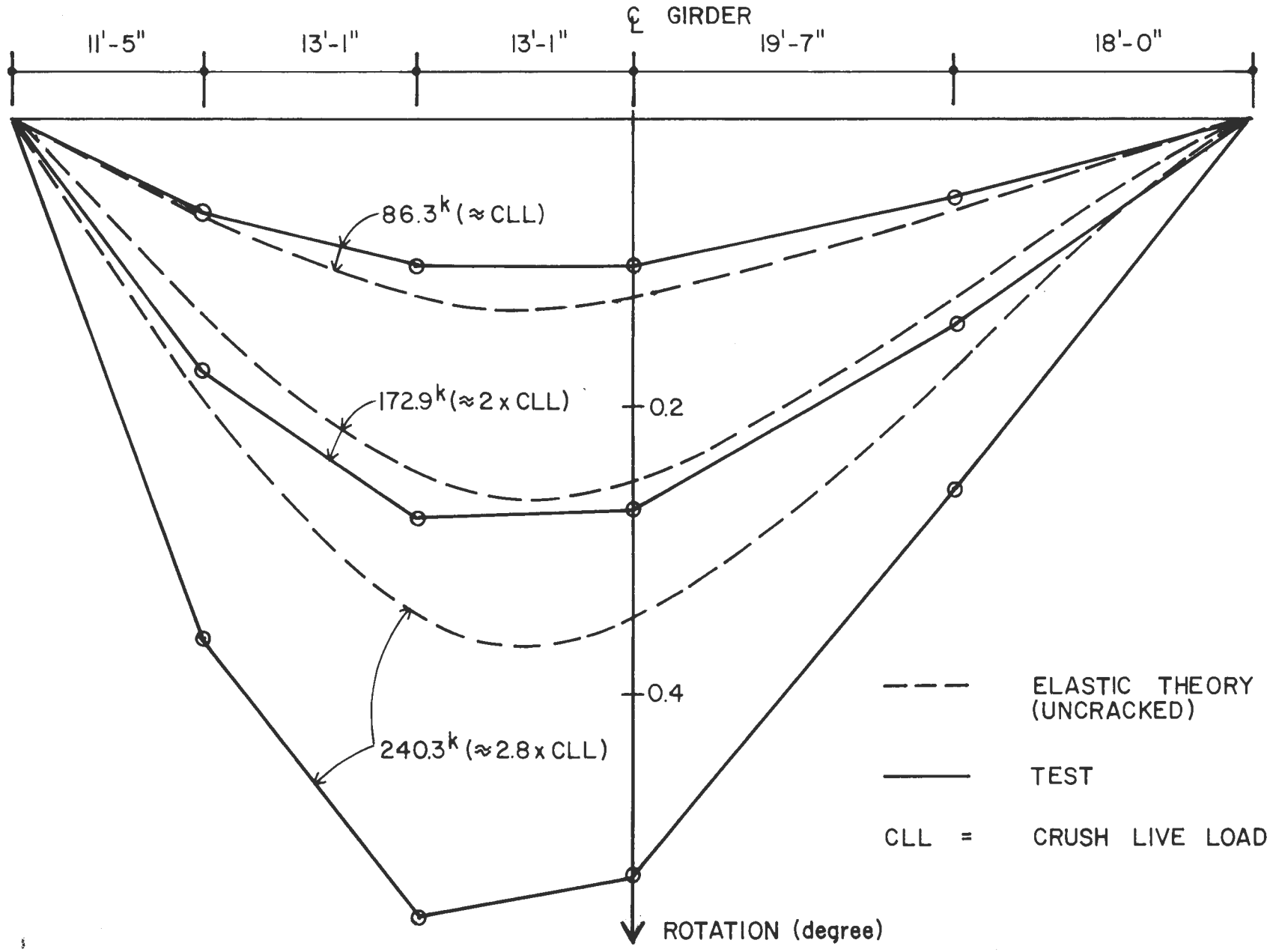

Fig. 54. Torsional Rotation Along Girder 3, Derailment Test.

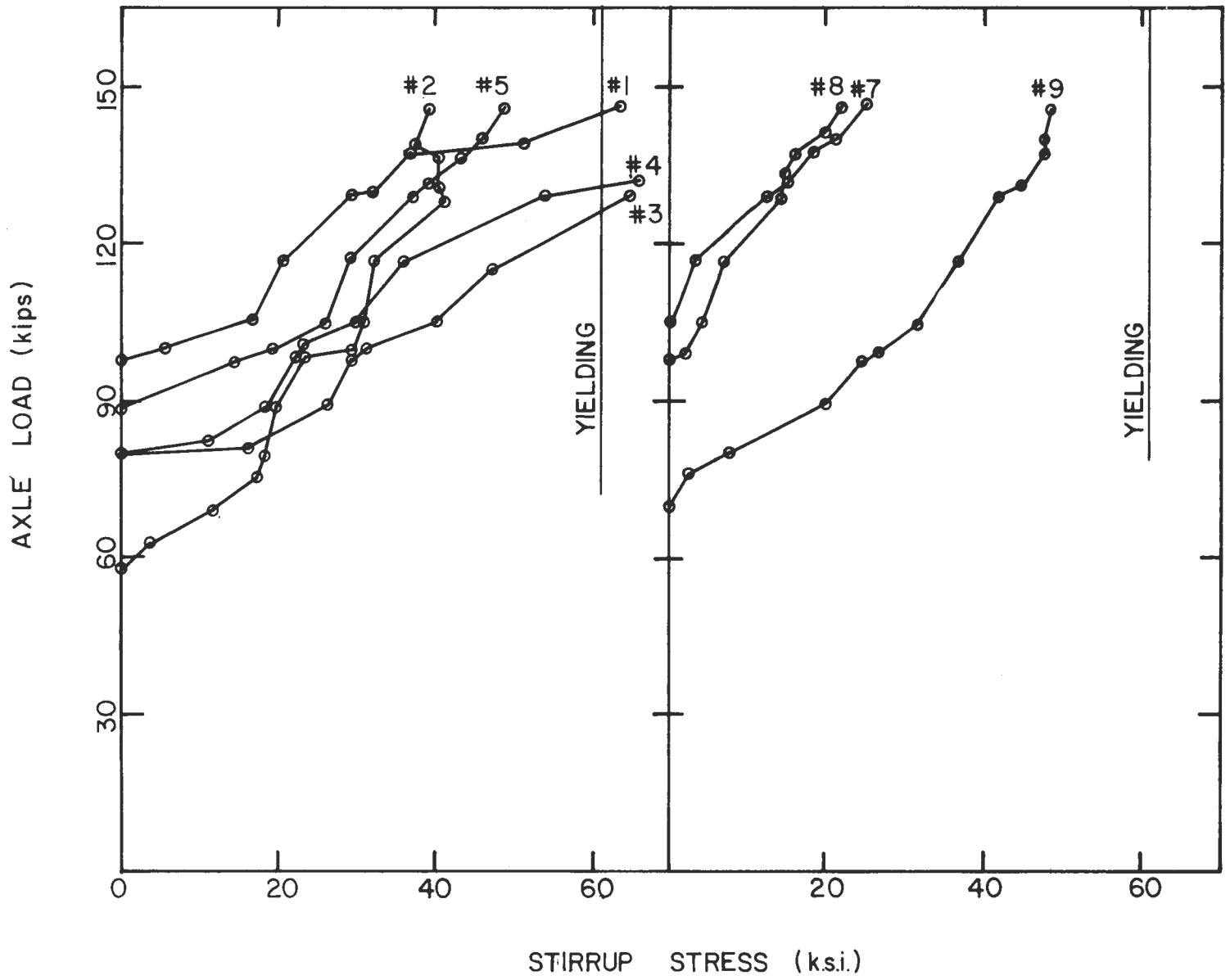

Fig. 55. Stresses in the Outer Legs of Stirrup in the Heavily-Loaded South Stem - Girder 3, Derailment Test.

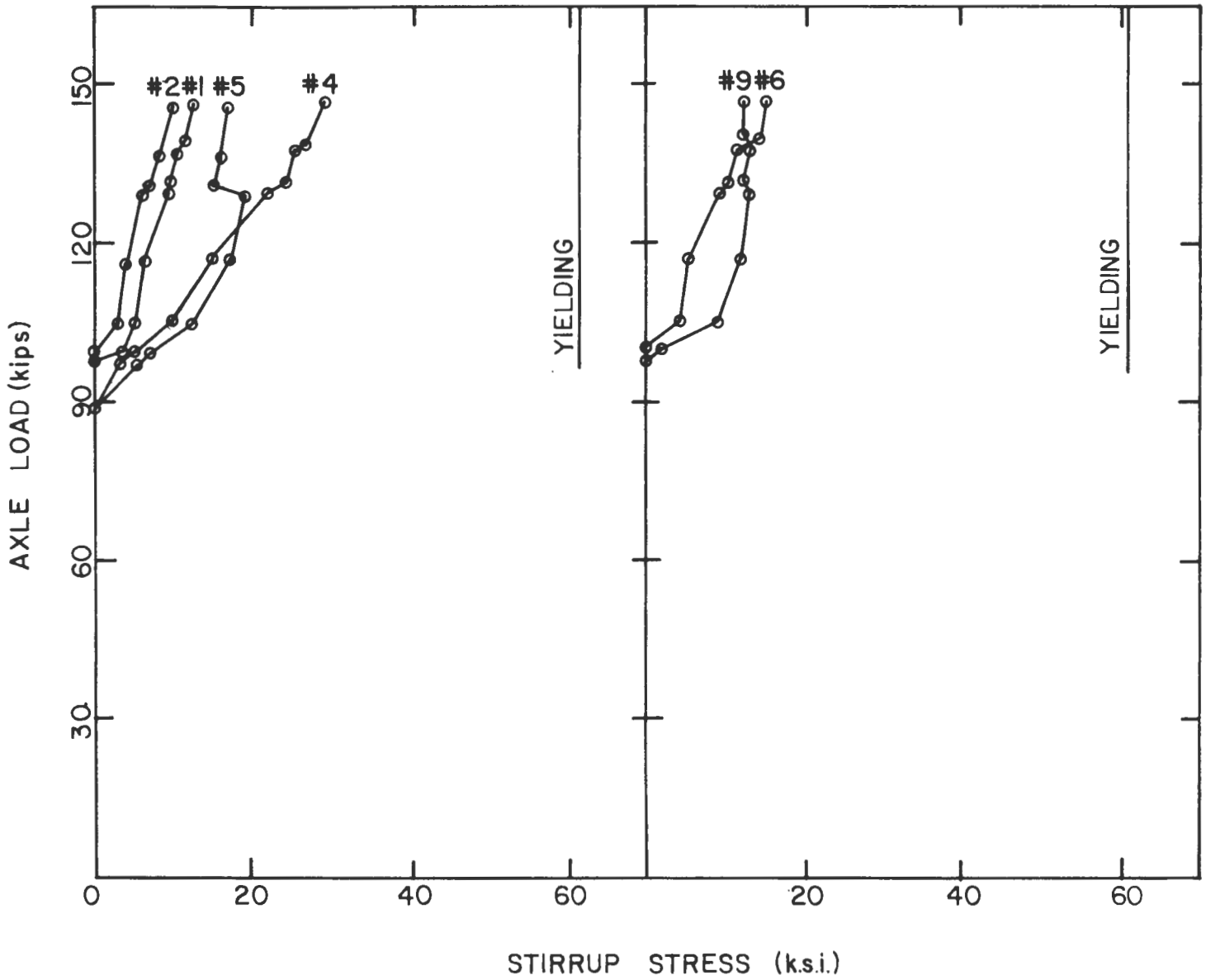

Fig. 56. Stresses in the Inner Legs of Stirrups in the Heavily-Loaded South Stem - Girder 3, Derailment Test.

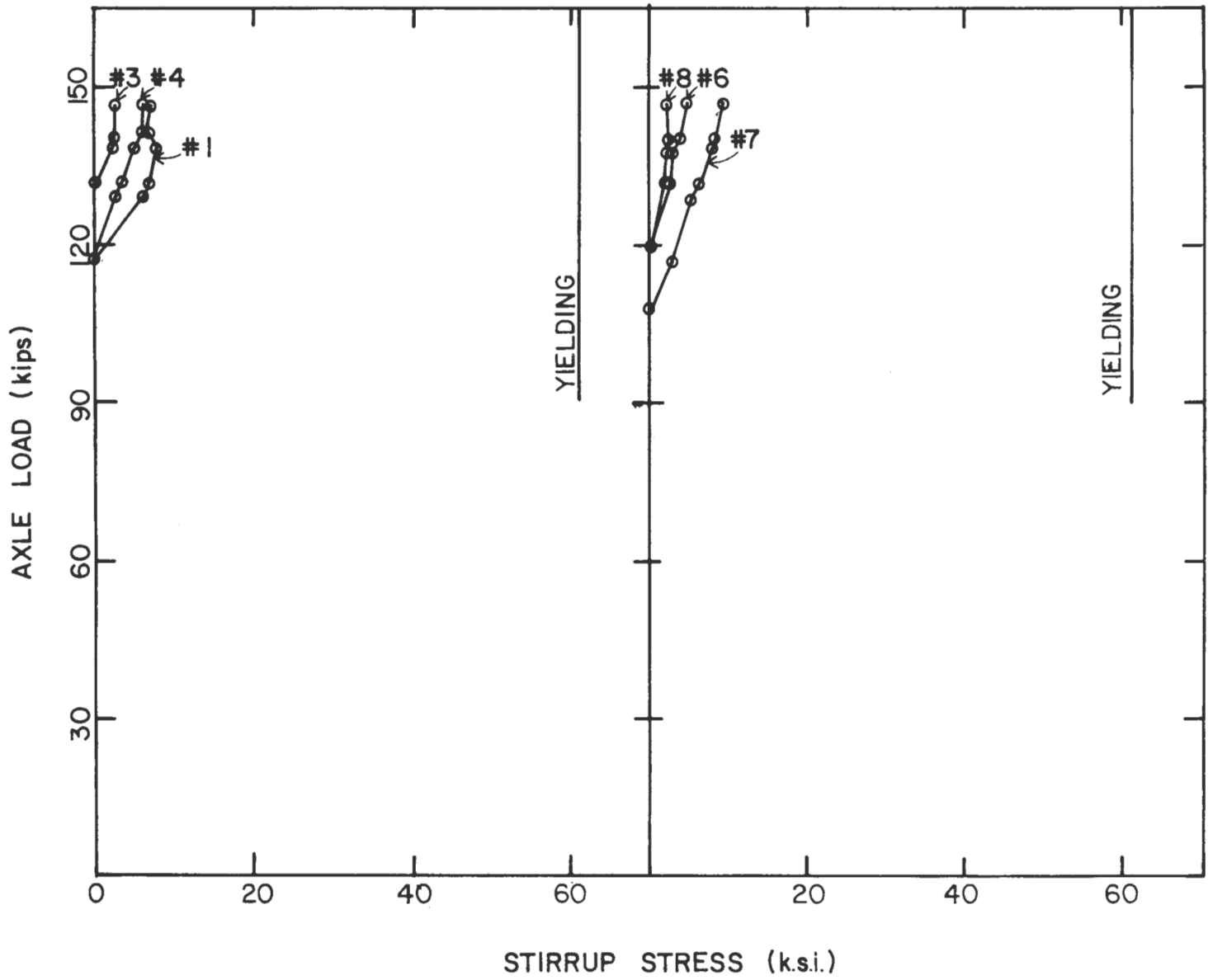

Fig. 57. Stresses in the Outer Legs of Stirrups in the North Stem - Girder 3, Derailment Test.

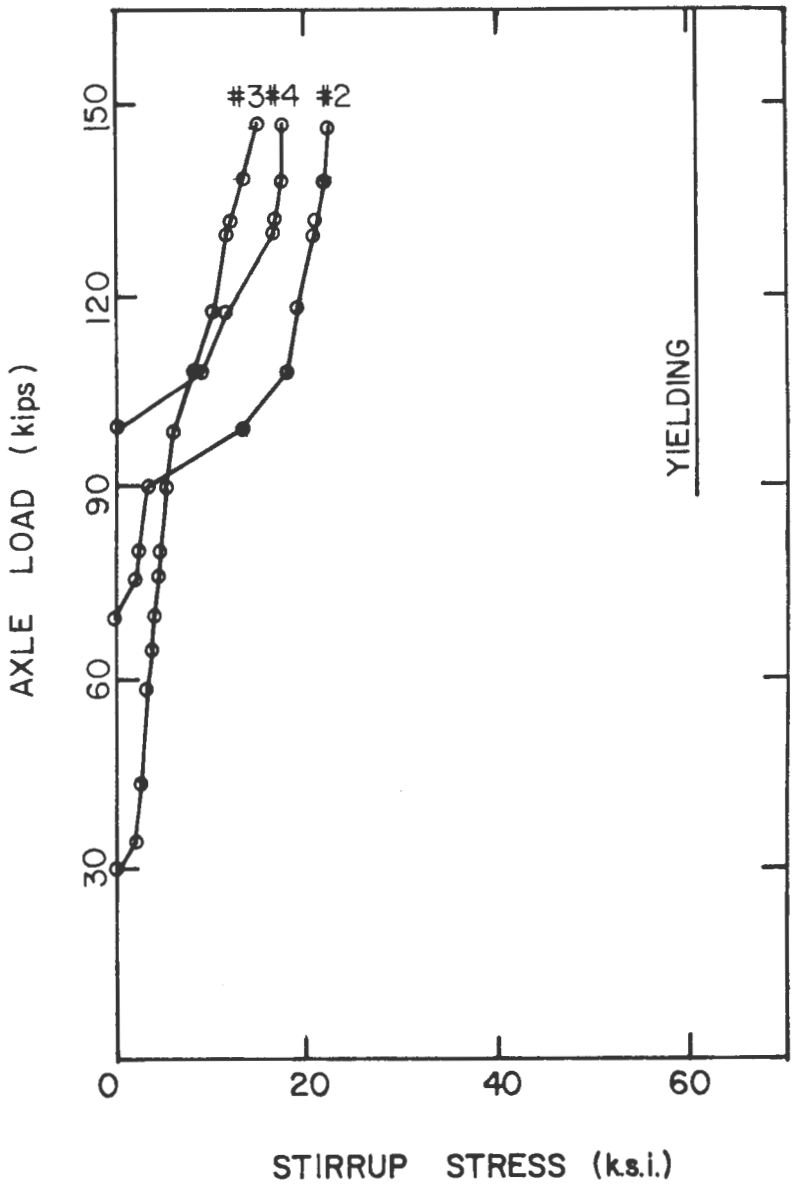

Fig. 58. Stirrup Stresses in the End Diaphragm - Girder 3, Derailment Test.

Fig. 59. Flexural Cracking Pattern - Girder 3 at
5.0 x crush Live Load (2.5 x Derailment Load)

Fig. 60. Shear Cracking Near Midspan - Girder 3, at 5.0 x Crush Live Load (2.5 x Derailment Load)

(a) At 2.0 x Crush Live Load

(b) At 5.0 x Crush Live Load

Fig. 61. Cracking Pattern at the Heavily-Loaded End - Girder 3

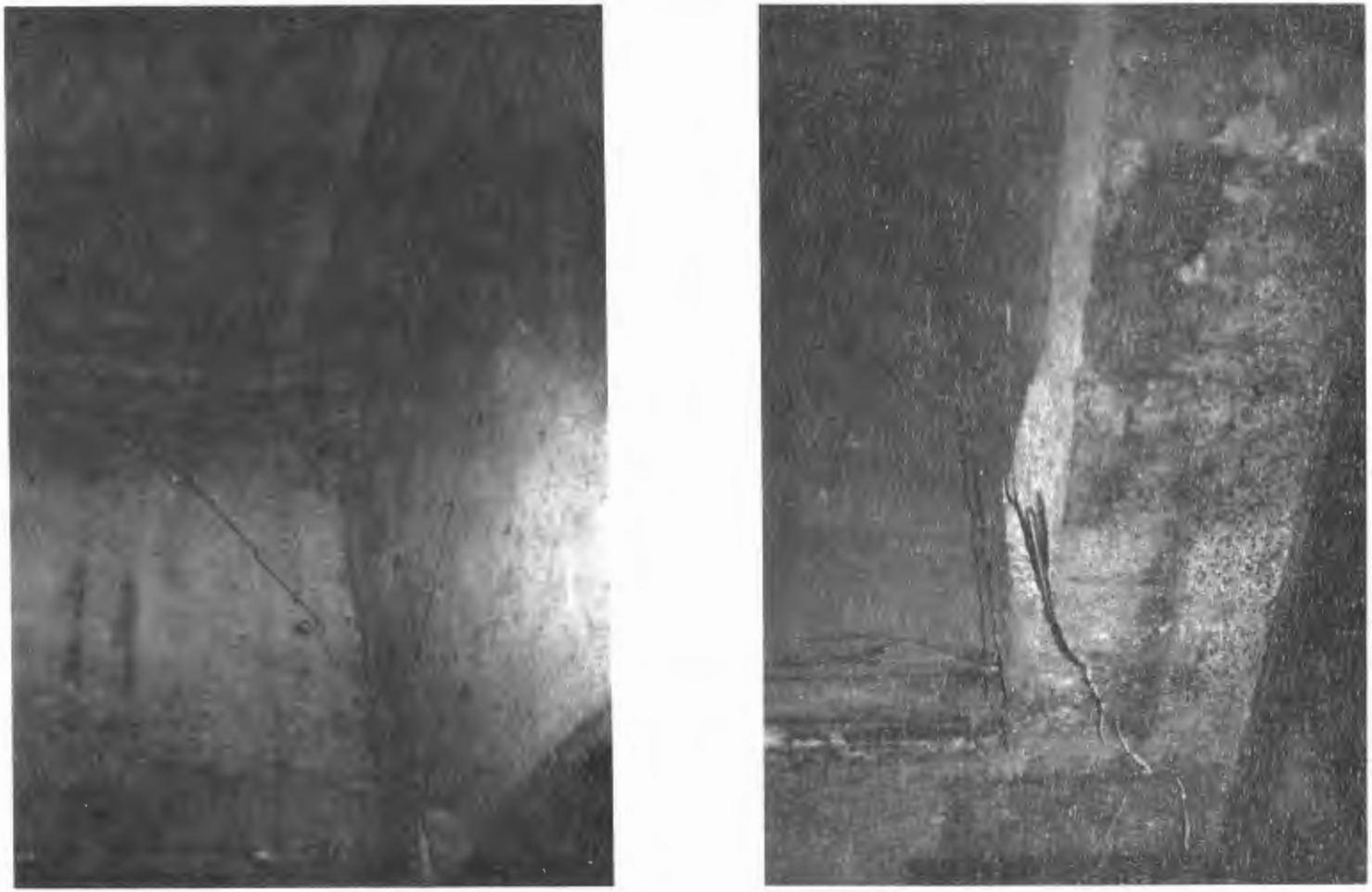

(a) (b)

Fig. 62 Crack Pattern at the Joint Between Stem and End Diaphragm - Girder 3, at 5.0 x Crush Live Load (2.5 x Derailment Load)

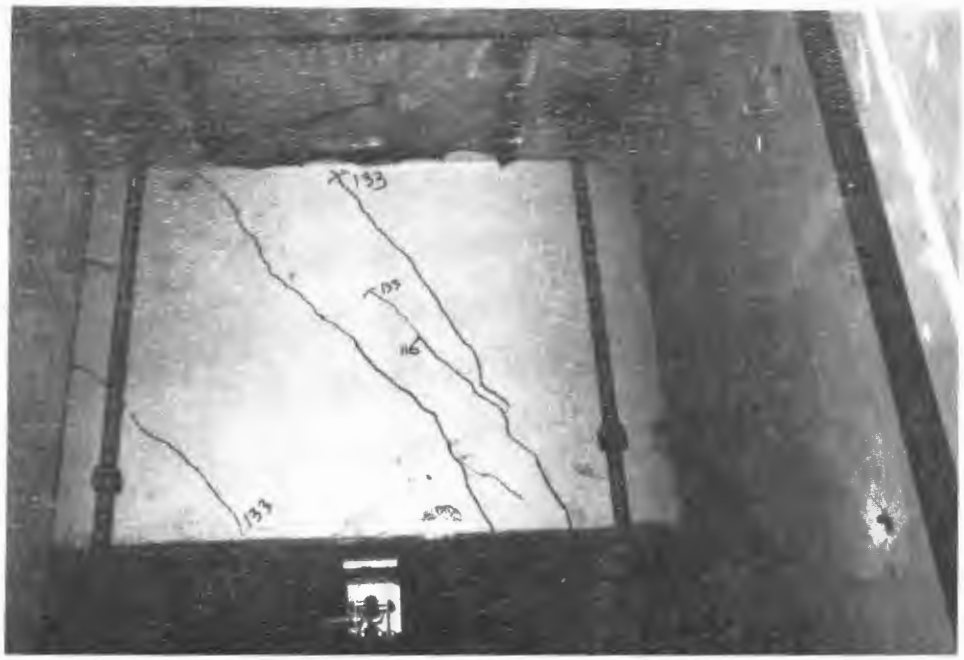

Fig. 63. Crack Pattern of End Diaphragm - Girder 3 at 5.0 x Crush Live Load (2.5 x Derailment Load)

(a) East Face

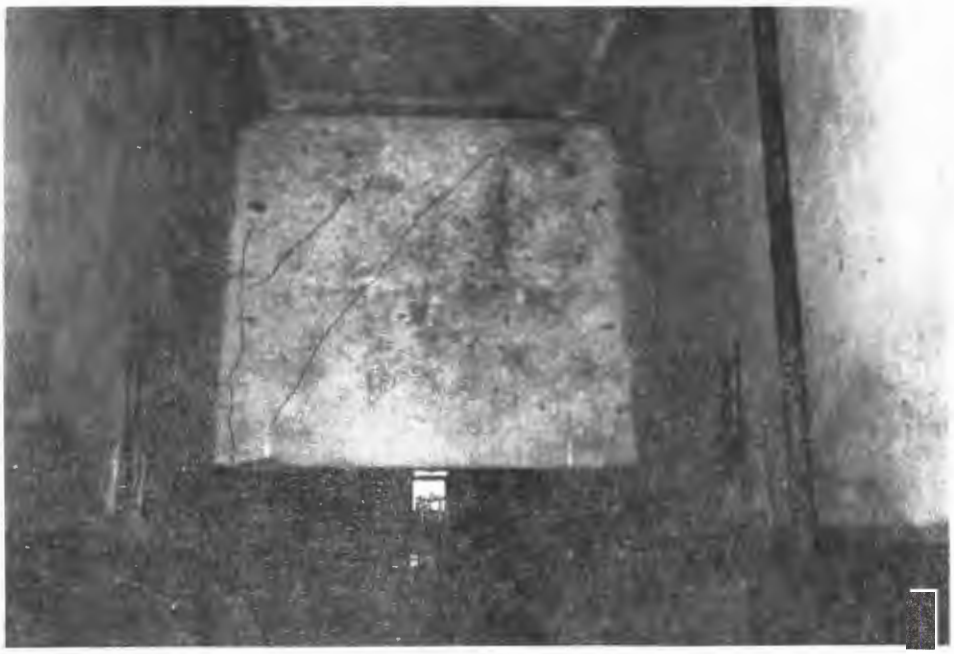

(b) West Face

Fig. 64. Crack Pattern of Midspan Diaphragm - Girder 3 at 5.0 x Crush Live Load (2.5 x Derailment Load)

Fig. 65. Local Horizontal Cracks at Midspan - Girder 3 at 5.0 x Crush Live Load (2.5 x Derailment Load)

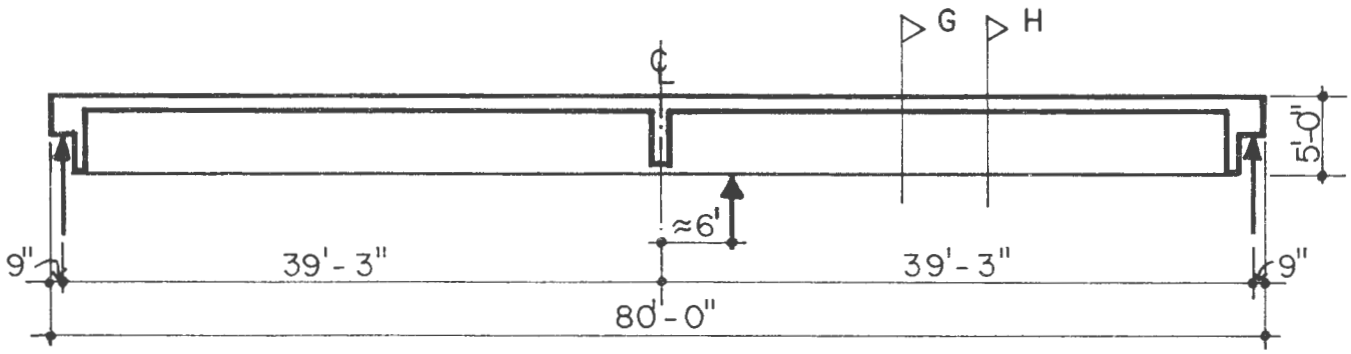

A. LONGITUDINAL SECTION

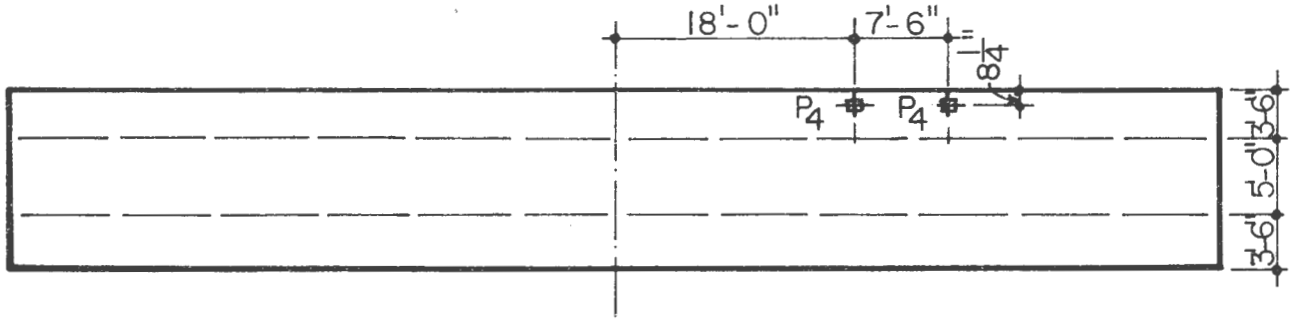

B. PLAN

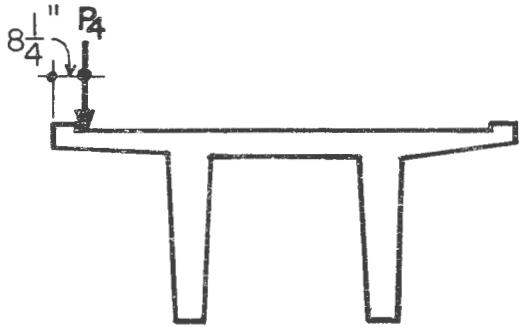

C. CROSS SECTION

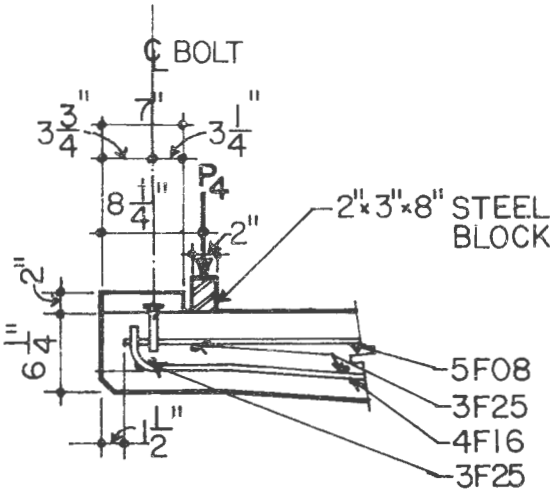

D. CURB DETAILS

Fig. 66 Location of Wheel Loads in Derailment Condition

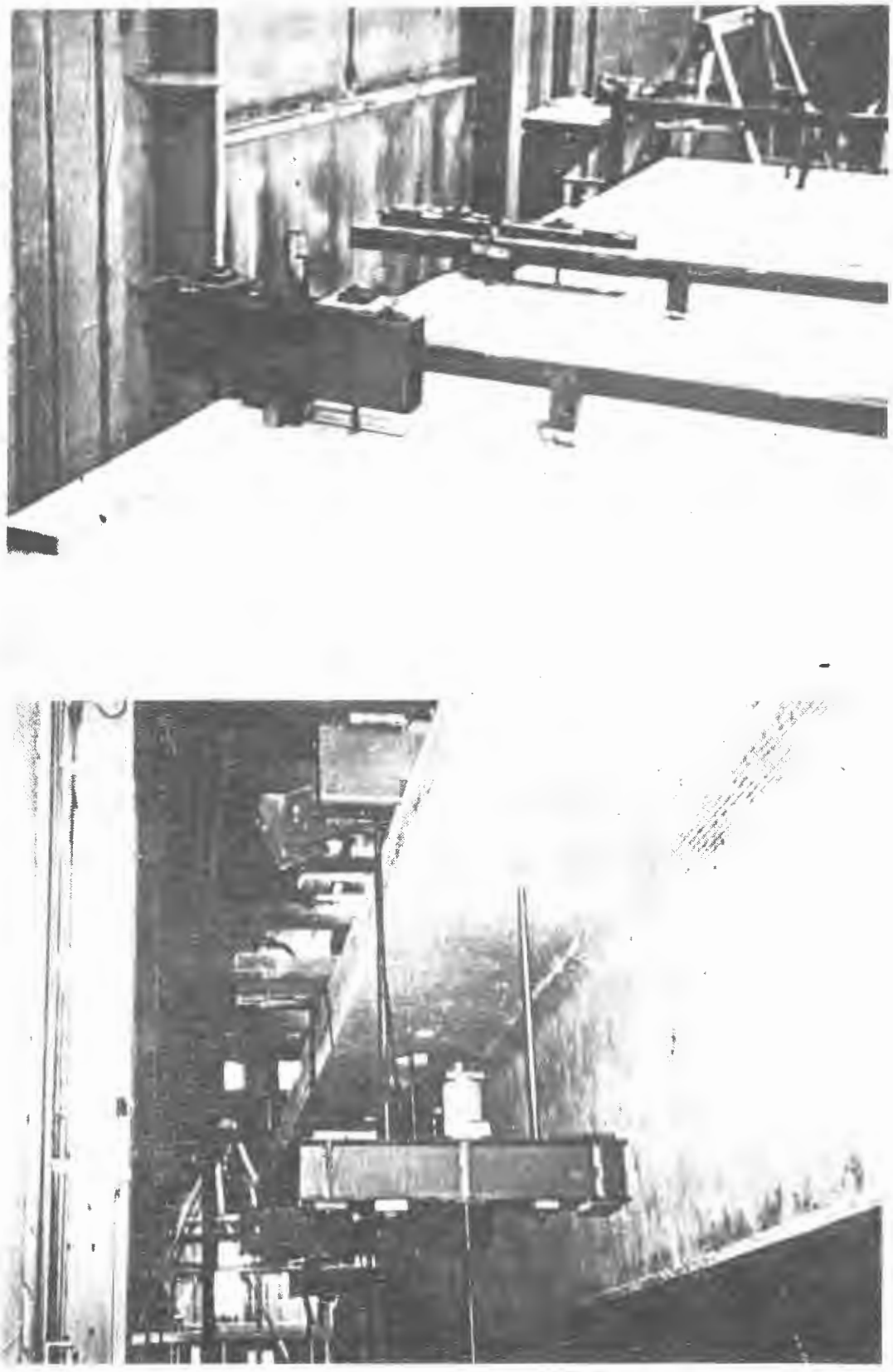

Fig. 67. Instrumentation in Flange Slab Test

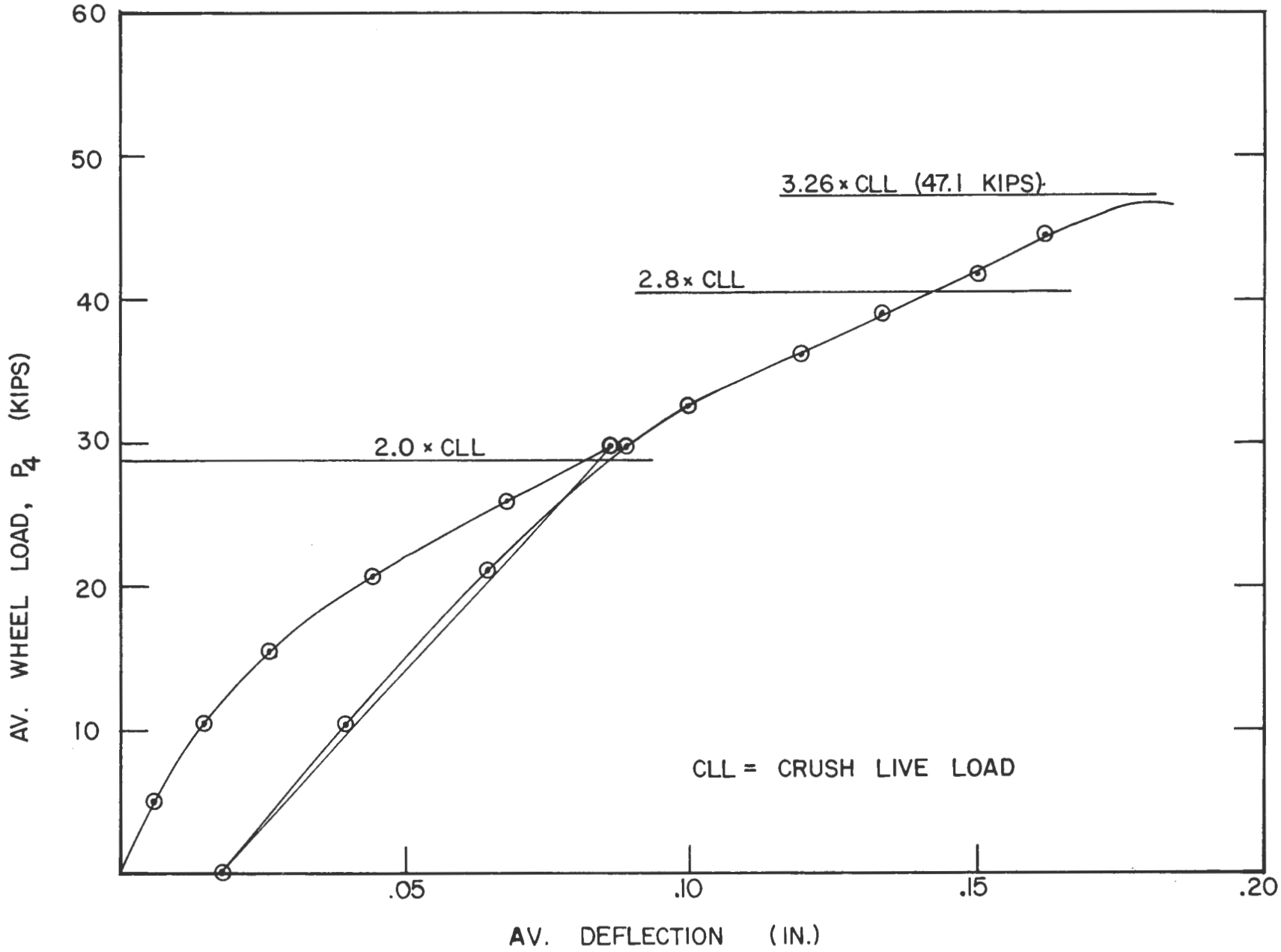

Fig. 68 Load vs. Deflection Curve for Flange Slab Test

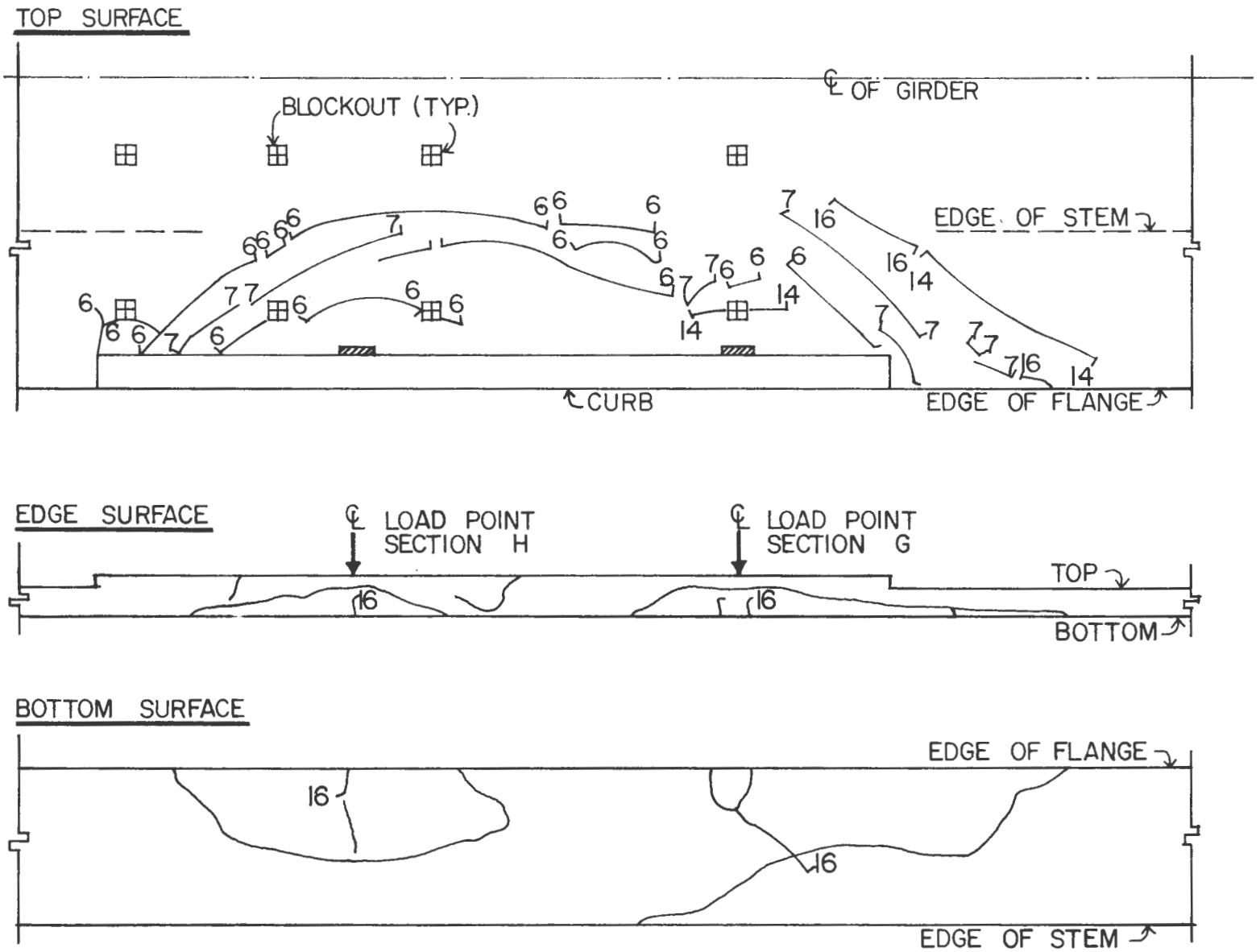

Fig. 69 Crack Pattern After Failure at 1.6 times Crush Live Load

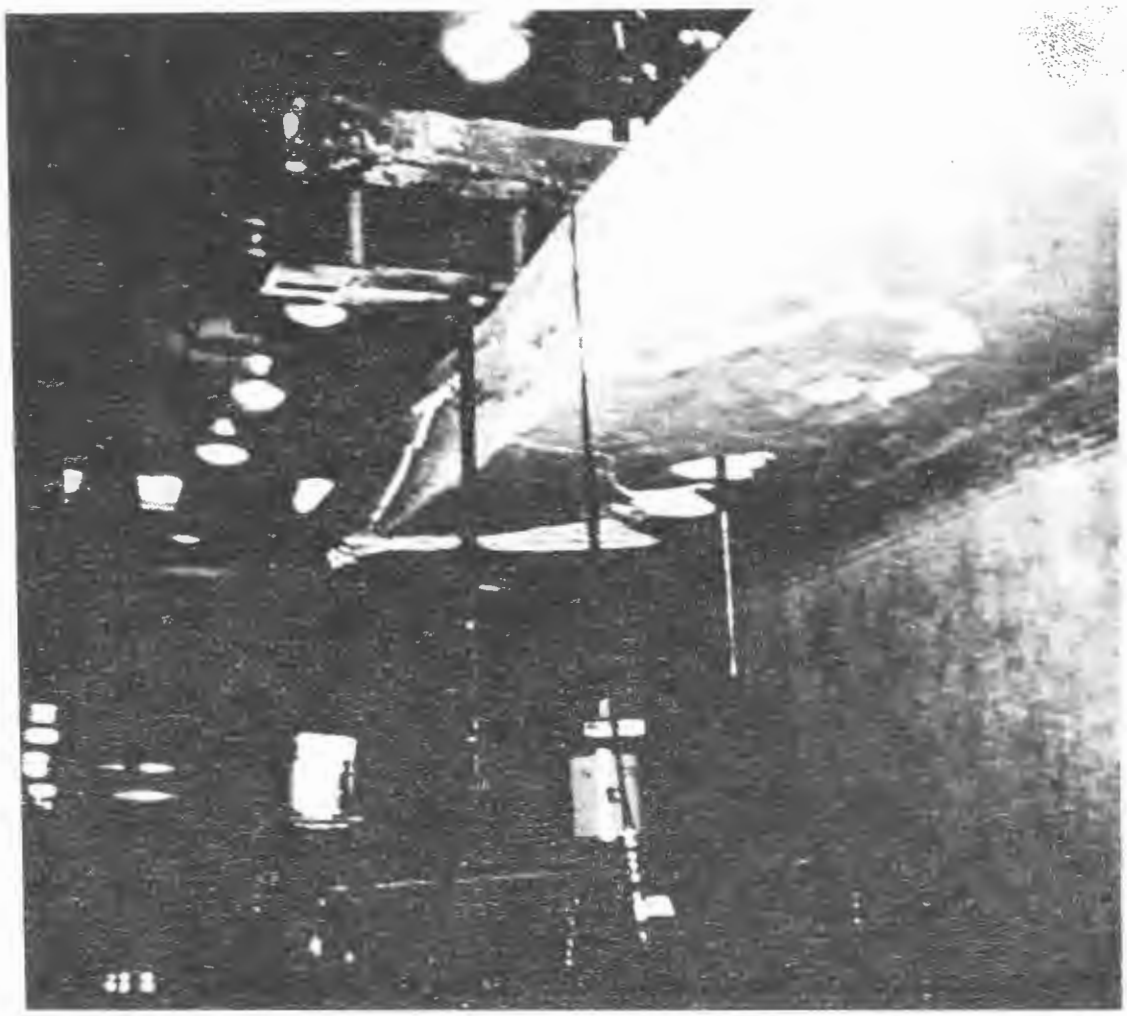

Fig. 70. Punching Shear Failure at Load Point H

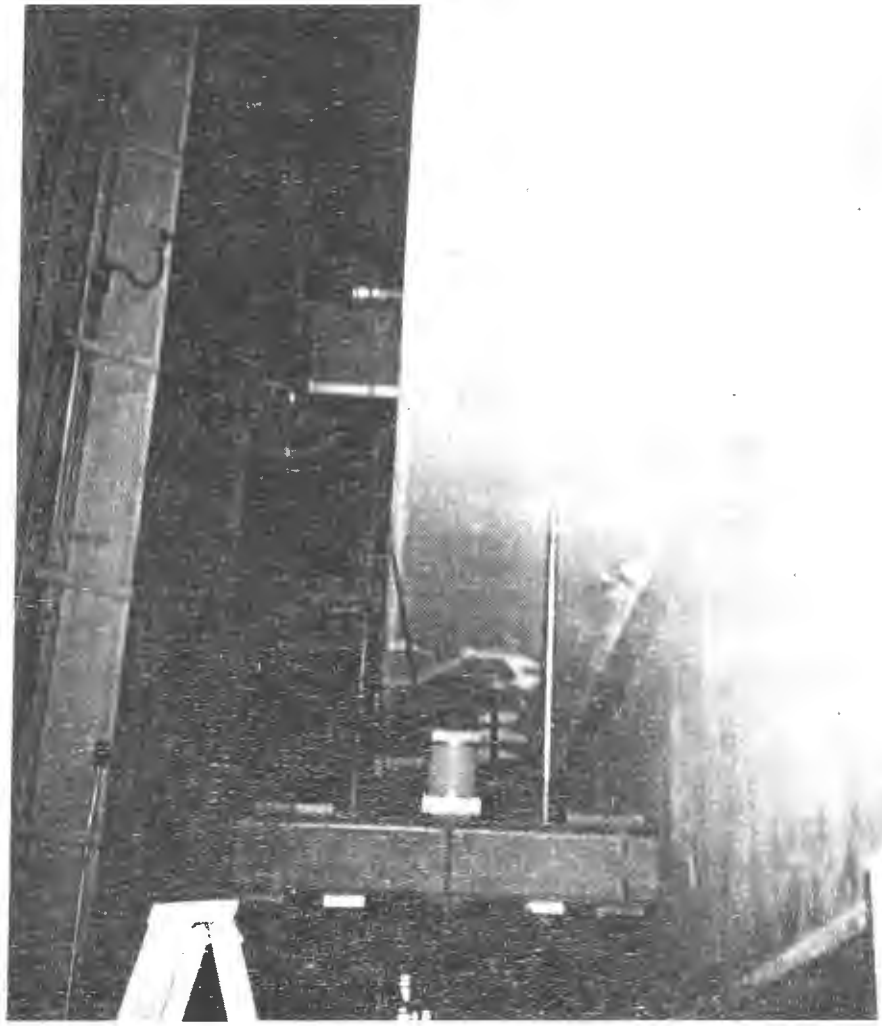

Fig. 71. Punching Shear Failure at Load Point G